Investigation of the genetic aetiology and pathogenetic mechanism of disease in patients with late-onset FGD

Dr Claire Hughes

Acknowledgements

I would like to thank Peter Nurmberg and his group for performing the exome sequencing and initial filtering to remove known varinats. I also thank our collaborators John Schimenti and his group for providing the MCM4 mutant and control mouse models and also Leo Guasti who provided Figure 6.7.

I would like to thank my supervisors and collegues in the endocrinology lab, especially Adrian, Lou, Helen, Rena, Peter, Paul, David, Rathi, Leo and Li for their guidance, advice, teaching and training.

I would really like to thank Colm Costigan and the endocrine nurses in Our Lady's Children's Hospital in Dublin who gave their continual suppport. I would also like to thank the patients and their families who gave their time so generously.

I would especially like to thank Adrian Clark and Lou Metherell who continually gave their expertise and advice.

Publications arising from this research

Clark, L. Metherell. **MCM4 mutation causes adrenal failure, short stature and natural killer cell deficiency in humans**. *Journal of Clinical Investigation 2012;122(3):814-820,* ***(front cover JCI March 2012 issue, comment in Nature Medicine)***

CR Hughes, Chung TT, Habeb AM, Kelestimur F, Clark AJL, Metherell LA. **Missense mutations in the Melanocortin 2 receptor accessory protein that lead to late onset Familial Glucocorticoid Deficiency type 2.** *J. Clin Endocrinol Metab. 2010 Jul; 95(7): 3497-501*

Contents Page

Chapter 2: Materials and Methods

Contents: Figures

Chapter 1: Introduction

Chapter 2: Methods

Chapter 3: Missense mutations in the Melanocortin 2 receptor accessory protein that lead to late onset Familial Glucocorticoid Deficiency type 2

Chapter 4: Identification of the gene causing FGD in the Irish traveller population

Contents: Tables

List of abbreviations

ACTH: Adrenocorticotrophin hormone

cAMP: cyclic adenosine monophosphate

CDK: cyclin dependent kinases

CREB: cAMP response element binding protein

CYP: cytochrome P450

DAX1: Dosage sensitive sex reversal Adrenal hypoplasia congenital critical region on the X chromosome

DHEAS: Dehydroepiandrosterone sulphate

DNA: Deoxyribonucleic acid

FGD: Familial Glucocorticoid Deficiency

FSH: Follicle stimulating hormone

GPCR: G protein-coupled receptor

HPA: hypothalamic-pituitary-adrenal

IGF1: insulin-like growth factor 1

IMM: inner mitochondrial membrane

LCAH: Non-classical Lipoid Congenital Adrenal Hyperplasia

LH: Luteinising hormone

LHR: luteinizing hormone receptor

MC2R: melanocortin 2 receptor

MCM4: Mini chromosome maintenance homologue 4

MRAP: Melanocortin 2 receptor accessory protein

MSH: melanotrophin stimulating hormone

NK: Natural Killer

NNT: nicotinamide nucleotide transhydrogenase

PC1: prohormone convertase 1

POMC: proopiomelanocortin

SF-1: steroidogenic factor-1

Shh: sonic hedgehog

StAR: steroidogenic acute regulatory protein

ZF: Zona fasciculate

ZR: Zona reticularis

ZR: zona reticularis

Abstract: Investigation of the genetic aetiology and pathogenetic mechanism of disease in patients with late-onset FGD

Familial Glucocorticoid Deficiency (FGD) is an autosomal recessive form of adrenal failure characterized by isolated glucocorticoid deficiency with preserved mineralocorticoid secretion. I studied two cohorts of patients who presented with late onset FGD.

Firstly I investigated 2 families of Turkish ethnicity who presented with delayed onset adrenal insufficiency and identified two novel missense mutations in the melanocortin 2 receptor accessory protein (MRAP). I characterised both these mutations in vitro and confirmed that both mutant MRAPs demonstrated reduced rather than absent function consistent with the phenotype of delayed presentation.

Secondly I studied 3 families from a genetically isolated Irish population who had an interesting variant of adrenal failure. Patients had typical biochemical features of FGD with isolated glucocorticoid deficiency, raised ACTH and normal renin and aldosterone levels. Unlike other forms of FGD, cortisol deficiency was often not as severe and onset was usually in childhood following a period of normal adrenal function. Affected children develop hypocortisolaemia but also growth failure, increased chromosomal breakage and natural killer (NK) cell deficiency.

Targeted exome sequencing identified a variant (c.71-1insG) in mini chromosome maintenance homologue 4 (*MCM4*) that segregated with the disease in all 3 families. RT-PCR of patient leucocyte RNA revealed this mutation leads to aberrant splicing of

exon 2 and a foreshortened ORF encoding a prematurely terminated translation product (p. Pro24ArgfsX4). Western blotting of patient lymphocytes revealed loss of the full length MCM4 protein but two smaller MCM4 isoforms were preserved.

Histological examination of the adrenals of an MCM4 depletion mouse model revealed an abnormal adrenal morphology. Small, spindle-shaped cells were present throughout the adrenal cortex. These cells did not express either CYP11A1 or CYP11B1 and significantly reduced the number of steroidogenic cells in the zona fasciculata. Further staining showed these cells expressed GATA4, a transcription factor expressed in foetal but not adult adrenals, and capsular markers, indicating that they may be non-steroidogenic capsular cells infiltrating the cortex.

MCM4 is one part of a heterohexameric complex essential for normal DNA replication and genome stability in all eukaryotes and no MCM mutation has ever been described in humans. I have identified a mutation in *MCM4* that results in adrenal failure, growth retardation, increased chromosomal fragility and NK cell deficiency. Animal models indicate that loss of MCM4 is lethal, but it is likely that the smaller isoforms I observe may rescue the patients from a lethal phenotype.

This research has revealed a novel mechanism of adrenal failure and potentially a novel function of MCM4. The seemingly specific impact on adrenal function may reflect a defect in adrenal stem cell differentiation and the inability of capsular cells to differentiate into steroidogenic cells.

Chapter 1: Introduction

1.1: Introduction

Familial Glucocorticoid Deficiency (FGD) is an autosomal recessive form of adrenal failure characterized by adrenocorticotrophin (ACTH) resistant isolated glucocorticoid deficiency with preserved mineralocorticoid secretion [1-3]. Patients with FGD usually present in the neonatal period or early childhood with symptoms relating to cortisol deficiency including hypoglycaemia, jaundice, recurrent infection and failure to thrive. Patients are hyperpigmented due to grossly elevated ACTH levels. A unique variant of FGD exists in the Irish travelling community, a genetically isolated population with high levels of consanguinity [4]. Affected children develop hypocortisolaemia and compensatory elevated ACTH, but retain normal renin and aldosterone levels as expected. However patients also have short stature, evidence of increased chromosomal breakage and natural killer (NK) cell deficiency.

FGD was first described in 1959 by Shepard *et al.* who reported 2 sisters as having Addison's disease without hypoaldosteronism [1]. Subsequently a number of patients were reported with an inherited form of adrenal insufficiency also without hypoaldosteronism [2, 3, 5, 6]. In contrast to Addison's Disease, FGD is a genetic disorder resulting from mutations in genes encoding essential proteins involved in the early response to ACTH.

1.2: Hypothalamic pituitary adrenal axis

1.2.1: Mechanisms controlling cortisol production

The adrenal gland consists of an outer adrenal cortex surrounding an inner adrenal medulla. The adrenal cortex comprises the zona glomerulosa secreting aldosterone,

the zona fasciculata secreting cortisol and the inner zona reticularis secreting adrenal androgen precursors. The anterior pituitary hormone ACTH controls cortisol synthesis and secretion from the zona fasciculata. ACTH secretion is stimulated by corticotrophin releasing hormone (CRH) from the hypothalamus and follows a circadian pattern. Cortisol secretion is an example of one of the classical endocrine feedback loops; it is under negative feedback control from the hypothalamic-pituitary-adrenal (HPA) axis (Figure 1.1). ACTH release occurs in response to low circulating cortisol levels and is inhibited by high circulating levels of cortisol or synthetic glucocorticoid. This negative feedback occurs at both the hypothalamic and pituitary level. ACTH is also released in response to stress such as trauma, hypoglycaemia, infection/fever, surgery or anxiety.

ACTH acts by binding to its specific cell-surface receptor, the ACTH receptor or melanocortin 2 receptor (MC2R) to induce adrenal steroidogenesis in all three zones of the adrenal cortex. The MC2R is the smallest member of the melanocortin receptor family, which includes five members MC1R – MC5R. The melanocortin receptors are seven transmembrane domain G protein-coupled receptors (GPCRs) which are involved in diverse functions including adrenal steroidogenesis, pigmentation and weight and energy homeostasis [7]. The sole natural ligand for MC2R is ACTH, in contrast to the other melanocortin receptors that show varying affinity to ACTH and α-, β- and γ-MSH [8].

ACTH binding to MC2R induces intracellular production of cyclic adenosine monophosphate (cAMP), one of the major actions of which is to stimulate cAMP-dependent protein kinase (protein kinase A). As a consequence of this stimulus

cholesterol ester is imported into the cell via the scavenger receptor B1 and hydrolysis of the ester by hormone sensitive lipase occurs. Cholesterol is then taken up into the mitochondrion by a complex including the steroidogenic acute regulatory protein (StAR). ACTH stimulates increased steroidogenic enzyme expression via a number of mechanisms including the activation of the cAMP response element binding protein (CREB), and ultimately results in an increased rate of cortisol synthesis. ACTH has also recently been shown to specifically increase StAR transcription via cAMP inhibition of salt inducible kinase (SIK), allowing phosphorylation of TORC (transducer of regulated CREB activity), which activates CREB and induces StAR transcription [9].

Figure 1.1

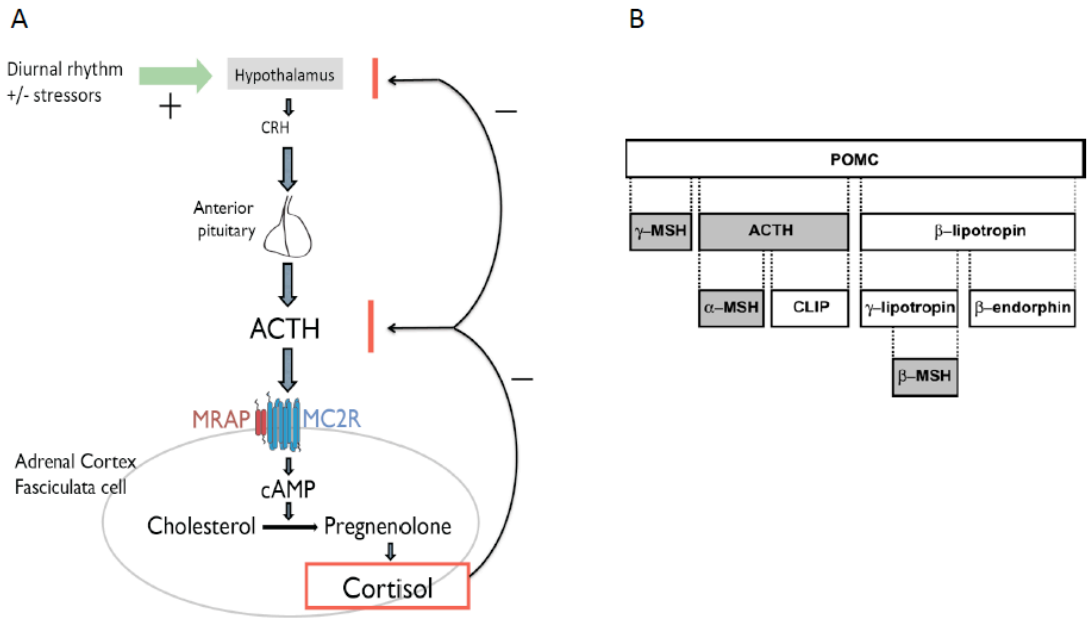

Figure 1.1. A. Hypothalamic Pituitary Adrenal Axis. Negative feedback regulation of cortisol secretion. B. POMC processing. The POMC gene leads to the generation of a prohormone POMC, which undergoes a series of proteolytic cleavages to give rise to ACTH as indicated.

1.2.2: Mechanisms controlling aldosterone production

The control of mineralocorticoid production is entirely separate from glucocorticoid production. This has important clinical consequences as some patients may have disorders affecting only one system or may have combined glucocorticoid and mineralocorticoid deficiency due to adrenal hypoplasia or destruction. The main factor controlling aldosterone production is angiotensin through the renin-angiotensin-aldosterone system.

Renin synthesis occurs from the juxtaglomerular cells of the kidney in response to low renal arteriolar pressure, hyponatraemia, hyperkalaemia, upright posture, vasodilatory drugs and β-adrenergic stimulation. Renin cleaves Angiotensinogen to form Angiotensin I, which in turn is converted to Angiotensin II by angiotensinogen converting enzyme (ACE). Angiotensin II has two principal actions both of which are mediated through the AT_1 receptor and both increase blood pressure. Firstly Angiotensin II stimulates arteriolar vasoconstriction within seconds. Secondly it is a potent stimulator of aldosterone secretion by increasing transcription of the cytochrome P450 enzyme, CYP11B2 within the zona glomerulosa cells of the adrenal cortex [10]. Increased plasma potassium is also a powerful stimulator of aldosterone production via membrane depolarization, calcium channel alteration and ultimately increased transcription of CYP11B2 [11]. Aldosterone causes renal sodium retention and potassium loss and consequently increases intravascular volume and blood pressure.

1.2.3: Mechanisms controlling adrenal androgen production

ACTH is capable of stimulating adrenal androgen synthesis however the pattern of secretion is very different from cortisol secretion. Androgen secretion is high in infancy, low during childhood and rises again in adolescence and early adulthood. This is in contrast to cortisol secretion which has a diurnal variation but levels remain similar throughout life. The exact control of adrenal androgen secretion together with the development of the zona reticularis (discussed below) remains to be elucidated.

1.3: Adrenal development

1.3.1: Embryology

The adrenal glands consist of an outer cortex and an inner medulla that are embryologically and physiologically distinct but often act together to coordinate the fight/flight response. The medulla consists of neuroectodermally derived chromaffin cells and secretes catecholamines including epinephrine and norepinephrine. During foetal life clusters of chromaffin cells are scattered throughout the adrenal cortex only coalescing into a separate identity after birth [12]. The adrenal cortex is derived from the intermediate mesoderm and produces many steroid hormones including mineralocorticoids, glucocorticoids and adrenal androgens.

The human foetus has very large adrenal glands relative to its size; by 20 weeks gestation the adrenal gland is approximately the same size as the foetal kidney. At birth the adrenal glands are approximately twice the weight of adult adrenals (8-9g) [13]. The growth of the foetal adrenal involves proliferation, migration, differentiation, hypertrophy and apoptosis of adrenal cells. The first evidence of adrenal development and adrenal specific cells *in utero* occurs at 4 weeks gestation when the

adrenogonadal primordium can be distinguished and identified by steroidogenic factor-1 (SF1) expression [14]. At approximately 8 weeks gestation the adrenal primordium separates from the gonadal primordium. At this stage the adrenal primordium consists of 2 zones, the definitive zone and the foetal zone both surrounded by a mesenchymal capsule [14]. The foetal zone consisting of large eosinophilic cells secretes vast quantities of steroids throughout pregnancy, principally DHEA and DHEAS. The placenta does not synthesise oestrogen from cholesterol but instead converts the DHEA and DHEAS from the foetal adrenal into oestrogen using placentally expressed aromatase. Oestrogen is important for the development of placental villous blood vessels and foetal ovarian development. The definitive zone consists of a thin layer of basophilic cells and is thought to act as a reservoir for progenitor cells which can then migrate into the foetal zone and differentiate into steroidogenic cells [15]. The transitional zone, lying between the definitive zone and the foetal zone, develops at approximately 24-28 weeks of gestation [16]. Transitional zone cells resemble those of the adult adrenal zona fasciculata and are capable of secreting small quantities of cortisol in late gestation. Postnatally the foetal zone regresses, presumably due to apoptosis, and the definitive zone differentiates into the zona glomerulosa, secreting mineralocorticoids and the zona fasciculata secreting glucocorticoids. Different studies provide conflicting evidence suggesting the regression of the foetal zone may be determined either by gestation or delivery [17, 18]. Later in childhood the zona reticularis develops and secretes adrenal androgens with the onset of adrenarche at around 6-8 years.

Most mechanistic studies on adrenal development have used rodent models, principally rats and, more recently, mice. Murine adrenal development proceeds in a

similar manner to the human, with the SF-1 positive adrenogonadal primordium first being identified in a thickening of the coelomic epithelium overlying the genital ridge at around embryonic day E9.5 [19]. At approximately E10.5 a subset of SF1 positive cells have coalesced into the adrenal anlagen which is then invaded by neural crest medullary precursors before mesenchymal cells encapsulate the gland by E13.5. By E16 the adrenal cortex and medulla are a distinct entity. As the adrenal grows SF1 dependent steroidogenic enzyme expression begins and steroidogenic zones segregate. In mice the zona glomerulosa forms perinatally. At birth a transient zone, termed the X-zone is detectable in the innermost part of the mouse adrenal cortex, this regresses at puberty in male mice and after the first pregnancy in females [20]. This zone has been postulated as being equivalent to the foetal zone in humans.

A number of different models have been proposed to explain growth of the foetal adrenal gland; the centripetal cell migration model, the transformation field model and the zonal model (Figure 1.2) [21]. The transformational field model suggests that there are two transformational fields; one located between the zona glomerulosa and the zona fasciculata and one between the zona fasciculata and the zona reticularis. Progressive transformation results in a proliferative increase of the fasciculata zone, regressive transformation leads to a narrowing and functional restriction. The zonal model postulates that specific undifferentiated stem cells exist for all zones. However most recent studies support the cell migration model, this model postulates that stem cell populations reside either in the adrenal subcapsular region or in the zona glomerulosa or zona glomerulosa/zona fasciculata border. These populations can proliferate and then migrate into the zona glomerulosa or zona fasciculata and differentiate into steroidogenic cells [22, 23]. Enucleation experiments indicate that

capsule and/or adherent subcapsular cells can differentiate to recreate an adrenal cortex with normal zonation. Although the exact origin of the stem cell population is unclear it has been suggested that these stem cells are SF1 negative cells that reside in the capsule or subcapsular region and that can migrate into the adrenal cortex in response to some unknown mitogenic signals, gain SF1 expression and differentiate into steroidogenic cells [24]. Studies have shown increased proliferation within the periphery of the gland and the definitive zone with hypertrophy predominantly occurring in the foetal zone in humans. Further studies show increased apoptosis occurring in the centre of the gland [25]. Taken together this indicates that cells proliferate in the periphery of the foetal adrenal gland and migrate centripetally differentiating into the different zones before undergoing senescence near the centre of the gland. In addition lineage tracing studies have demonstrated that both sonic hedgehog (Shh) expressing cells in the subcapsular mouse cortex and Shh signal receiving capsule mesenchyme cells have properties of adrenocortical stem/progenitor cells with their progeny populating the entire cortex [21]. Recent preliminary work has further supported this hypothesis; genetically engineered mice expressing Cre-recombinase under the control of aldosterone synthase, a specific zona glomerulosa cell marker were created. These mice had GFP labeled cells in the zona glomerulosa on postnatal day 1, these cells encompassed most of the zona glomerulosa by 3 weeks of age and by 5 weeks of age there was considerable GFP labeling in the zona fasciculata suggesting the zona fasciculata cells arise from the zona glomerulosa. However when zona glomerulosa cells were ablated the zona fasciculata was still able to develop normally suggesting an alternative mechanism independent of the zona glomerulosa can also give rise to a functional zona fasciculata [26].

Figure 1.2

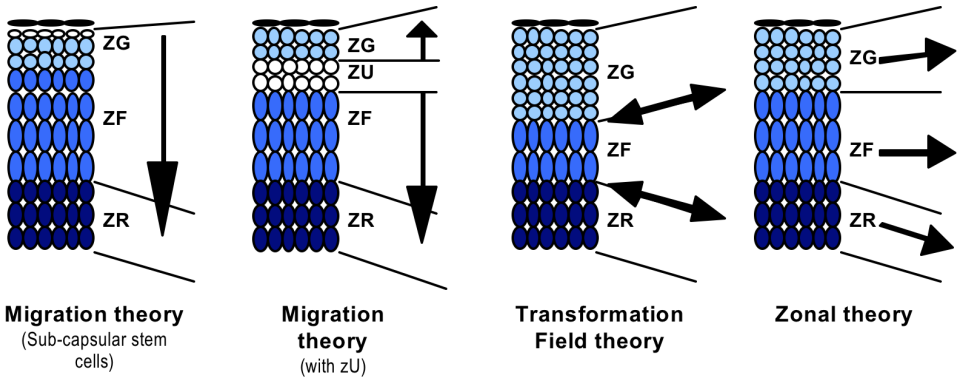

Figure 1.2. Different models proposed to explain growth of the fetal adrenal gland. The origin of the arrows indicate the place of cell renewal and proliferation. The tips of the arrows indicate the direction of growth and / or migration. ZG, zona glomerulosa; ZF, zona fasciculata; ZR, zona reticularis; ZU; undifferentiated zone.

1.3.2: ACTH

ACTH is accepted as one of the primary regulators of adrenal development. However this is not mediated solely by MC2R. ACTH stimulates proliferation of adrenocortical cells *in vivo* but not *in vitro* suggesting that it acts through other mitogenic factors produced locally [27]. This has important implications for children with familial glucocorticoid deficiency (described in detail below) due to ACTH receptor pathway defects. These children present postnatally with isolated glucocorticoid deficiency but importantly they have had some degree of normal adrenal development. Although the adrenals are reported as being small these children have an intact renin – aldosterone system and can produce mineralocorticoids as normal from the zona glomerulosa, indicating that ACTH driven adrenal development is not only mediated through MC2R [28]. Babies with anencephaly (and therefore presumably very low levels of ACTH) have normal adrenal development at 10-15 weeks gestation indicating that early development of the foetal adrenal is ACTH independent [29].

Mutations in the proopiomelanocortin (POMC) gene or the prohormone convertase 1 (PC1), which cleaves POMC to ACTH, give rise to a similar phenotype as that seen in FGD. However patients with POMC mutations also have red hair, pale skin and obesity as well as adrenal insufficiency as melanotrophin stimulating hormone (MSH) and β-endorphin will also be affected. Those patients with mutations in PC1 can also present with abnormalities in glucose metabolism, obesity, hypogonadotrophic hypogonadism and malabsorptive diarrhoea [30]. ACTH deficiency can also exist as part of multiple pituitary hormone deficiency or as an isolated deficiency secondary to TPIT mutations, a T-box factor that controls transcription of the POMC gene [31].

ACTH up-regulates vascular endothelial growth factor (VEGF)-A, a pro-angiogenic factor and potent mitogen for endothelial cells. ACTH also increases expression of Angiopoietin (Ang)-1 and Ang-2 growth factors that mediate angiogenesis allowing increased blood supply to the rapidly enlarging foetal adrenal gland [32]. In addition ACTH can up-regulate expression of FGF-2, and IGF-II which act as growth factors stimulating adrenocortical cell growth. Each zone of the foetal adrenal gland expresses ACTH receptors and it has been postulated that different expression levels of the ACTH receptor and therefore different responsiveness to ACTH between the zones may help control zonation of the adrenal cortex [33].

1.3.3: SF1 and DAX1

Adrenal development and the appropriate differentiation of progenitor cells within the adrenal cortex depend on the normal spatiotemporal expression of a wide range of signalling molecules. Steroidogenic Factor 1 (SF1) and Dosage sensitive sex reversal Adrenal hypoplasia congenital critical region on the X chromosome (DAX1) are

members of the nuclear hormone receptor family of transcription factors. Both are expressed in the adrenal primordium from its earliest stages in development, throughout prenatal life and postnatally in the adult adrenal cortex [14, 34]. Although both are essential for normal adrenal (and gonadal) development they seem to have antagonistic actions as well as synergistic actions.

SF1 expression is initiated by Pbx1 (pre-B-cell leukaemia transcription factor 1) within a complex with Prep1, a homeobox protein, and Hox (Homeobox gene) 9b that together activate a *F*oetal *Ad*renal *E*nhancer (FAdE), which lies within intron 4 of SF1 [34]. This initially occurs on separation of the adrenogonadal primordium after which SF1 autoregulates its own expression. FAdE is an adrenal specific promoter and is not active in other SF1 expressing tissues, for example the gonad, hypothalamus or pituitary gonadotropes. SF1 regulates the transcription of many genes involved in steroidogenesis [35]. SF1 knock out mice have adrenal agenesis and gonadal dysgenesis. A recent paper from Achermann's group has reviewed the wide clinical spectrum of human disease associated with SF1 mutations [36]. Two case reports describe the classical human phenotype of primary adrenal failure and gonadal dysgenesis in XY individuals (1 homozygous and 1 heterozygous mutation in SF1) and one reports primary adrenal failure but normal gonadal development in a 46XX individual with a heterozygous mutation in SF1. Conversely 46XX patients with SF1 mutations have also been reported as having normal adrenal function but primary ovarian failure. Interestingly a number of cases with heterozygous mutations in SF1 have been reported in 46XY patients who have gonadal anomalies ranging from gonadal dysgenesis and sex reversal to milder abnormalities such as hypospadias and male factor infertility but all have normal adrenal function. In contrast overactivity or

overexpression of SF1 may also be a potential cause or modifier of human disease. Somatic duplications of 9q33 (SF1 locus) have been described in a cohort of children from Brazil with adrenocortical tumours [37]. Subsequently increased SF1 expression has been seen in adult adrenocortical tumours and has also been associated with a worse prognosis [38].

Human mutations in DAX1 cause X-linked adrenal hypoplasia congenita which usually presents as primary adrenal failure at birth with hypogonadotrophic hypogonadism [39, 40]. DAX1 is one of the target genes for SF1 but it also inhibits SF1 mediated transcription; DAX-1 null mice do not present with adrenal hypoplasia or adrenal failure however the adrenal failure in the SF1 knockout mouse is partially rescued by knockout of DAX1 [41]. DAX1 human mutations give rise to hypoplasia of the human foetal adrenal with little or no evidence of a definitive zone and a poorly organised foetal zone. In the human foetal adrenal DAX-1 shows nuclear localisation in the definitive zone cells perhaps preventing SF1 expression and therefore inhibiting steroidogenesis in these cells. In contrast DAX-1 is less abundant and localises to the cytoplasm in foetal zone cells, possibly releasing the inhibition of SF1 and allowing steroidogenesis[42]. DAX-1 is also specifically enriched in the subcapsular region similar to sonic hedgehog (Shh) (see below). This data suggests that DAX-1 loss of function leads to depletion of steroidogenic progenitor cells with enhanced differentiation of definitive zone cells secondary to reduced inhibition on SF1 and therefore ultimately adrenal hypoplasia.

1.3.4: Hedgehog signalling

Hedgehog (Hh) signalling is required for the growth and normal development of a number of tissues and has been identified as a regulator of both adult stem cell populations and embryonic stem cells [43, 44]. Sonic hedgehog (Shh) in the adrenal gland binds to its receptor (Patched-1) and releases inhibition of the Smoothened membrane protein allowing downstream activation of Gli transcription factors (Gli1-3). Gli1 expression is absolutely dependent upon Hh signalling and is only seen in the capsule and a few subcapsular, non-steroidogenic, cells. Recently King *et al.* showed that Shh mRNA is expressed in the mouse adrenal cortex and also identified Gli-1 and Shh expressing cells as candidate adrenoprogenitor and stem cell populations [21]. They identified Shh signalling as the potential mechanism underlying the cell migration model (discussed above) of adrenal growth and maintenance in mice. In this model there are 2 populations that contain adrenocortical progenitors. Firstly, SF1 positive cells derived from the adrenogonadal primordium delaminate and establish a primary adrenal lineage (the foetal zone/X zone). Some of these cells initiate Shh signalling and can differentiate into any steroidogenic lineage. These Shh positive, SF1 positive progenitors within the zona glomerulosa can populate the cortex throughout development and promote adrenal maintenance in later life. The Shh positive cells signal to the surrounding mesenchymal cells, acting possibly as a chemoattractant or mitogen for the coalescing capsule. These mesenchymal derived cells that are Gli1 positive (Sf1 negative, Shh negative) within the adrenal capsule or subcapsular mesenchyme can also give rise to Sf1 positive cells and these cells can also subsequently differentiate and contribute to all steroidogenic lineages, at least in part via a Shh expressing intermediate population. Huang *et al.* and King *et al.* showed that tissue specific knockout of Shh led to small adrenals but proper zonation

was maintained indicating that Shh has a role in the growth of the adrenal cortex but not its differentiation in mice [21, 45]. King *et al.* also showed that in the absence of Shh proliferation indices of the cortical cells are relatively normal but that the capsule is very thin, indicating that the conversion of capsule cells to cortical cells is disrupted accounting for the growth failure.

Interestingly a recent paper examining the effects of eliminating SF1 sumoylation *in vivo* provided further evidence suggesting correct Shh signalling is required for normal adrenal and gonadal development [46]. Sumoylation is generally considered to repress transcriptional activation of its given substrate. However by creating a knockin mouse with a mutant unsumoylatable SF1 homozygous allele Lee *et al.* showed that disrupting the SF1 sumo cycle leads to increased activation of Shh and the Shh signalling pathway in the adrenal gland. Shh positive cells, which are usually restricted to the immediate subcapsular layer, were seen penetrating deep into the cortex. Additionally there was a notable expansion of Gli1 positive cells in the subcapsular layer and definitive zone suggesting that loss of SF1 sumoylation elevates Shh expression to amplify hedgehog signalling. This was in contrast to a number of known SF1 targets, for example CYP11A1, in which the expression levels remained unchanged. In addition the authors found the mutant adrenals expressed a number of testicular markers, for example SOX9, and also exhibited a persistent foetal X zone suggesting eliminating SF1 sumoylation interferes with normal adrenal maturation. Paradoxically they noted reduced Shh expression and a thinner subcapsular layer of Gli-1 cells in older mutant adrenals together with reduced adrenal weights. They proposed that the early expansion of Shh positive adrenal progenitors would interfere with the adrenal stem cell niche and potentially disrupt steroidogenic cell

differentiation by recruiting progenitors prematurely, consistent with the role of Shh in adrenal stem cell proliferation and maintenance discussed above.

Mutations in Shh and other genes involved in the hedgehog signalling pathway can lead to holoprosencephaly, which is frequently associated with secondary adrenal insufficiency. Pallister-Hall syndrome, which has been associated with adrenal hypoplasia and insufficiency in humans, has been shown to be caused by a frame shift mutation in Gli-3, although the adrenal phenotype may also be secondary to pituitary defects [47].

1.3.5: Wnt/β-catenin

Wnt/β-catenin signalling is essential for normal embryonic development and maintenance and differentiation of stem cell populations in many tissues including the adrenal. Among Wnt factors Wnt 4 is specifically required for adrenal development [15]. Wnt activation allows cytoplasmic and nuclear accumulation of β-catenin, leading to activation and transcription of downstream genes. Specific inactivation of B-catenin in a mouse model, using cre-lox techniques to target only SF-1 expressing cells, showed adrenal hypoplasia at birth with high SF-1 cre transgene expression [48]. In mice with lower levels of Cre expression the phenotype was delayed and the mice displayed increased cortical thinning and adrenal failure later in life. The cortical depletion is hypothesised to be secondary to a reduction in adrenocortical progenitor cells as B-catenin/Wnt signalling has been demonstrated to be essential in a number of progenitor cell systems. It is possible that hedgehog signalling and Wnt/B-catenin signalling regulate adrenocortical progenitor populations in concert as B-catenin has been shown to be required for SF1 positive cell proliferation and survival and

hedgehog and Wnt signals are frequently reciprocally regulated [49]. Overexpression of β catenin causes adrenal hyperplasia and a secondary zona glomerulosa situated next to the medulla. Wnt4 deletion causes absence of the zona glomerulosa [50].

Many other transcription factors have been identified as being essential for normal adrenal development in mice including, SALL1, CITED2, FoxD2 and WT1. Knockout of any of these factors in mice leads to an adrenal phenotype however only mutations in Gli-3 have been associated with adrenal hypoplasia and insufficiency in humans (Pallister-Hall syndrome).

1.3.6: *Acd* and chromosomal instability

An interesting spontaneous autosomal recessive mutant with developmental defects in organs derived from the urogenital ridge was identified in an inbred mouse strain from the Jackson laboratory [51]. This mouse, named the *Acd* mouse, has adrenocortical dysplasia, with hypoplastic adrenals, skin hyperpigmentation, growth retardation, infertility and hydronephrosis. Biochemically female mice had lower baseline corticosterone levels and both sexes had elevated ACTH levels compared to wild type but interestingly aldosterone levels were normal indicating a normal functioning zona glomerulosa. Subsequently Keegan *et al* identified the cause of the *Acd* mutant phenotype, a novel splice mutation in the *Acd* gene which encodes the telomere protein Tpp1 [52]. This protein is a component of the shelterin complex that maintains telomere integrity and protects the telomere from telomerase activity. Therefore these mice had telomere dysfunction and genomic instability. They further characterised the adrenal defect showing that the mutant adrenals consisted of enlarged cortical cells with irregular nuclei, The adrenals lacked an X-zone at any age

indicating that the developmental program yielding a mature adrenal cortex was interrupted. However the fundamental defect leading to the adrenal phenotype remains unknown, it was presumed to be caused by a defect in cellular proliferation but this is unproven and so the role of Acd in adrenal cortical development is still to be established. No human mutations in Acd /Tpp1 have been identified. However other human syndromes caused by genomic instability including Werner syndrome (caused by mutations in the RecQ DNA helicase RECQL2) and dyskeratosis congenita (caused by mutations in the TERC gene) have similar features to the Acd mouse including germ cell failure, adrenal insufficiency and skin abnormalities [53, 54]. Therefore genomic instability, through an as yet undiscovered mechanism, can lead to adrenal insufficiency both in mice and humans.

1.3.7: GATA transcription factors

GATA4 and GATA6 are expressed in both human and mouse adrenals [55]. GATA1-6 are zinc finger transcription factors that bind to gene promoters and enhancers to regulate gene expression. GATA1-3 are primarily expressed in haematopoetic lineages whilst GATA4-6 regulate cellular proliferation, differentiation and apoptosis in mesoderm and endoderm derived tissues including the adrenal cortex. Null mutations for any of the GATA transcription factors (except GATA5) are embryonic lethal. GATA4 is only expressed in the foetal adrenal cortex, i.e in less differentiated proliferating cells whilst GATA6 is present in both foetal and adult adrenal cells. GATA6 acts with SF1 to upregulate StAR, CYP11A1, CYP17A1, HSD3B2 and SULT2A1 while GATA4 upregulates inhibin-α, CYP 17A1 and StAR [55]. In adult mouse gonads GATA4 expression is most readily detected during periods of active proliferation in ovarian granuloma cells and testicular sertoli cells [56, 57]. Up-

regulation of GATA4 expression has been identified in a small number of adrenocortical tumours and has been linked to more aggressive tumour behaviour [58].

1.3.8: Adrenal maintenance and zonation

The adult adrenal cortex is a dynamic organ that is constantly remodelling to meet the steroidal requirements of the animal and thus maintain homeostasis. The zona glomerulosa is under the control of the renin-aldosterone system so that activation, by for example, placing animals on low sodium or high potassium diets leads to a rapid expansion of the zona glomerulosa whereas inhibition, by for example ACE inhibitors, leads to its rapid diminution. Similarly, the ZF, under the control of the HPA, can be expanded by ACTH treatment but reduced by chronic exposure to glucocorticoids [59]. It is proposed that remodelling occurs in a similar way to the growth and development of the foetal adrenal gland, by recruitment of differentiated steroidogenic cells into the zona fasciculata or zona glomerulosa from stem/progenitor populations within the adrenal capsule, although transdifferentiation between zona glomerulosa and zona fasciculata cells cannot be ruled out. It has been theorized that there may be progenitor cells within each zone but the most accepted concept as discussed above is that cells initially reside in the capsule or subcapsular region or the zona glomerulosa, then successively become zona fasciculata cells then zona reticularis cells through either centripetal migration or as the whole tissue is pushed down by pressure of cell division. Freedman *et al.* recently presented preliminary data suggesting zona fasciculata cells arise from the zona glomerulosa using fate mapping studies in which CYP11B2 –Cre mice were crossed with reporter lines to mark zona glomerulosa cells [60]. It is then presumed that the zona fasciculata cells eventually become zona reticularis cells in the human adrenal however

experiments to prove this have not been performed since the zona reticularis only develops in humans and some higher primates and so this cannot be explored using mouse or rodent models.

The actual regulation controlling the zonation of the adrenal cortex remains poorly understood; there are a number of hypotheses to explain potential methods of zonation but no definitive method. The first hypothesis is that the development of the zona fasciculata and zona reticularis is related to the growth and development of the adrenal cortex so that differentiation of cells into zones is regulated by the gradient of a morphogen such as hedgehog, Wnt or Notch. This hypothesis is consistent with the observed cell migration model involved in adrenal development and maintenance. It is proposed that the morphogen would be at its highest concentration near the capsule and reducing to a low level adjacent to the medulla. This is most likely given the blood supply within the adrenal gland as the arterial supply reaches the capsule first before entering and supplying each layer from the zona glomerulosa to the zona reticularis, when the blood reaches the medulla it flows into the medullary vein. This is similar to that observed in the colon where the gradient of morphogens has been shown to influence cellular differentiation in the colonic crypts [61].

A second hypothesis, especially when considering development of the zona reticularis, proposes that a specific hormone may act on a precursor cell (either a stem cell or zona fasciculata cell) to cause development of the zona reticularis [62, 63]. A number of different hormones have been postulated including leptin, as adrenarche occurs with pre-adolescent increases in adiposity and leptin levels. Alternatively a pituitary hormone such as POMC or a Pit1/POU1F1 dependent factor, for example prolactin,

may be involved. The development of the adrenal reticularis, adrenarche and adrenal androgen synthesis is becoming more important as several recent research papers have indicated that children with premature adrenarche may be at increased risk of PCOS and metabolic syndrome in later life [64]. The factors controlling DHEAS secretion are especially intriguing given the function of DHEAS in children and adults remains elusive. Although DHEAS is the major precursor in sex steroid synthesis and its deficiency causes androgen deficiency in females, many additional functions distinct from its role in sex hormone production have been proposed. These include neurosteroid properties as DHEAS can cross the blood brain barrier and perhaps plays a role in human brain maturation [65]. Additional research, perhaps using novel pluripotent stem cell techniques, is required to further scrutinise adrenocortical zonation.

1.4: Steroidogenesis

1.4.1: Foetal cortisol synthesis

Goto *et al.* suggest that human foetal adrenals secrete cortisol from as early as 8 weeks gestation. Type 2 3β hydroxysteroid dehydrogenase (HSD3B2) expression can be identified in the foetal zone from about 6 to 14 weeks peaking at approximately 8-9 weeks [66]. HSD3B2 expression is required for cortisol synthesis and to shift steroid synthesis away from the androgen-secreting pathway. This period is also the critical time for sexual differentiation. The ability of the foetus to synthesise cortisol at this time allows negative feedback on the HPA axis, reducing steroid production, but most importantly reducing androgen synthesis. This protects the female foetus from excess androgens allowing normal female genital development. From 14 weeks gestation onwards HSD3B2 expression is very low and therefore the foetal adrenal

gland predominantly secretes large quantities of the androgen precursors DHEAS and DHEA [66]. However at this time placental aromatase activity increases substantially and converts DHEA and DHEAS to oestrogens thereby protecting the female foetus from excess androgens and virilisation. From 24 weeks gestation HSD3B2 expression is present in the definitive zone and the transitional zone consistent with the ability of the foetus to make cortisol in the third trimester [67]. The spatiotemporal regulation of HSD3B2 expression is poorly understood.

1.4.2: Post-natal steroidogenesis

Steroidogenesis requires the concerted action of a number of different enzymes including cytochrome P450 (CYP) and hydroxysteroid dehydrogenase enzymes (Figure 1.3). The steroid produced depends on the stimulus, ACTH or angiotensin II and therefore whether the zona fasciculata or zona glomerulosa is stimulated and also the specificity of steroidogenic enzyme expression within each zone. Zona glomerulosa cells lack CYP17A1 and therefore cannot produce cortisol and conversely zona fasciculata and reticularis cells lack CYP11B2 and therefore cannot synthesise aldosterone. Specific cofactors are also required for the CYP enzymes. These are present either within the endoplasmic reticulum and depend on electron transfer from NADPH via the electron donor enzyme P450 oxidoreductase or are present in the mitochondria and require electrons donated from adrenodoxin/adrenodoxin reductase for normal activity (Figure 1.3).

Cortisol is produced at an average production rate of 9-11mg/m^2/day (approximately 10-30mg daily) but aldosterone is produced in much smaller quantities of approximately 100-150 micrograms daily [11, 68]. The adrenal androgens are

produced in the highest quantities in adults; DHEAS is the most abundant steroid in the adult human circulation [69].

Figure 1.3

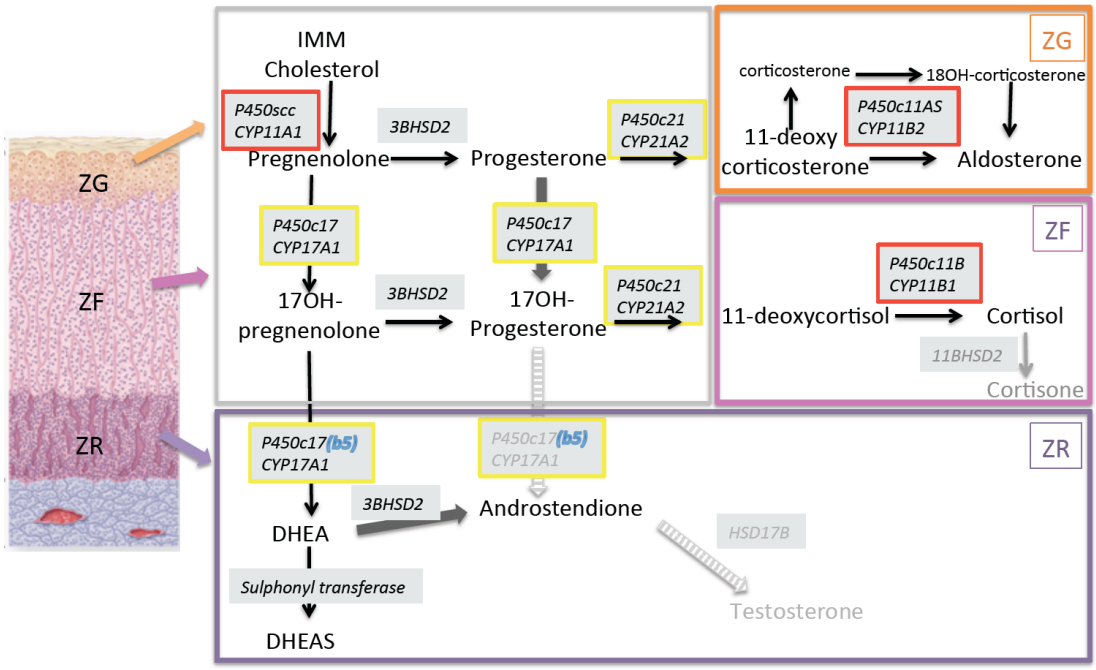

Figure 1.3. Pathway of adrenal steroid synthesis. Enzymes required for a steroidogenesis are indicated in the shaded grey boxes, those outlined in red are CYP type I enzymes requiring electron transfer via adrenodoxin reductase and adrenodoxin. Those outlined in yellow are microsomal CYP type II enzymes receiving electrons from P450 oxidoreductase. The 17-20 lyase reaction catalysed by CYP17A1 also requires cytochrome b5 (b5). Enzyme expression specific to each zone is indicated using the coloured boxes. Enzymes common to more than one zone are shown in the grey box. ZG, zona glomerulosa; ZF, zona fasciculata; ZR, zona reticularis; IMM, inner mitochondrial membrane.

1.5: Adrenal Insufficiency

Adrenal insufficiency can be classified as either primary or secondary adrenal failure. Secondary adrenal failure may be iatrogenic or can be caused by pituitary or hypothalamic disease. The latter is most commonly due to a space-occupying lesion

resulting in panhypopituitarism due to mass effect but may also occur following treatment with surgery or radiotherapy [70]. Iatrogenic adrenal insufficiency follows withdrawal of exogenous glucocorticoids but is usually transient. A number of rare genetic disorders may also lead to secondary adrenal insufficiency. These include defects in genes involved in pituitary and hypothalamic development including *HESX1, LHX3, LHX4, PROP1* and *SOX3* all of which can lead to combined pituitary hormone deficiency including ACTH deficiency [31]. Congenital isolated ACTH deficiency is due to mutations in Tpit or T-box 19 genes or POMC as discussed above. Pituitary destruction from infiltration, apoplexy (Sheehan's syndrome) or trauma can also lead to ACTH deficiency. Secondary adrenal failure leads to isolated glucocorticoid deficiency due to ACTH deficiency; the mineralocorticoid axis is unaffected and aldosterone production is normal.

The most common cause of primary adrenal failure in the developed world is autoimmune adrenalitis either as isolated adrenal failure or as part of an autoimmune polyendocrine syndrome (APS) [71]. APS type 1 also termed autoimmune polyendocrinopathy – candidiasis – ectodermal dystrophy (APECED) includes adrenal insufficiency, hypoparathyroidism and chronic mucocutaneous candidiasis. APS type 2 can also include chronic active hepatitis, type 1 diabetes mellitus, thyroid disease and malabsorption [71]. In the developing world tuberculous adrenalitis remains an important cause of primary adrenal failure; 5% of patients with active tuberculosis have adrenal involvement [72]. Destruction of the adrenal gland can also be due to other infectious agents for example fungi, HIV and associated CMV or adrenal haemorrhage (including Waterhouse-Friderichsen syndrome) or infiltration.

Table 1.1

Diagnosis	Clinical features in addition to AI	Steroid deficiency	Gene mutation
Congenital adrenal hyperplasia			
21 hydroxylase deficiency	46,XX DSD	GD +/-MD	*CYP21A2*
11β-hydroxylase deficiency	46,XX DSD & HTN	GD	*CYP11B1*
17α-hydroxylase deficiency	46,XY DSD, HTN & no puberty in either sex	GD, MD, SD	*CYP17A1*
3ß-HSD deficiency	46,XY DSD, postnatal virilisation in females	GD, MD	*HSD3B2*
P450 oxidoreducatase deficiency	46,XX DSD 46,XY DSD and skeletal anomalies	GD, MD, SD	*POR*
P450 SCC deficiency	46,XY DSD	GD+/-MD/SD	*CYP11A1*
Congenital lipoid adrenal hyperplasia (CLAH)	46,XY DSD	GD+/-MR/SD	*STAR*
Familial Glucocorticoid Deficiency			
FGD type 1	FGD 1: tall stature	GD	*MC2R*
FGD type 2	Isolated glucocorticoid	GD	*MRAP*
FGD type 3/Non-classical CLAH	deficiency with normal	GD	*STAR*
FGD type 4	aldosterone secretion	GD	*NNT*
Triple A syndrome	Alacrima, achalasia & neurological defects	GD	*AAAS*
Adrenal hypoplasia congenital			
X linked AHC	Hypogonadatrophic hypogonadism	GD, MD	*DAX 1*
Xp21 contiguous gene syndrome	Duchenne Muscular Dystrophy + GK def	GD, MD	*Xp21 deletion; DAX1, GK & DMD*
SF1 linked AHC	46,XY DSD	GD, MD+/-SD	*SF-1 (NRB5A1)*
Adrenoleucodystrophy/ Adrenomeyloneuropathy	CNS demyelination & neurological defecits	GD +/-MD	*ABCD1*
IMAGe syndrome	IUGR, metaphyseal dysplasia and genital anomalies	GD, MD	*CDKN1C*
Smith-Lemli Opitz syndrome	Growth failure, Craniofacial malformations developmental delay	GD, MD	*DHCR7*

Table 1.1. Differential diagnosis of genetic defects leading to primary adrenal insufficiency. DSD; Disorder of sexual differentiation, HTN; hypertension, GD; glucocorticoid deficiency, MD; mineralocorticoid deficiency, SD; sex hormone deficiency

The aetiologies of primary adrenal failure described above invariably lead to both glucocorticoid and mineralocorticoid deficiency. However there are a number of genetic defects that also lead to primary adrenal failure but these can present with either mineralocorticoid and glucocorticoid deficiency or isolated glucocorticoid deficiency (Table 1.1).

1.6: Familial Glucocorticoid Deficiency

Familial Glucocorticoid Deficiency (FGD) also known as isolated glucocorticoid deficiency or hereditary unresponsiveness to adrenocorticotrophin (ACTH) is a rare, genetically heterogeneous autosomal recessive disorder. It is characterised by resistance of the adrenal cortex to ACTH resulting in adrenal failure with isolated glucocorticoid deficiency. Mineralocorticoid production by the adrenal gland remains near normal.

1.6.1: Aetiology and molecular genetics of FGD

FGD is characterised by ACTH resistance due to defects in the early events of ACTH action leading to failure of cortisol synthesis. The resulting cortisol deficiency causes failure of the negative feedback loop to the pituitary and hypothalamus and hence grossly elevated ACTH levels. A number of autosomal recessive causes of FGD have been described and include FGD type 1 resulting from mutations in *MC2R* and FGD type 2 resulting from mutations in the melanocortin 2 receptor accessory protein (*MRAP*). A third sub-group of patients presenting with FGD have been shown to have mutations in the steroidogenic acute regulatory protein (*STAR*), and recently Meimaridou *et al.* have identified mutations in nicotinamide nucleotide transhydrogenase (NNT) as a fourth cause of FGD [73].

1.6.2: FGD Type 1

MC2R was first cloned in 1992 by Mountjoy *et al.* [74]. Subsequently researchers have been able to identify more than 30 point mutations in *MC2R* in patients with FGD [75, 76]. The majority of these mutations are missense mutations occurring as either homozygous or compound heterozygous mutations. Nonsense mutations are uncommon and are usually associated with a missense mutation on the other allele. Mutations in *MC2R* are distributed throughout the gene (see figure 1.4) and have been found in approximately 25% of patients with FGD.

Figure 1.4

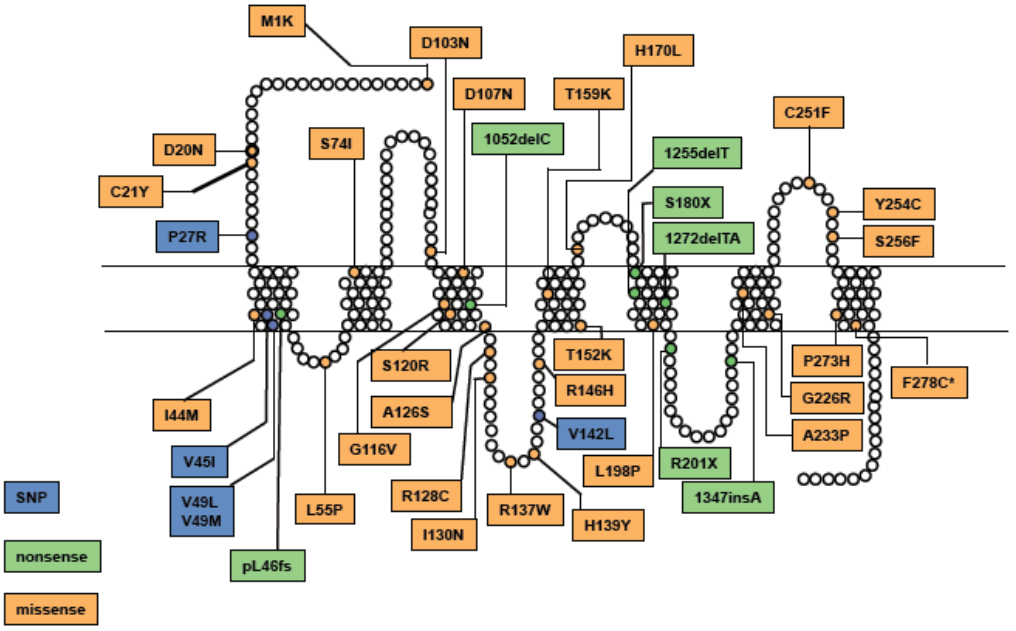

Figure 1.4 Schematic diagram showing the locations of all *MC2R* mutations that are known to be associated with FGD type 1. Those shown in orange are missense mutations, those in blue are probable benign polymorphisms and those in green are nonsense or frameshift mutations. Reprinted from [77] with permission.

The identification of homozygous mutations in affected individuals is highly suggestive of a causative role in the disease but does not provide conclusive proof. Functional analysis showing reduced function of mutant protein compared to wildtype is required for appropriate verification. However functional analysis of any MC2R mutation was problematic as it was difficult to achieve cell surface expression of the receptor in transfected cells [78]. This observation led to the hypothesis that a specific accessory factor, present in adrenal cell types is required to facilitate trafficking of MC2R to the cell surface.

1.6.3: FGD type 2

Metherell *et al.* carried out homozygosity mapping in 2 consanguineous families with FGD but without *MC2R* mutations. This identified a disease associated locus on chromosome 21q22.1. Further studies identified 2 different mutations in the 2 families in a candidate gene in this region which showed high adrenal expression. This gene was subsequently named the melanocortin 2 receptor accessory protein (*MRAP*) [79]. MRAP is a small single transmembrane domain protein. Functional analysis of MRAP revealed that it was essential for normal MC2R function [79]. MRAP forms a unique antiparallel homodimer, which directly interacts with the MC2R at the endoplasmic reticulum and is required for correct folding or trafficking of the receptor to the cell surface. Current evidence suggests that MRAP is also required at the plasma membrane for ACTH binding and signal transduction [80].

Since the discovery of MRAP it has been possible to prove using *in vitro* studies that mutations in *MC2R* are associated with loss of receptor function. The majority of

mutations lead to failure of the receptor to traffic to the cell surface, probably because the mutation leads to defective folding of the receptor at the time of its synthesis [81].

Ten *MRAP* mutations causing FGD have been reported (see figure 1.5), all these result in either an absent or severely truncated protein. Mutations in *MRAP* account for approximately 20% of cases of FGD [82].

Figure 1.5

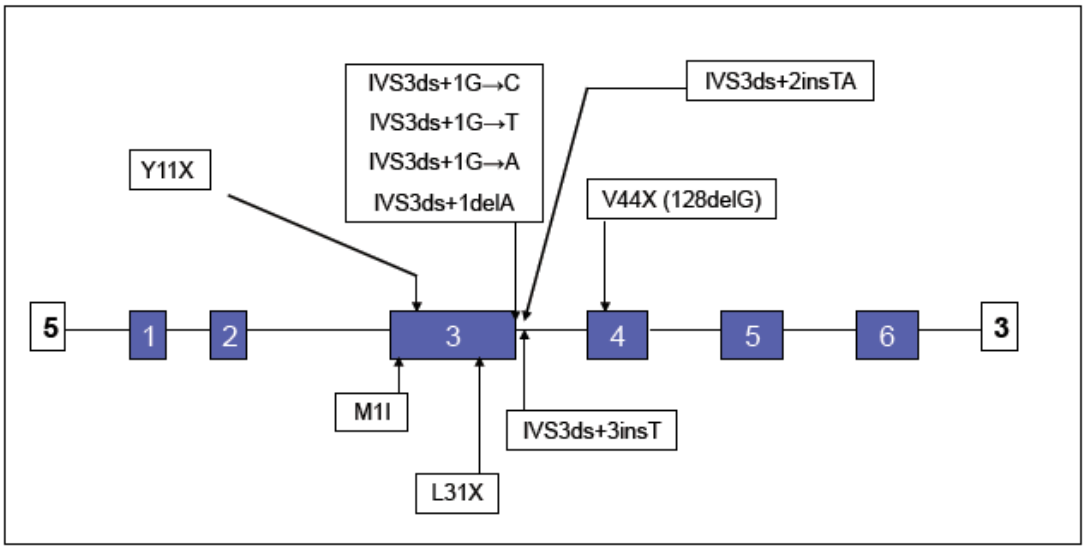

Figure 1.5 Schematic diagram of human MRAP showing the location of all known mutations

1.6.4: FGD type 3/ Non-classical Lipoid Congenital Adrenal Hyperplasia (LCAH)

StAR is a mitochondrial phosphoprotein that mediates the acute response to steroidogenic stimuli by increasing cholesterol transport from the outer to the inner mitochondrial membrane. Defects in StAR usually result in Lipoid Congenital Adrenal Hyperplasia, a severe form of congenital adrenal hyperplasia. However a small percentage of patients presenting with classical FGD were found to have mutations in *STAR* [83]. Review of history, examination, and biochemical data in the

individuals diagnosed with FGD confirmed they had isolated glucocorticoid deficiency with normal or near normal renin and aldosterone levels. However some patients did have mild reproductive anomalies including hypospadias and cryptorchidism, which had not previously been connected to their adrenal failure. The mutations found in *STAR* in FGD appear to lead to only partial impairment of the cholesterol uptake function of this protein. Thus classical LCAH is caused by mutations that completely abolish any functioning StAR while mutations that allow the protein to retain some function are associated with a non-classical LCAH or FGD [84].

Recently a case report described clinically isolated adrenal insufficiency in two brothers with a partially inactivating mutation in P450 Side Chain Cleavage Enyzme (CYP11A1). The younger brother had evidence of glucocorticoid deficiency but not mineralocorticoid deficiency as his electrolytes and plasma renin levels were normal [85]. This report together with the paper describing mutations in the *STAR* gene discussed above illustrates the need for genetic screening following careful clinical phenotyping. Determining the correct genetic diagnosis can be important for genetic counselling and providing families with the most appropriate screening and follow-up care.

1.6.5: FGD type 4; Defects in antioxidant pathways

Targeted exome sequencing in additional families identified mutations in nicotinamide nucleotide transhydrogenase (NNT) as another cause of isolated glucocorticoid deficiency [73]. These mutations were spread throughout the gene and included abolition of the initiating methionine, splice mutations and many mis- and

nonsense mutations. NNT is a highly conserved gene that encodes an integral protein of the inner mitochondrial membrane. Under most physiological conditions, this enzyme uses energy from the mitochondrial proton gradient to produce high concentrations of NADPH. Detoxification in mitochondria of reactive oxygen species (ROS) by glutathione peroxidases depends on this NADPH for regeneration of reduced glutathione (GSH) from oxidized glutathione (GSSG) to maintain a high GSH/GSSG ratio. The finding of NNT mutations in FGD suggests that, at least in humans, NNT is of primary importance for ROS detoxification in adrenocortical cells, highlighting the susceptibility of the adrenal cortex to this type of pathological damage [73].

1.6.6: Clinical features of FGD

Patients with FGD usually present during the neonatal period or early childhood with symptoms related to cortisol deficiency and ACTH excess. The most common presenting features are those secondary to hypoglycaemia including jitteriness, tremors, hypotonia, lethargy, apnoea, poor feeding and hypoglycaemic seizures. In a small number of patients undiagnosed hypoglycaemia in infancy may have been sufficiently severe to cause serious long-term neurological sequelae. Neonates may also present with jaundice, failure to thrive, collapse and very rarely transient neonatal hepatitis [86].

Hyperpigmentation will usually develop by a few months of age due to the over stimulation of the melanocortin 1 receptor (MC1R) by high circulating ACTH levels, although there are exceptions to this [87]. Older children may present with a variety of features including increased pigmentation, recurrent infections, hypoglycaemia,

lethargy and shock. As this is an autosomal recessive disorder there is frequently a history of consanguinity and there may also be a history of unexplained neonatal or childhood deaths in FGD families.

A feature that has been observed in patients with FGD type 1 is tall stature [88]. The underlying mechanism is not clear but hydrocortisone replacement appears to stop this excessive growth [88]. This suggests that either the high ACTH levels or the cortisol deficiency itself may have a causative role. It has been proposed that ACTH at high concentrations may activate melanocortin receptors in bone and in the growth plate and stimulate growth [89]. Alternatively it has been reported that cortisol inhibits the synthesis of IGF binding protein 5 (IGFBP5) in the osteoblast suggesting that perhaps cortisol deficiency could result in a lack of inhibition and hence increased growth [90]. Tall stature is not a recognised feature of FGD type 2, which tends to present at an earlier age than FGD 1, meaning patients are treated earlier and do not have chronic exposure to high ACTH or low cortisol levels [91].

ACTH also stimulates adrenal androgen synthesis from the zona reticularis and is required for normal adrenarche in children. Children with FGD can have an absent adrenarche with delayed or absent pubic hair development [92]. However normal pubertal development controlled by the hypothalamic-pituitary-gonadal axis is unaffected and fertility is normal.

1.6.7: Investigation and diagnosis of FGD

The characteristic biochemical features of FGD are low or undetectable cortisol paired with high ACTH levels and normal electrolytes, renin and aldosterone levels. ACTH levels are often extremely high, often greater than 1000pg/ml (normal range <

80pg/ml). A standard ACTH stimulation test will confirm an impaired cortisol response (<550nmol/l) and verify adrenal insufficiency.

The most important feature to distinguish FGD from other causes of adrenal insufficiency is the absence of mineralocorticoid deficiency. However FGD patients frequently present with minor abnormalities of the renin-aldosterone axis for various reasons. Firstly, at presentation, children with FGD are usually stressed and may be hypovolaemic, or pyrexial. Alternatively they may be relatively water overloaded as a result of intravenous fluid replacement and because of reduced free water clearance associated with glucocorticoid deficiency. Usually, after introduction of appropriate hydrocortisone replacement any minor derangements in renin and aldosterone levels normalise and fludrocortisone replacement is not required.

A conclusive diagnosis of FGD can be confirmed by identifying a mutation in *MC2R, MRAP, STAR* or *NNT* in these patients. However approximately 40% of patients have no mutation in any of the associated genes.

1.6.8: Management of FGD

The treatment is with physiological glucocorticoid replacement. This is usually given in the form of oral hydrocortisone 8-10 mg/m^2/day in children and 20mg/day in adults. The total daily dose is given in 3-4 divided doses throughout the day. Prednisolone and rarely dexamethasone can also be used in certain circumstances. In individuals with adequate replacement therapy ACTH levels often remain elevated and therefore cutaneous pigmentation can persist. Attempting to suppress the ACTH levels must be

avoided as it will lead to over treatment, potentially iatrogenic Cushing's syndrome and poor growth in children.

Hydrocortisone dosing must be increased during times of stress to 2-3 times the maintenance dose. It is important to ensure the patient and their family have adequate education and understand when and how to increase hydrocortisone doses and emergency management with intramuscular hydrocortisone or hydrocortisone suppositories.

1.7: Aims of this research

This research aims to investigate the genetic aetiology and pathogenetic mechanism of disease in patients with late-onset FGD. As described above FGD patients usually present with adrenal failure in infancy or early childhood, however there are a number of families in which affected individuals either have "mild" disease and present later in life or develop isolated glucocorticoid deficiency following a period of normal adrenal function.

This project aims to study two such groups of patients; firstly two families of Turkish ethnicity who presented with late onset disease and secondly eight patients from the Irish travelling community, a genetically isolated population with high levels of consanguinity.

Patients will first be screened for mutations in *MC2R, MRAP, STAR* and *NNT*. If sequencing is normal novel genetic loci for the disease will be sought by SNP genotyping. Once a significant locus is identified this can then be investigated for

likely disease causing genes. Potential genes can be studied *in silico* and *in vitro* and subsequently sequenced in affected patients to identify disease causing mutations.

These mutations will be functionally characterised *in vitro* to determine if the disease severity in these patients with FGD reflects the functional significance of the underlying mutation.

Chapter 2: Materials and Methods

2.1 DNA extraction

Genomic DNA was extracted from peripheral blood leucocytes following patient's informed consent. Blood was collected in sodium EDTA tubes and DNA was extracted using the Illustra Nucleon Genomic DNA extraction kit (GE Healthcare), according to the manufacturer's instructions. Briefly, this involves cell lysis using reagent A (10mM Tris-HCl, 0.32M Sucrose, 5 mM $MgCl_2$, 1% (v/v) Triton x-100, pH 8.0) and nucleic lysis with reagent B (detergent). Four times the volume of reagent A was added to the blood sample using aseptic techniques, mixed on a rotary wheel for 4 minutes at room temperature and centrifuged at 1300g for 5 minutes. The supernatant was discarded and the pellet vortexed with 2ml reagent B, then transferred to a clean 15ml polypropylene centrifuge tube. Deproteinisation was carried out by adding 500µl sodium perchlorate solution and mixing by hand. 2ml of chloroform was subsequently added and the sample again mixed by hand to extract the DNA. 300µl Nucleon resin was then added and the sample centrifuged at 1300g for 3 minutes. The resin separates the chloroform and protein (lower phase) from the aqueous solution containing the DNA in the upper phase. This upper phase was removed to a clean tube with a minimum volume of 7.5ml. 2 volumes of cold absolute (100%) ethanol was added to precipitate the DNA. This can be removed by 'fishing' using a Pasteur pipette whose end has been sealed and shaped into a U by heating in a flame. The DNA was washed in 70% ethanol, allowed to dry and then dissolved in water.

2.2 PCR and sequencing

2.2.1 Oligonucleotide design

After establishing the gene sequence of interest using ENSEMBL, primer pairs were designed by following the guidelines below:

- Primers should ideally be 17-25 bp in length
- Sequences should be non-repetitive and non-palindromic
- G/C content should be 40-60%
- Forward and reverse primers should anneal at approximately the same temperature
- T_m should be between 58-68^{o}C and was calculated approximately as
    - Melting temperature (^{o}C) = 4(number of C/G bases) + 2(number of A/T bases)
- Primers should not form secondary structures

2.2.2 PCR

Each exon of genes of interest including intronic boundaries was amplified by PCR using specific primers (for these and all subsequent primer sequences see Table 2.2). The basic principle involves denaturing double stranded DNA at high temperatures, followed by annealing of sequence specific oligonucleotide primers typically at temperatures in the range of 50-60^{o}C before synthesis of complementary DNA strands from 5' to 3' using a thermostable DNA polymerase. Repeated cycling allows exponential amplification of a specific portion of DNA.

The reaction mixture contained 100ng of DNA template, 1 × PCR buffer (Sigma, Poole, UK) (100nM Tris-HCl, pH 8.3, 500mM KCl, 15mM $MgCl_2$, 0.01% gelatin) 200µM each dNTP, 200nM each primer and 1U *Thermus aquaticus* (*Taq* DNA

polymerase (Sigma-Aldrich) with total volume typically 25µl. Cycling conditions were 95^{o}C for 5 min (one cycle); 95^{o}C for 30 sec, 55^{o}C for 30 sec, and 72^{o}C for 30 sec (30 cycles); and 72^{o}C for 5 min. Alternatively the cycling conditions were based on touchdown PCR, where the annealing temperature starts high and decreases by a single degree with every cycle, until a suitable annealing temperature is reached. In this way non-specific binding of primers can be reduced. PCR products were separated and visualized using agarose gel electrophoresis. This technique applies an electric field across an agarose gel which induces the nucleic acids loaded into it to migrate towards the anode due to the net negative charge of the sugar-phosphate backbone of the nucleic acid chain. Different sized molecules move through the gel at different speeds with longer molecules moving more slowly as they experience more resistance. The PCR products were visualized on 1-2% agarose gel made in 1x TAE buffer (40mM Tris-acetate, 2mM disodium ethylenediaminetetraacetate (Na_2EDTA), pH 8.3; National Diagnostics, UK) alongside DNA markers (GeneRuler^{TM} DNA Ladder Mix, 0.5 mg DNA/ml, Fermentas) with ethidium bromide (0.2 µg/ml) or GelRed (Biotium) staining. Usually 5µl of each reaction was mixed with 1 µl of loading dye solution (40% w/v sucrose, 0.25% w/v bromophenol blue or Orange G, 1mmol EDTA ph 8.0, prior to loading into the wells. Electrophoresis was carried out at approximately 100-120 V for 20-30 minutes or until clear separation of products was obtained. Ethidium bromide/GelRed intercalated into DNA will fluoresce under UV light at 300nm allowing the DNA and therefore the PCR product to be visualized. An Uvitec transluminator was used to visualize the bands and capture an image of the gel. The approximate size of the PCR product can then be determined by comparison with the DNA markers on the agarose gel.

2.2.3 Sequencing

The PCR products were sequenced using the ABI Prism Big Dye sequencing kit and an ABI 3730 automated DNA sequencer (Applied Biosystems, Foster City, CA) by the Genome Centre in Bart's and the London, QMUL. This is based on the Sanger dideoxy-mediated chain termination method [93]. This method requires a DNA template, a DNA primer, DNA polymerase, conventional deoxynucleotide-triphosphates (dNTPs) and modified nucleotides that terminate DNA strand elongation (ddNTPs). In this method the double stranded DNA fragment is denatured into single DNA strands and a primer complementary to the known DNA sequence binds to the single stranded DNA template. DNA polymerase then binds to the primer and synthesizes a new strand of DNA incorporating free nucleotides that are complementary to the target fragment of DNA. The fluorescently labeled chain terminating nucleotides are modified to lack the 3'OH group required for the formation of the phosphodiester bond between two nucleotides thus terminating each DNA strand at the point of inclusion. This process is repeated many times generating many fragments of different lengths that all terminate in fluorescently labeled bases that correspond to A, T, G and C. The reaction is then transferred into thin glass capillaries where an electrical charge moves the negatively charged particles through a gel matrix. Similarly to electrophoresis described above the DNA fragments are then separated according to size and a laser used to excite the chain terminating fluorescent base, which is recorded as a coloured peak or band by the automated sequencer.

2.2.4 Sequence Analysis

Analysis of sequence chromatograms was carried out using BioEdit URL: http://www.mbio.ncsu.edu/BioEdit/ (BioEdit is a biological sequence alignment editor and analysis program for Windows 95/98 NT. Nucleic Acids Symposium Series 41, 95-98). BioEdit is a freeware program that allows a DNA sequence to be compared to a reference sequence [94]. This allows the user to readily identify differences between 2 or more sequences by eye allowing the detection of potential mutations in the chromatograms generated from patient samples.

2.3 Homozygosity mapping

2.3.1 Genome wide mapping Array

For the whole-genome scan, the GeneChip mapping 10 K array *Xba*131 (Affymetrix) was used in accordance with the manufacturer's guidelines. These are described in detail in the GeneChip Mapping 10K 2.0 Assay manual (https://www.affymetrix.com/user/login.jsp?toURL=/support/file_download.affx?onloadforward=/support/downloads/manuals/10k2_manual.pdf). This version of the Mapping 10K array comprises a total of 11,555 single nucleotide polymorphisms (SNPs) with a mean intermarker distance of 210 kb, equivalent to 0.32 cM.

High quality, double stranded, uncontaminated genomic DNA that is free from PCR inhibitors is required. The assay overview is described in Figure 2.1 and briefly outlined below. All reagents used in this assay are from New England Biolab (NEB) unless otherwise stated.

Figure 2.1

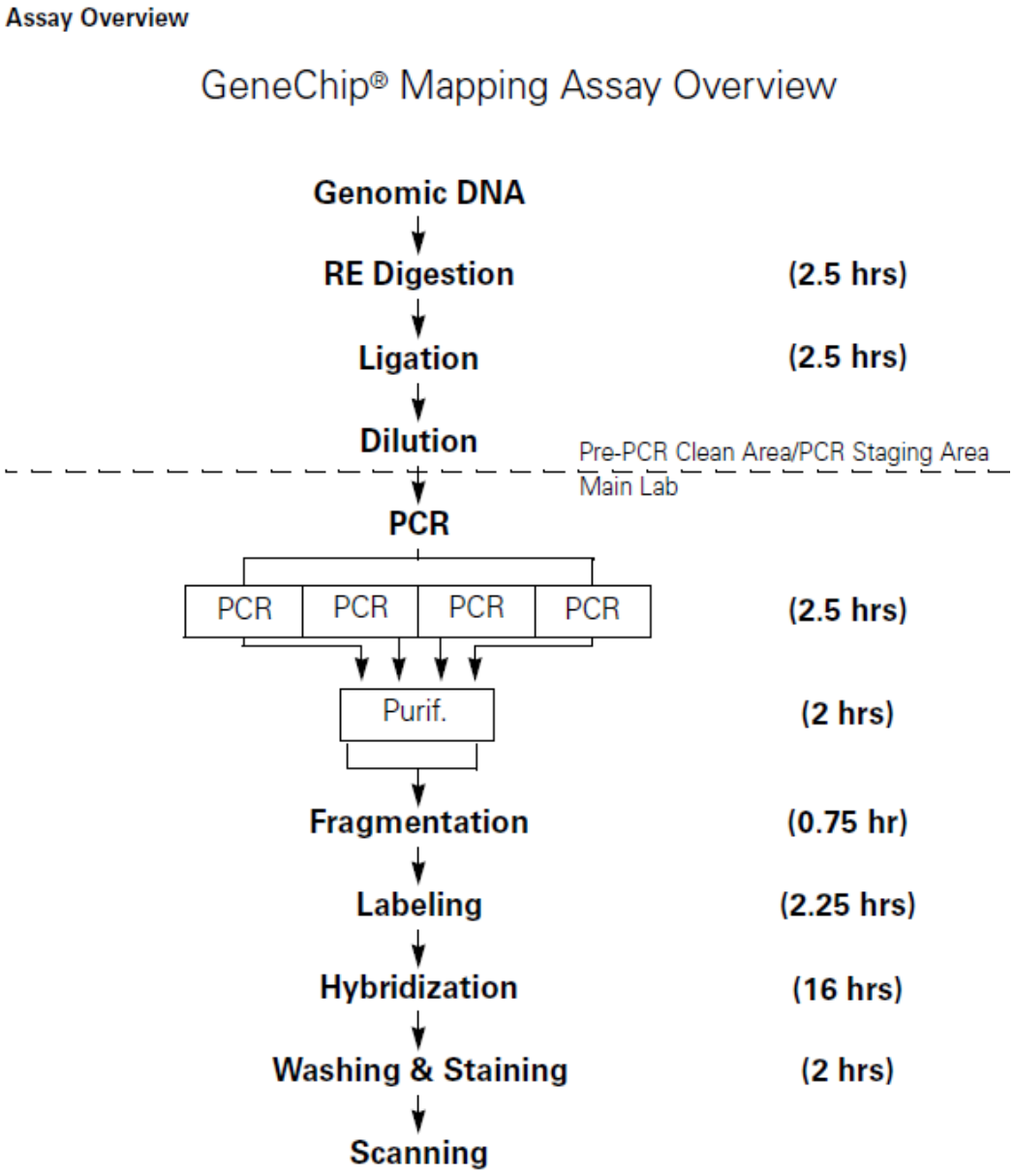

Figure 2.1: Reprinted from Affymetrix Genechip Mapping 10K 2.0 Assay Manual.

250ng of genomic DNA (50ng/µl) was digested using *Xba*1 restriction enzyme. The digested DNA fragments were ligated to adapters (Adaptor Xba) using T4 DNA ligase. Following thermal cycling the ligated DNA was diluted using molecular biology grade water. The diluted ligated DNA was then amplified using PCR. The

PCR master mix contains PCR primer Xba, which specifically targets the adapters on the ligated DNA fragments and PCR conditions are optimized to preferentially amplify fragments in the 250-1000 base-pair size range.

The PCR reaction was prepared in a pre-PCR Clean Room but once the reaction was complete the PCR product should only be handled in a "post PCR" main lab to prevent contamination of future experiments. The PCR products were eluted and concentrated before fragmentation using DNase 1. The fragmented DNA was denatured and end-labeled using DNA GeneChip DNA labeling Reagent. The sample was hybridized onto a GeneChip Mapping probe array. The steps following hybridization were carried out by colleagues in the Genome Centre. Briefly, hybridized arrays were processed with an Affymetrix Fluidics Station 450 and fluorescence signals were detected using the Affeymetrix GeneChip Scanner 3000. Signal intensity data was analysed by the GeneChip DNA analysis software based on a model algorithm to generate SNP calls [95].

SNP genotypes then scanned for regions of homozygosity using IBDFinder from the Centre for Autozygosity (http://autozygosity.org). This tool allows the identification of regions of homozygosity that are linked with or associated with a particular phenotype. IBDfinder does not calculate formal linkage probabilities but generates a graphical display of a numerical score that changes as the genotype data are scanned [96].

2.4 Targeted Exome sequencing

2.4.1 Sequence capture array and sequencing

A custom sequence capture array targeting the exons, 50bp up- and downstream, plus 1Kb upstream of the transcription start site for each REFSEQ gene within the areas of homozygosity (coordinates 4:96.3-100.3, 8:36.8-51.9 and 8:62.1-64.5) was designed and manufactured by Roche NimbleGen (Madison, WI) using a 385K custom sequence array. DNA (5μg) from one affected individual was subjected to target enrichment and sequencing. High quality DNA was required with a concentration between 50 -100ng/μl and OD_{260}/OD_{280} ratio > 1.8, which was measured using a NanoDrop ND-1000 spectrophotometer at λ=260nm/280nm. The enrichment and sequencing was carried out by collaborators in Germany, briefly, the sequencing library was prepared using standard techniques including end repair, A-tailing, paired end adaptor ligation and amplification by PCR.

A 472-fold enrichment of the targeted regions was achieved and the resultant library was subjected to massively parallel sequencing performed on a single lane of the Illumina GAII analyzer. Single Nucleotide Polymorphisms, with a threshold coverage of at least 10 reads on the respective nucleotide, were called with the MAQ alignment and downstream analysis tools [97]. Variants were checked against the Ensembl SNP database, release 54. Functional characteristics of the SNPs were checked with a pipeline based on an in-house variant database maintained by Dr. Hogler Theile. Novel SNPs that were non-synonymous coding variants, splice site mutations or coding insertions or deletions were prioritized for further analysis.

2.4.2 Genotyping of 200 control alleles

PCR products (PCR method as above) for *MCM4* exon 2 were digested by *Alu*1 restriction digest. *Alu*1 cleaves the PCR product from a wild-type sequence once but does not cut the mutant sequence. 10µl of a PCR product was incubated with 10 U of *Alu*1 (1µl) (NE Biolabs), 3µl N4 10x Buffer, 0.3µl bovine serum albumin and 17.5µl double distilled (dd) water in a 30µl reaction at 37°C for 2 hours. Digestion products were resolved on a 2% agarose gel. Wild-type samples gave rise to 2 bands following digestion, PCR products from DNA with c.71-1insG were not digested and remained as 1 band, heterozygotes resulted in 3 bands.

2.5 RNA extraction and cDNA sequencing

2.5.1 RNA extraction from whole blood

Total RNA was isolated and purified from patient and control leucocytes using the PAXgene Blood RNA system (Qiagen). 2.5 ml blood were collected into PAXgene Blood RNA tubes which allows storage, transport and stabilization of intracellular RNA in a closed tube.

PAXgene Blood RNA Tubes contain a proprietary reagent composition based on a patented RNA stabilization technology (US Patents 6,602,718 and 6,617,170), this reagent composition protects RNA molecules from degradation by Rnases. This additive stabilizes the *in vivo* gene transcription profile by reducing *in vitro* RNA degradation and minimizing gene induction. A major challenge in analysing RNA is the instability of intracellular RNA, which rapidly degrades within hours after blood collection. Furthermore, certain RNA transcripts, through the process of gene induction, increase *in vitro* after blood collection. Both *in vitro* RNA degradation and gene induction can lead to an under- or overestimation of *in vivo* relative gene

transcript number. After blood is introduced into the tube, the intracellular RNA profile remains stable for 3 days at 18^{o}C to 25^{o}C, 5 days at 2^{o}C to 8^{o}C, or for a minimum of 50 months at -20^{o}C or -70^{o}C/-80^{o}C (Paxgene protocol).

After storage for 2-3 days at 4^{o}C, the samples were processed as per the PAXgene Blood RNA Kit handbook to extract RNA. Briefly the blood sample was incubated in the PAXgene Blood RNA tube for a minimum of 2 hours at room temperature in order to achieve complete lysis of blood cells. The tube was then centrifuged for 10 minutes and the resuspended pellet was incubated in optimized buffers (PAXgene) together with proteinase K to bring about protein digestion. An additional centrifugation through the PAXgene Shredder spin column was carried out to homogenize the cell lysate and remove residual cell debris, and the supernatant of the flow-through fraction was transferred to a fresh microcentrifuge tube. Ethanol was added to adjust binding conditions, and the lysate was applied to a PAXgene RNA spin column. During a brief centrifugation, RNA was selectively bound to the PAXgene silica membrane but contaminants passed through. Remaining contaminants were removed in several wash steps. Between the first and second wash steps, the membrane was treated with DNase I to remove trace amounts of bound DNA. After the wash steps, RNA was eluted in elution buffer and heat-denatured. RNA yields from 2.5ml healthy human blood are >3µg for over 95% of samples tested.

2.5.2 cDNA synthesis and sequencing

For cDNA production via reverse transcription, 2µl of 2mg/ml RNA in 15µl RNase free water was incubated with 2µl random primers (Promega, Southampton, UK) at 70°C for 5 minutes, then incubated for 2 minutes on ice. 1µl of reverse transcriptase

enzyme was added, with 5µl 5x reverse transcriptase buffer (50mM Tris-HCl (pH8.3), 75mM KCl, 3mM $MgCl_2$ and 10mM DTT), 1.25µl dNTPs (deoxynucleotides; consisting of 10mM dATP, 10mM dCTP, 10mM dGTP, 10mM dTTP) and 0.75µl RNase inhibitor (RNasin, Promega, Southampton, UK), and the entire mixture was incubated at 37ºC for 60 minutes. The resulting cDNA was used as a template for PCR amplification and sequencing of *MCM4* exons 2-4 (for primers see table 2.2) as described above.

2.6 Leucocyte separation

Fresh whole blood was collected into sample tubes containing EDTA. Mononuclear cells were extracted using a gradient density centrifugation method with Histopaque 1077 as per the manufacturer's protocol (Sigma, Poole, UK). Histopaque solution 1077 has a density of 1.077. When blood is layered onto this solution and subjected to centrifugal forces, mononuclear cells are held at the plasma – histopaque interphase while erythrocytes gravitate to the bottom (figure 2.2). Briefly 6 ml histopaque-1077 were added to a 15ml centrifuge tube and 6 ml blood carefully layered onto it. This was centrifuged at 700g for 30 minutes at room temperature (18-26ºC). The plasma was carefully aspirated and discarded to within 0.5cm of the mononuclear layer. The mononuclear layer was then removed into a clean tube. This was washed with 10ml isotonic phosphate buffered saline and centrifuged for 10 minutes at 200g. The supernatant was aspirated and discarded and the cells resuspended and washed again as above.

Figure 2.2

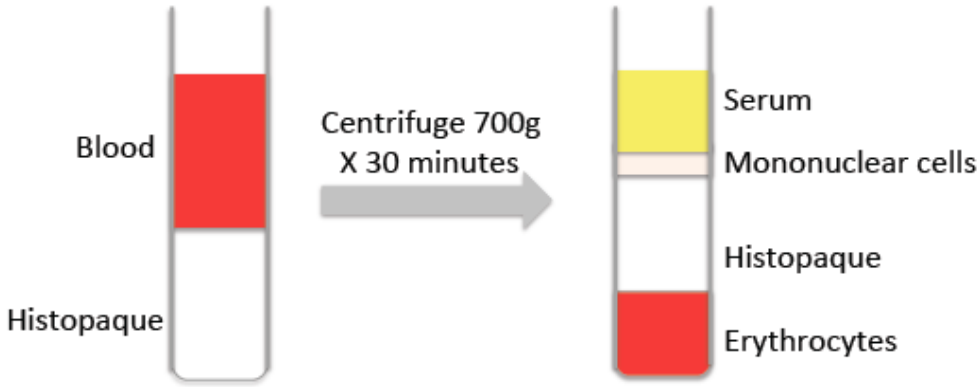

Cells were lysed by addition of RIPA buffer (50mM Tris-HCl, pH 8.0, with 150mM sodium chloride, 1% Igepal CA-630 (NP-40), 0.5% sodium deoxycholate and 0.1% sodium dodecyl sulphate), supplemented with Mini, EDTA-free Protease Inhibitor Cocktail Tablets (Roche) on ice for 30 minutes. Samples were then centrifuged at 17g for 12 minutes at 4°C and the supernatant added to an equal volume of 1 x Laemmli loading buffer [98] (Sigma, Poole, UK).

2.7 Cloning MCM4 constructs

Briefly, FLAG-MCM4 constructs were prepared using human *MCM4* cDNA (Source Bioscience), which was cloned into a p3xFLAG-CMV10 expression vector (Sigma Aldrich) after PCR amplification. *MCM4* cDNAs from the 2nd and 3rd in-frame ATGs were amplified using specific primers (for primer sequence see table 2.2) and cloned into the same p3xFLAG-CMV 10 expression vector (Sigma Aldrich). Alternatively, PCR amplification generated MCM4 with a C-terminal HA tag, which was then cloned into a pcDNA 3.1 expression vector (Invitrogen). The initiating methionine

was mutated using site directed mutagenesis. The sequence of all constructs was verified by DNA sequencing.

2.7.1 Purification of plasmid DNA

MCM4 cDNA in a Bluescript vector was purchased from Source Bioscience. Clones were streaked onto LB Agar containing 100μg/ml ampicillin. p3xFLAG-CMV-14 expression vector clones were also purchased and clones restreaked onto LB Agar plates with 100μg/ml ampicillin. Plates were left overnight at 37°C to obtain single colonies. To purify plasmid DNA a single bacterial colony was inoculated in 5ml LB broth containing ampicillin overnight at 37°C shaking at 220rpm. After 14 hours the bacterial cells were centrifuged at 5400x*g* for 10 minutes at 4°C, and the supernatant was discarded. The DNA was purified from the bacterial pellet using a modification of the alkaline lysis procedure [99]. Briefly, the cells were resuspended in buffer P1 (50mM Tris-HCl ph 8.0, 10mM EDTA, 100μg /ml RnaseA) and lysed in an alkaline buffer (200mM NaOH with 1% SDS) before neutralisation with an acidic buffer (4.2 M Gu-HCl, 0.9 M potassium acetate, pH 4.8). The lysate was cleared via centrifugation before transfer to a silica DNA-binding column from the QIAprep Miniprep kit (Qiagen, Crawley, UK). Endonucleases present were removed by washing and salt was also subsequently removed by a brief wash step. DNA was eluted in distilled water and the concentration measured using a Nanodrop ND-1000 spectrophotometer at λ=260nm.

2.7.2 PCR of MCM4

MCM4 cDNAs from the initiating methionine to the terminal stop codon (amino acids 1-863), from the 2nd initiating in frame methionine (amino acid 51-863), 3rd initiating

in frame methionine (amino acid 75-863) or 4th initiating in frame methionine (amino acid 194-863) were amplified individually using specific primers incorporating *Eco*R1 and *Bam*H1 restriction sites at the 5' and 3' ends of the cDNAs respectively (see table 2.2 for primers). PCR was performed as described above and the products were visualised by agarose gel electrophoresis on a 1% gel.

Additionally an MCM4 insert with a C-terminal HA tag was synthesised using PCR (for primers see table 2.2) to introduce an *Eco*R1 and *Bam*H1 restriction site for cloning as above.

2.7.3 Gel extraction

The PCR bands were cut out of the gel and purified using the Qiagen QIAquick Gel extraction kit (Qiagen, Crawley, UK). Briefly, the excised bands were incubated in a solubilisation buffer at 50°C until the agarose had melted, before the resolubilised DNA was applied to a silica DNA-binding membrane. The membrane was washed once in solubilisation buffer and once in ethanol-containing buffer to remove salts. DNA was eluted in water before 1µl of sample was re-run on 1% agarose gel to confirm efficient purification.

2.7.4 Restriction enzyme digestion of purified plasmid DNA

10µl of PCR product was incubated with 10U of both *Bam*H1 (1µl) and *Eco*R1 (1µl) (NE Biolabs), 3µl N2 10x Buffer, 1x (0.3µl) bovine serum albumin and 14.7µl ddH_2O in a 30µl reaction at 37°C for 1 hour. Flag empty vector containing *Eco*R1 and *Bam*H1 restriction sites was also digested; 500ng Flag vector (1.2µl) was incubated with 10U of both *Bam*H1 (1µl) and *Eco*R1 (1µl) (NE Biolabs), 3µl N2 10x Buffer, 1x

(0.3µl) bovine serum albumin and 23.5ul ddH_2O in a 30µl reaction at 37°C for 1 hour before being treated with 2µl alkaline phosphatase for 30 minutes at 37°C, to help prevent re-annealing of the vector. Both samples were run on a 1% agarose gel, visualised using GelRed and gel extracted as above. Purified insert (MCM4 cDNA) was then ligated into the digested Flag vector.

2.7.5 Ligation into p3xFLAG-CMV-14 expression vector

4µl purified MCM4 PCR product was incubated with 2µl p3xFLAG-CMV-14 expression vector (Sigma Aldrich) and 1µl T4 DNA ligase in ligase buffer (300mM Tris-HCl (pH 7.8), 100mM $MgCl_2$, 100mM DTT, 10mM ATP; Promega, Southampton, UK) made up to 10µl total with ddH_2O overnight at 16°C before transformation into competent JM109 *E.coli*.

2.7.6 Ligation into pGEMT-Easy

If direct cloning was unsuccessful the insert was cloned into a pGEMT-Easy vector (Promega, Southampton, UK) before subcloning into p3xFLAG-CMV-14 expression vector. 5µl purified PCR product was incubated with 1µl pGEMT-Easy vector and 1µl T4 DNA ligase in ligase buffer (300mM Tris-HCl (pH 7.8), 100mM $MgCl_2$, 100mM DTT, 10mM ATP; Promega, Southampton, UK) made up to 10µl total overnight at 4°C before transformation into competent JM109 *E.coli*. The DNA was purified, then digested, gel extracted and ligated into the p3xFLAG-CMV-14 expression vector.

2.7.7 Transformation of DNA into competent bacteria

E.coli strain JM109 highly competent cells (>10^8 cfu/μl) (Promega, Southampton, UK) were thawed on ice and mixed gently after thawing. 25μl of cells were transferred to a pre-chilled 1.5ml tube and 5μl of plasmid DNA was added to the cells. The cell-DNA mixture was incubated on ice for 10 minutes. After incubation the cells were heat-shocked at exactly 42°C for 45 seconds before being returned to ice for 2 minutes. 900μl of LB media was added to the cells and then the cells were incubated at 37°C with shaking (230-250rpm) for 45 minutes. The cells were then centrifuged at 4000 g for 4 minutes. The cells were resuspended in 100μl of LB media and spread onto LB agar plates containing 100μg/ml ampicillin overnight at 37°C. For blue white selection of pGEMT-Easy containing clones, the LB agar was supplemented with 100μg/ml IPTG (Promega, Southampton, UK) and 50μg/ml X-Gal (Promega, Southampton, UK). Correct insertion of the PCR product disrupts the *lacZ* operon and stops the bacteria synthesising the blue coloured substrate. Therefore only white colonies were picked for inoculation.

Plasmid DNA was purified as above (section 2.7.1) and 1μg digested using *Bam*H1 and *Eco*R1. The resulting fragments were run on 1% agarose gel and visualised using GelRed to confirm an insert was released. Colonies that released the correct size of insert were then sequenced to confirm the insert was both the correct sequence and in-frame.

2.8 Site directed mutagenesis

2.8.1 Abolition of initiating methionine of MCM4 with C-terminal HA tag in pcDNA 3.1 expression vector

MCM4 with a C-terminal HA tag in a pcDNA 3.1 expression vector was synthesised as described above. The initiating methionine was then abolished using site directed mutagenesis using the QuikChange XL Site-Directed Mutagenesis Kit according to the manufacturer's instructions (Stratagene) using primers "SDM MCM4" table 2.2.

2.9 Cell culture

The human kidney cell line HEK293 and the human cancer adrenal cell line H295R were purchased from the European Collection of Cell Cultures (ECACC) at the Health Protection Agency (HPA; Salisbury). HEK293T cells were maintained in Dulbecco's Minimum Eagle Medium (DMEM) with 10% heat inactivated foetal calf serum (FCS; Invitrogen, Paisley, UK) and 50U/ml penicillin and 50μg/ml streptomycin (Pen/Strep; Invitrogen, Paisley, UK;). H295R cells were maintained in DMEM/F12 (Sigma, Poole, UK), (1:1) supplemented with 2% NU serum, ITS and penicillin/streptomycin. Cells were kept in a constant humidified atmosphere of 5% CO_2 at 37ºC.

Cells were harvested as follows: after growing in a $75cm^3$ (T75) cell culture flask to 80-90% confluency, cells were washed twice with 10ml phosphate buffered saline (PBS). Cells were incubated with 3ml Trypsin/Ethylenediaminetetraacetic acid (EDTA; Invitrogen, Paisley, UK) until detachment from the flask had occurred.

Trypsin/EDTA was neutralised with 7ml media and the cells were split into additional flasks or collected and spun gently at 100 g for 5 minutes until a pellet had formed.

2.9.1 Transfections

Cells were seeded either in 8 well chamber slides (Nunc, VWR, Leicester, UK), 12 well plates, 6 well plates or 25cm^3 (T25) cell culture flasks (VWR, Leicester, UK) until 60% confluent. Cells were transfected using the Lipofectamine and Plus reagent system (Invitrogen, Paisley, UK) as per Table 2.1 and according to the manufacturer's instructions.

Table 2.1

	Optimem	Plus	DNA/RNA	Optimem	Lipofectamine
8 well slide	12.5	1	100ng	100	1
12 well plate	50	2	500ng	200	2
6 well plate	100	4	1µg	400	4
T25 flask	250	10	2µg	1.5ml	10

Table 2.1. Transfection mixtures for various cell culture vessels. Volumes (in µl) are shown for a single well of each vessel included.

For example; for 8 well chamber slides, 100ng of siRNA or DNA was incubated at room temperature with 1µl Plus reagent in 12.5µl serum free media (Optimem; Invitrogen, Paisley, UK) for 20 minutes. 1µl Lipofectamine and 100µl Optimem were added to the mixture and incubated for 15 minutes. Cells were washed twice with serum free media before the transfection mixture was added to the cells. Total plasmid DNA amounts were kept constant. Whole-cell lysates were prepared 24 or 48

hours after transfection.

2.9.2 siRNA sequences and tranfection

Small interfering RNAs (siRNAs) were purchased from Applied Biosciences, Warrington, UK. Two siRNA molecules that target the *MCM4* gene at exons 5 (s69687) and exons 12 (s8592) or a scrambled control siRNA were transfected at concentrations of 50nM or 100nM for 24-48 hours, depending on the experimental design, and cells lysed as below.

2.10 Western blotting

2.10.1 Cell lysate preparation

Cell lysates were prepared by washing cells 3 times with PBS. Cells from a 6 well plate were incubated in 150µl RIPA buffer (as above) supplemented with complete, Mini, EDTA-free Protease Inhibitor Cocktail Tablets (Roche) on ice for 30 minutes. Samples were then centrifuged at 17g for 12 minutes at 4°C and the supernatant added to the same volume of 1x Laemmli loading buffer [98] (Sigma, Poole, UK). The samples were heated at 100°C for 10 minutes and centrifuged at 17 g for 1 minute before loading.

2.10.2 SDS-PAGE

The samples were run on precast 4-12% or 10% polyacrylamide NuPage BisTris gels (Invitrogen, Paisley, UK). The gels were run in 1x 3-(N-morpholino)propanesulfonic acid (MOPS) running buffer (Invitrogen, Paisley, UK), consisting of 50mM MOPS, 50mM Tris, 0.1% SDS, 1mM EDTA, pH 7.7. A High Molecular Weight Marker

protein ladder (Invitrogen, Paisley, UK) was run alongside all samples. 10-40µl of sample per well (depending on sample, ie 20µl harvested cell lysate vs 30-40µl lymphocyte cell lysates) was loaded and the samples were run at 150V for 60 minutes.

2.10.3 Immunoblotting

After separation by electrophoresis, the samples were transferred to a nitrocellulose membrane by semi-dry transfer using a Trans-Blot SD semi-dry transfer cell (Bio-Rad, Hemel Hempstead, UK). The transfer buffer consisted of 20mM Tris, 120mM glycine and 10% methanol. The semi-dry transfer of proteins was performed for 30 minutes at 15V. After transfer the nitrocellulose membranes were blocked with 5% milk powder in PBS with 0.05% Tween20 (PBST) for 1 hour. After blocking, membranes were incubated in 10ml 5% milk in PBST containing appropriate primary antibodies overnight at 4^{o}C. The primary antibodies used included a polyclonal anti-MCM4 antibody (Abcam, Cambridge, UK; targeting MCM4 exon 14, or Santa Cruz, CA, USA; targeting the N-terminal of MCM4, at 1:2000 and 1:500 dilution in milk/PBST respectively), anti-FLAG at 1:1000 (Sigma, Poole, UK) and β-actin or GAPDH at 1:10000 (Sigma Poole, UK) as a loading control. Following overnight incubation the membranes were washed in PBST three times for 10 minutes and then incubated in appropriate species-specific infra-red secondary antibodies (Licor, Cambridge, UK) at a dilution of 1:10000 for 1 hour. After two washes in PBST and a single wash in PBS, the membranes were imaged using the Licor Odyssey infrared scanner.

2.11 Fluorescent cAMP reporter assay (dose response study)

2.11.1 MRAP DNA constructs and site directed mutagenesis

MRAP-3XFLAG vector had already been constructed in our laboratory by directional cloning of MRAPα into the *Hin*dIII and *Eco*R1 restriction sites of the p3xFLAG-CMV-14 expression vector (Sigma, Poole, UK) after PCR amplification of human MRAPα (for primer sequences see table 2.2).

Mutant MRAP vectors were then synthesised from this by site directed mutagenesis using the QuikChange XL Site-Directed Mutagenesis Kit according to the manufacturer's instructions (Stratagene). A haemagglutinin-tagged human wild-type MC2R construct (HA-MC2R) was used for all experiments.

2.11.2 cAMP Luciferase assay

cAMP production can be assayed using Promega's Dual-Luciferase Reporter Assay System which assays the activities of firefly (*Photinus pyralis*) and *Renilla* (*Renilla reniformis*/sea pansy) luciferases which are measured sequentially from the same sample. The 2 plasmids used in the assay are pRL-CMV *Renilla* Luciferase plasmid, this is driven by the CMV immediate-early enhancer/promoter. The second is a α GSU – 846 luciferase plasmid, containing luciferase driven by the cAMP responsive promoter α GSU -846.

To measure the cAMP response in the presence of the mutant MRAP constructs, MC2R and the MRAP constructs were co-transfected with a cAMP-responsive luciferase reporter gene (-846αGSUluc, figure 2.3) along with pRL-CMV renilla.

Figure 2.3

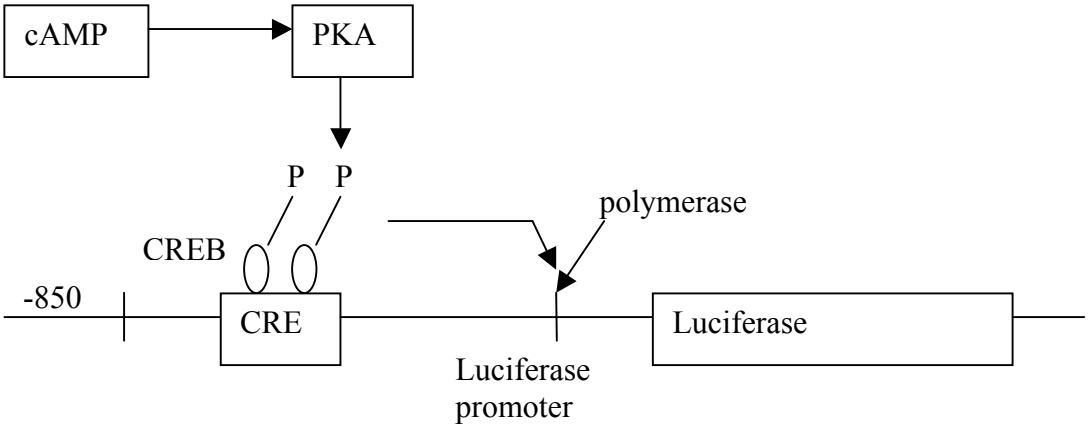

Figure 2.3 Schematic diagram of cAMP activation of the Luciferase Reporter Construct. cAMP generates protein kinase A (PKA) which in turn leads to phosphorylation of CREB (cAMP repsonse element binding protein) allowing it to bind to co-activators, leading to the recruitment of RNA polymerase II to the αGSU promoter and transcription of luciferase.

Five to six hours after ACTH stimulation (allowing for transcription and translation of luciferase) the amount of luciferase is assayed. This technique assumes luciferase production will be proportional to cAMP production. Luciferase is then measured via its ability to catalyse the formation of light (from ATP and luciferin according to the following reaction).

$$\text{ATP} + \text{Luciferin} + O_2 \xrightarrow[Mg^{2+}]{\text{Luciferase}} \text{Oxyluciferin} + \text{AMP} + \text{PPi} + CO_2 + \text{LIGHT}$$

The intensity of light emission has a linear relationship to the concentration of luciferase and is measured using a luminometer. Before Luciferase expression can be measured by bioluminescence, the enzyme must first be extracted from the cells. The Luciferase assay system facilitates the simultaneous extraction and measurement of luciferase from cells.

Luciferase Assay Buffer II which contains luciferin is mixed with the experimental cell lysate. Firefly luciferase produces an initial burst of light that decays over about 15 seconds to a low level of sustained luminescence, this is measured by the Luminometer. Following this Stop and Glo solution is added, this simultaneously quenches the Firefly luciferase reaction and initiates the *Renilla* luciferase reaction. This produces a stabilized signal from the *Renilla* luciferase, which decays slowly over the course of the measurement. The *Renilla* measurement acts as an internal control. The luminometer then quantifies the luciferase and *Renilla* bioluminescent reactions which can be displayed in tables or graphically, allowing comparison between the degree of bioluminescence (and therefore cAMP production) in cells transfected with wild type or mutant MRAP.

HEK293 cells grown in 6 well plates were co-transfected with HA-MC2R and either wild type MRAP, mutant MRAP or an empty vector (total plasmid per well - 1000ng) plus both α-GSU-846 luciferase (900ng) and pRL-CMV Renilla luciferase (100ng) reporter constructs. After 48 hours cells were stimulated with ACTH (concentration range 10^{-6} to 10^{-11}) for 6 hours, lysates were harvested and cAMP production assayed as described previously [100].

2.11.3 Statistical Analysis

Results are stated as mean +/- SEM of at least 4 independent experiments. EC_{50} values were obtained from Prism software. Statistical analysis was performed using the Mann-Whitney Test ($p<0.05$ is significant).

2.11.4 Immunofluorescence

HEK293 cells were transfected with wild type HA-MC2R and either FLAG-wild type, mutant Y59D or mutant V26A MRAP and grown on coverslips in 12 well plates or glass 8-well chamber slides ((Nunc, VWR, Leicester, UK) until 80% confluent or 48 hours post-transfection, depending on the experiment. Cells were washed twice in PBS, treated with either ice cold 100% methanol for 20 minutes at -20ºC to fix and permeabilise the cells, or 3.7% formaldehyde for 10 minutes to fix the cells. This was followed by PBS with 0.05% TritonX100 for 10 minutes to permeabilise the cell membranes. The cells were washed three times for 5 minutes in PBS, and then blocked in PBS containing 10% NDS and 0.3% bovine serum albumin (BSA), hereafter called Buffer A, for 1 hour. After blocking the cells were incubated with primary antibodies, either AntiRabbit HA 1:500 or Anti Mouse Flag 1:500 (Sigma, Poole, UK) in Buffer A for 3 hours. After incubation with primary antibodies the cells were washed three times in PBS and then incubated with species-specific secondary antibodies in Buffer A for 1 hour. Cells were washed three times in PBS, briefly (1 minute) incubated with 2μg/ml 4',6-diamidino-2-phenylindole dihydrochloride (DAPI, Sigma, Poole, UK) to counterstain nuclei and then washed again for 10 minutes in PBS. The chamber or coverslip was removed from the slide and Fluorescent Mounting Medium (Dako, Ely, UK) was used to apply coverslips.

Cells stained for MC2R and MRAP were visualised and imaged using the Zeiss LSM510 laser scanning confocal microscope. Images were taken using a 63x objective.

2.12 Mouse methods

2.12.1 Generation and validation of mouse lines

All mice used in these studies were obtained from our collaborators in Cornell University, New York and have been reported previously, along with genotyping protocols [101, 102].

2.12.2 Chaos mice

Male C57/BL6J mice (Stock No. 000664) were treated with multidose N-ethyl-N-nitrosourea (ENU) and then bred to C3HeB/FeJ (Stock No. 000658). The resulting male pups were then bred to C3HeB/FeJ females to obtain second generation mice, which were subsequently intercrossed to obtain third generation mice. A mutagenesis screen was then performed to select mice for chromosome instability (as assessed by micronucleus levels in erythrocytes). One of these mutants in which the tendency to form micronuclei segregated in a monogenic, autosomal recessive manner was termed Chaos3 (or chromosome aberrations occurring spontaneously 3). Further studies revealed that Chaos3 is a hypomorphic allele of Mcm4, containing a T to A transversion at nucleotide 1033 of the coding region that defines an amino acid change from phenylalanine to isoleucine at residue 345 (F345I). These mice have been backcrossed to C3HeB/FeJ for at least 8 generations prior to arrival at The Jackson Laboratory.

2.12.3 MCM4 null mice

Mice that carry a disruption allele of Mcm4 (referred to as *Mcm4*$^{-}$) were generated. *Mcm4*$^{-}$ is derived from BayGenomics embryonic stem cell line RRE056 that contains a gene trap vector inserted between exons 12 and 13 of Mcm4, disrupting the highly

conserved MCM domain. Embryonic stem cell culture; Clone RRE056 cells (derived from the 129/Ola strain) were cultured in DMEM (GibcoBRL) supplemented with 15% FBS (HyClone), 0.1 mM MEM nonessential amino acids, 2 mM GlutaMAX-1, penicillin-streptomycin (100 units/ml), β-mercaptoethanol (Sigma) and leukemia inhibitory factor (produced in-house). Cells were microinjected for chimera production into B6 blastocysts by standard methods.

2.12.4 *Mcm4*$^{+/-}$ *Mcm3*$^{+/-}$ mice

To generate the mice analyzed here, mice of the genotypes *Mcm4*$^{Chaos3/Chaos3}$ (chromosome aberrations occurring spontaneously 3) and *Mcm4*$^{+/-}$ *Mcm3*$^{+/-}$ were crossed to generate the control (*Mcm4*$^{Chaos3/+}$ *Mcm3*$^{+/-}$) and mutant (*Mcm4*$^{Chaos3/-}$ *Mcm3*$^{+/}$) animals.

2.12.5 Mouse histology

Adult mouse adrenals were fixed in 4% paraformaldehyde (Sigma, Poole, UK) and embedded in paraffin. Sections were obtained using a microtome (Leitz 1512) at 6 μm thickness and mounted onto SuperFrost Plus slides (VWR). Sections were deparaffinised with 3 washes in xylene, followed by one wash in 100% ethanol. This was followed by incubation in 3% hydrogen peroxide in methanol (Fisher Scientific) to block endogenous peroxidase activity. Ethanol washes were then continued using 100%, 90%, 70% and 50% solutions in H_2O, followed by two washes in water to rehydrate. Haematoxylin and eosin staining was performed using standard procedures [103].

2.12.6 GATA-4 immunohistochemistry

Preliminary experiments showed that anti GATA-4 antibody (C-20, Santa Cruz Biotechnology) required antigen unmasking to give a clear and specific signal. To achieve that, the slides were boiled for 30 minutes in 10mM sodium citrate buffer pH6.

After a 5 minute wash in PBS Triton X-100 0.1% (T-PBS), the slides were blocked for 30 minutes with 10% normal horse serum (Sigma Aldrich) and treated with biotin blocking reagent (Vector Laboratories) to prevent non-specific secondary antibody and tertiary reagent binding. They were then incubated overnight with goat anti GATA-4 diluted 1:250 in T-PBS. Any unbound antibody was removed by washing three times in T-PBS. This was followed by incubation with a biotinylated horse anti-goat secondary (Vector Laboratories) diluted 1:500 in T-PBS, for 2 hours at room temperature. The slides were washed three times in T-PBS, treated with avidin-biotin complex (ABC Elite kit, Vector Laboratories) according to the manufacturer's instructions, rinsed again and incubated with 3-3'diaminobenzidine/nickel (Vector Laboratories). The reaction was stopped with H_2O and slides were dehydrated and coverslipped using DPX mounting medium (Fisher). Images were acquired using a Leica DMR microscope (Leica), and digital images were captured using a Leica DC200 camera (Leica) and DCViewer software (Leica).

2.12.7 CYP11A1 / YP11B1 immunofluorescence

Sections were processed as above up to the blocking step, incubated with mouse anti-CYP11B1 (1:20 in T-PBS) and rabbit anti-Side Chain Cleavage (Millipore, 1:1000 in T-PBS). After three washes with T-PBS, slides were incubated for 2 hr with goat anti-

mouse Alexa Fluor 488 and goat anti-rabbit Alexa Fluor 568 (Invitrogen) diluted 1:1000 in T-PBS and, after further washes, coverslipped. Images were acquired as above. CYP11B1 antibody was a kind gift of Dr C. Gomez-Sanchez (University of Mississippi Medical Center, Jackson, Mississippi).

2.12.8 Non-radioactive *in situ* hybridisation (NR-ISH)

Digoxigenin (DIG)-labeled antisense and sense Gli1 cRNA probes were available as they had been synthesized previously by *in vitro* transcription in the presence of DIG-labeling mix (Roche) using ~1 μg of linearized template and T7 or SP6 RNA polymerase (New England Biolabs) [103]. All probes were used at a concentration of 400-800ng/ml of hybridization buffer. Paraffin sections were dehydrated through an ascending alcohol series and NR-ISH performed as described previously [104].

Table 2.2. Primer sequences

	Forward Primer	Reverse primer
gMCM4	AAAAGACAAATCCAGGAAGGC	AACCTGAGCAGATAAAGCATCAG
cMCM4	GAGCTACTCGCCAGGTGG	GGAGTGCCGTATGTCAGTGG
1st ATG MCM4	ATAGAATTCAATGTCGTCCCCGGCGTCGAC	GAGGGATCCTTGCTCACAAGGC
2nd ATG MCM4	ATAGAATTCAATGCCAACCTCG	GAGGGATCCTTGCTCACAAGGC
3rd ATG MCM4	ATAGAATTCAATGCATTCTTCA	GAGGGATCCTTGCTCACAAGGC
gANK1	CAGCCTCCCCTCTTCCC	GGAGGCGGCTCGTACTG
gADAM5P	CGAAATGCATTGTAAAC	CTTAAGAAGACAAAATTG
Cloning MCM4-HA	GAGGGATCCTTGCTCACAAGGC	GATGGATCCTCAAGCGTAATCTGGCACATCGTATG GGTAGAGCAAGCGCACGGTCTTCC
SDM MCM4	CGACGGAATTCAAAGTCGTCCCCGG	CCGGGGACGACTTTGAATTCCGTCG
MRAPα	ACGCTGAAA GCTTAGTGCCACAGAGATG	ACCAGTTGAATTCGCTATGGC CACGAT
Y59D	CTCATCTTGCTCGACATGTCCTGGT	ACCAGGACATGTCGAGCAAGATGAG
Y59F	TCATCTTGCTCTTCATGTCCTGGTC	GACCAGGACATGAAGAGCAAGATGA
V26A	ACCTCATTCCCGCGGACGAGAAGAA	TTCTTCTCGTCCGCGGGAATGAGGT

Chapter 3: Missense mutations in the Melanocortin 2 receptor accessory protein that lead to late onset Familial Glucocorticoid Deficiency type 2.

3.1 Introduction

Twenty percent of patients with Familial Glucocorticoid Deficiency (FGD) have mutations in the MC2R accessory protein (MRAP). The *MRAP* gene spans a 23 kb region on chromosome 21q22.1 and consists of 6 exons that are alternatively spliced to form two isoforms, *MRAPα* (exons 1-5) or *MRAPβ* (exons 1-4 &6) [79]. MRAPα encodes a 172 amino acid protein in contrast to MRAPβ encoding a 102 amino acid protein. The proteins have identical N terminal and transmembrane domains but differ at their C termini (Figure 3.1).

Figure 3.1

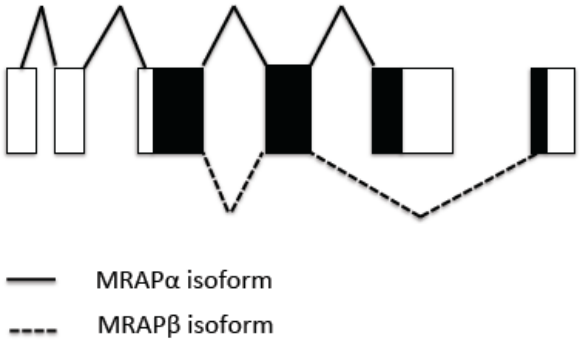

Figure 3.1. MRAP α and β isoforms. MRAP is alternatively spliced into either MRAPα or MRAPβ. Both proteins have identical N termini and transmembrane domains but diverse C termini.

Previous work in our laboratory has shown that MRAP is essential for normal MC2R function. MRAP forms a unique antiparallel homodimer that colocalises and directly

interacts with MC2R and is required for normal MC2R cell surface expression [79, 105]. MRAP may also be involved in ligand interaction and signal transduction [106, 107]. *MRAP2* has been identified as a paralogue to *MRAP*, this gene encodes a 205 amino acid protein with a single transmembrane domain and shows 27% homology to *MRAPα*. Like MRAP, MRAP2 is expressed in the adult adrenal gland, however it is also expressed in the ventromedial hypothalamus in the brain [108]. Similar to MRAP it has the ability to traffic MC2R to the cell surface leading to the formation of a functional ACTH receptor which responds to high levels of ACTH (10^{-6}M) stimulation.

Ten different MRAP mutations have been associated with FGD, all occurring in the N terminus or transmembrane domains. Interestingly, although MRAP2 may be able to replace MRAP function *in vitro*, MRAP2 clearly cannot replace MRAP function *in vivo*, as MRAP mutations present with FGD. This may be because of the relatively high concentration of ACTH required for MC2R signalling in the presence of MRAP2, which would exceed physiological circulating ACTH levels. Typically FGD patients with MRAP mutations present early with a severe phenotype, usually in the neonatal period (median 0.1 years) [91]. No patient reported to date has presented after 1.6 years. This most likely reflects the molecular basis of all MRAP mutations reported to date; all result in either an absent or severely truncated protein. In contrast most MC2R mutations are missense mutations, nonsense mutations being uncommon and usually present in compound heterozygosity with a missense mutation.

Two families with late onset FGD were referred to our group for genetic analyis (Figure 3.2). The proband in family 1 was diagnosed aged 4 years. Following family

review it was apparent that 2 older siblings had undiagnosed FGD. One sibling was well but the second had cerebral palsy likely secondary to hypoglycaemic seizures. The proband in family 2 was diagnosed aged 18 years with symptoms of fatigue, weight loss and depression.

3.2 Patients

3.2.1 Index Patient I

Family 1 is a consanguineous Saudi-Arabian family with 6 children, 3 of whom have FGD (Figure 3.2). The proband (II:6) was diagnosed aged 4 years following a severe exacerbation of asthma on the background of recurrent intermittent asthma requiring inhaled steroid treatment. He was noted to be hypotensive, hypoglycaemic and hyperpigmented. Electrolytes were normal (Na 134mmol/l, K 4.1mmol/l). Investigations revealed a grossly elevated ACTH level, 1050pg/ml (10-50) with a low paired cortisol level, < 25nmol/l (200-550). Plasma renin (2.1 ng/ml/h [1.9–3.7]), VLCFA (C26:0 = 0.68, C24:0/C22:0 ratio = 0.85, C26:0/C22:0 = 0.011) and 17 hydroxyprogesterone (6.1 nmol/l [0-10]) were all normal. Adrenal autoantibodies were negative.

A family review revealed a brother aged 15 years (II:2) and sister aged 20 years (II:1) who were both severely pigmented with high ACTH and low cortisol levels. The brother had no significant medical history and had never required hospitalisation, he was thriving and was developmentally normal. His sister suffered a hypoglycaemic seizure in infancy and subsequently developed cerebral palsy, however a causal relationship between the two cannot be assumed. Otherwise she had been relatively

well and had no history of further hypoglycaemic episodes later in childhood. Neither sibling had been treated for their FGD. Another sister (II:3) who was reported to have been very pigmented, died during an intercurrent illness aged 11 years. Both parents and 2 further siblings were unaffected.

Figure 3.2

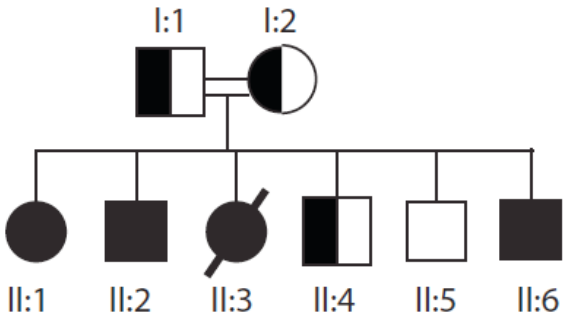

Figure 3.2: Pedigree of family 1 indicating affected siblings. All affected individuals (black symbols) were homozygous for the Y59D mutation, unaffected parents and siblings (where characterised) were heterozygous (half-filled symbol) or wild type (open symbol).

3.2.2. Index Patient II

The index patient was a 38 year old male of Turkish origin, first diagnosed aged 18 years after psychiatry review for symptoms of fatigue, weight loss and depression. On examination he was noted to have skin and mucosal hyperpigmentation, ACTH was grossly elevated at 1000 pg/ml with paired cortisol 345 nmol/l. He was commenced on Prednisolone 7.5 mg/day but discontinued the medication after 6 months. He was relatively asymptomatic for the next 20 years suffering only prolonged minor infections. On second review hyperpigmentation remained and repeat ACTH was again markedly elevated at 3359 pg/ml with paired cortisol of 438

nmol/l. Standard low dose ACTH stimulation test showed basal cortisol of 522 nmol/l with no increase on stimulation. Plasma renin activity (1.32 ng/ml/h [0.5-1.9])/ h), aldosterone: 246 pmol/l (30-420 pmol/l) and 17 OH- progesterone (3.4nmol/l [0-10 nmol/l]) were all within normal limits. He remains untreated with glucocorticoids.

3.3 Sequencing Results

The coding exons of *MC2R* and *MRAP* were sequenced in these families. In both families the *MC2R* sequence was normal. In family I *MRAP* sequencing in affected individuals (patients II:1 II:2 and II:6) revealed a novel homozygous missense mutation c.175T>G, predicted to cause the substitution of tyrosine with aspartic acid at position 59 (p.Y59D) (figure 3.3A and 3.4). The mother and one unaffected sibling (I:1 and II:4) were heterozygous at this position and one sibling (II:5) was homozygous for the wild type sequence. Paternal DNA was unavailable for analysis.

In family II, sequencing of *MRAP* identified a novel homozygous missense mutation c.76T>C, predicted to cause the substitution of valine with alanine at position 26 (p.V26A) (figure 3.3B and 3.4). Parental DNA was unavailable for analysis.

Figure 3.3

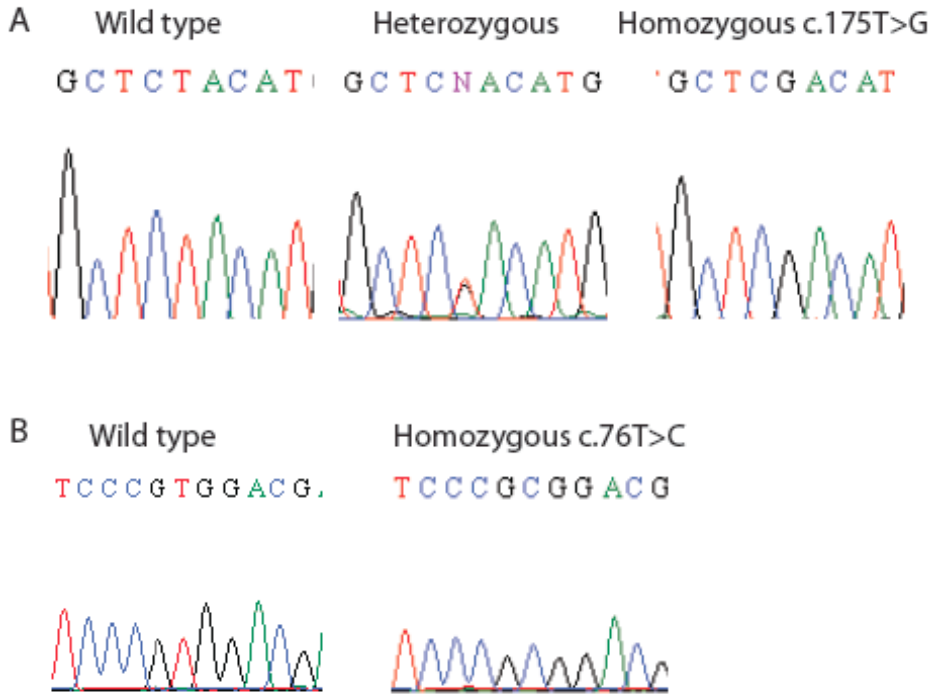

Figure 3.3 A. Partial sequence chromatograms showing wild type, heterozygous and homozygous missense mutation c.175T>G; this is predicted to cause substitution of tyrosine with aspartic acid at position 59 (p.Y59D). B. Partial sequence chromatograms showing wild type and novel homozygous missense mutation c.76T>C; this should cause substitution of valine with alanine at position 26 (p.V26A).

Figure 3.4

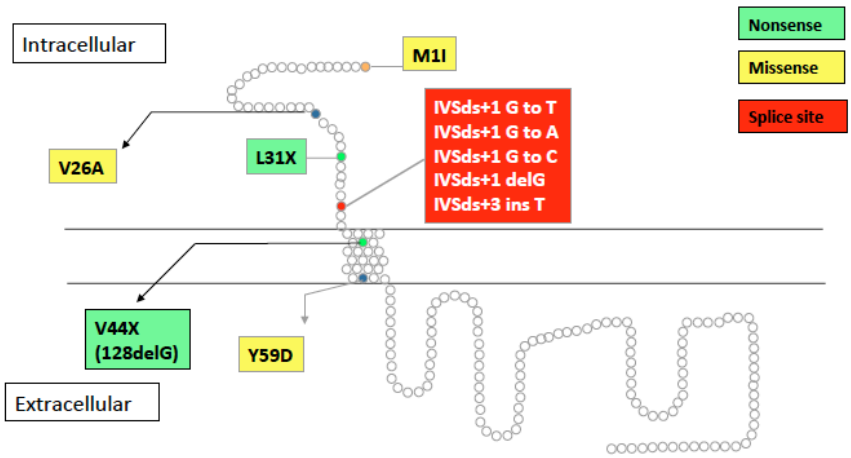

Figure 3.4 Schematic diagram of human MRAP illustrating the intracellular, extracellular and transmembrane domains. The locations of all known mutations including the novel mutations Y59D and V26A are shown.

3.4 cAMP luciferase reporter assay

As discussed in the introduction, in the early stages of steroidogenesis ACTH binds to MC2R which induces intracellular production of cAMP, one of the major actions of which is to stimulate cAMP-dependent protein kinase (protein kinase A). Steroidogenic enzyme expression is stimulated via a number of mechanisms including activation of the cAMP response element binding protein (CREB), and ultimately results in an increased rate of cortisol synthesis. It has previously been shown that both MC2R and MRAP are essential for a normal cAMP response [79].

HEK293 cells do not contain any endogenous MRAP or MC2R but do contain all other components necessary to allow a normal cAMP response to ACTH. Therefore when wildtype MC2R and MRAP constructs are transfected into HEK293 cells a normal cAMP response can be elicited [109]. By transfecting wild type MC2R in conjunction with either mutant or wildtype MRAP, cAMP production can be compared in the two cell systems and the difference in function between wild-type and mutant MRAP inferred. By stimulating with varying doses of ACTH, dose response curves can then be generated for each construct.

MRAP-3XFLAG vector had already been constructed in our laboratory by directional cloning of MRAPα into the *Hin*dIII and *Eco*R1 restriction sites of the p3xFLAG-CMV-14 expression vector (Sigma, Poole, UK) after PCR amplification of human MRAPα [80]. The Y59D and V26A mutant MRAPα constructs were created by site directed mutagenesis of MRAP-3XFLAG vector as described in section 2.11.1.

HEK293 cells were seeded into 6 well plates and then transfected with HA-MC2R and either wild type MRAP, mutant MRAP or an empty vector. In addition each well was transfected with equal quantities of αGSU and Renilla. After 48 hours each well was stimulated with ACTH in concentrations ranging from 10^{-6} to 10^{-11}M and one control well with MC2R and wildtype MRAP was left unstimulated. After 6 hours the cells were washed, lysed and cell lysate collected to be read in duplicate in a luminometer. Dose response curves were generated from the raw data and EC_{50} measurements for all wildtype and mutant constructs were obtained using Prism (Prism Software Corp., Irvine, CA). The EC_{50} or half maximal effective concentration refers to the concentration of ACTH when 50% of its maximal effect is observed.

In cells with either wild-type or mutant MRAP, ACTH stimulated the production of cAMP in a concentration dependent manner (Figure 3.5). In cells with Y59D mutant MRAP there was a significantly lower cAMP response and the dose response curve was shifted to the right when compared to cells with wild type MRAP; wild-type EC_{50} $3.2x10^{-9}$M, Y59D mutant EC_{50} $3.1x10^{-8}$M ($p=0.0058$) (Figure 3.5). In cells with V26A mutant MRAP there was a smaller but still significant shift in the dose response curve to the right; V26A mutant EC_{50} $6.6x10^{-9}$M ($p=0.0263$) (Figure 3.5).

These data reveal that the mutations have a deleterious effect on the ability of MRAP to facilitate ACTH signalling via MC2R. Phosphorylation of serine, threonine or tyrosine residues is a common post-translational mechanism by which mammalian cells regulate protein function. The substitution of aspartic acid, being a negatively charged amino acid, at position 59, may mimic a phosphorylated tyrosine and hence affect protein function. To investigate the possibility that the negative charge may be

responsible for the loss of function of the Y59D mutation, phenylalanine, which is a similar but non-polar aromatic amino acid to tyrosine, was substituted at this position by site-directed mutagenesis and the activity of these two mutants was compared.

Figure 3.5

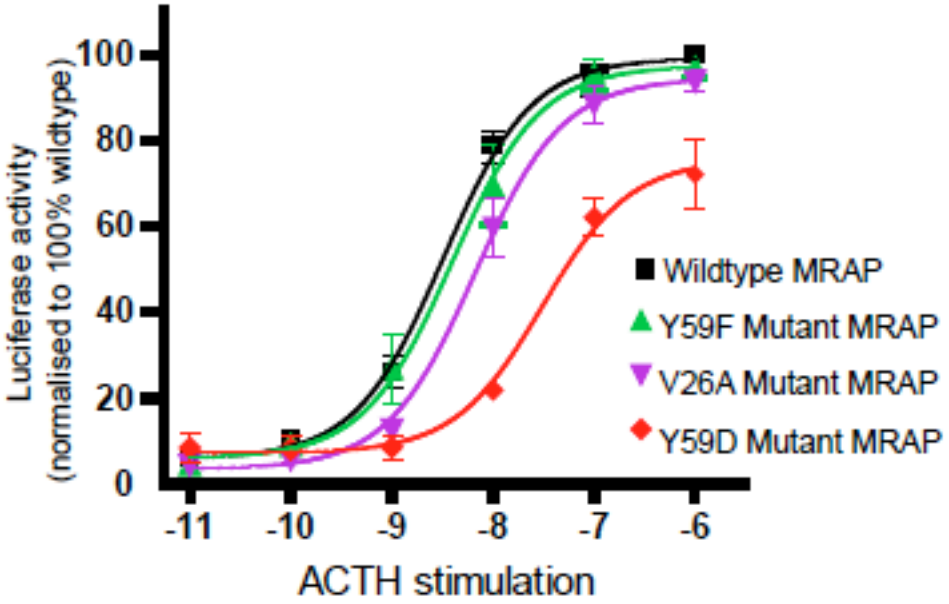

Figure 3.5 Graph showing dose response curves (DRC) for all mutants compared to wild type. There was a significant shift in DRC for Y59D mutant MRAP (family I) (n=4), and a smaller but still significant shift in the DRC in V26A (family II) (n=8). There is no significant difference in function with Y59F (phenylalanine substitution) (n=4) compared to wild type, indicating that the negative charge associated with aspartic acid or the significant change in structure may be interfering with function.

In cells with both wild type and Y59F mutant MRAP, ACTH again stimulated the production of cAMP in a concentration dependent manner, however there was no significant difference between wild type and mutant. The dose response curve was similar in both cases; mean EC_{50} wild type $3.2x10^{-9}$M, mutant Y59F $3.9x10^{-9}$M

(p=0.9436) (figure 3.5), indicating that the negative charge of aspartic acid may be the cause of the reduced activity of the Y59D mutant.

3.5 Immunofluorescence

Confocal immunofluorescence studies were performed to try to establish whether this decreased function was caused by a trafficking or cell signalling defect. Consistent with previous studies, wild type MC2R and MRAP are required for cell surface expression of MC2R (Figure 3.6 A-B). However the mutant MRAP Y59D and V26A were also detected at the cell surface with MC2R suggesting that both MRAP mutants are trafficking competent (Figure 3.6 C-D).

Figure 3.6

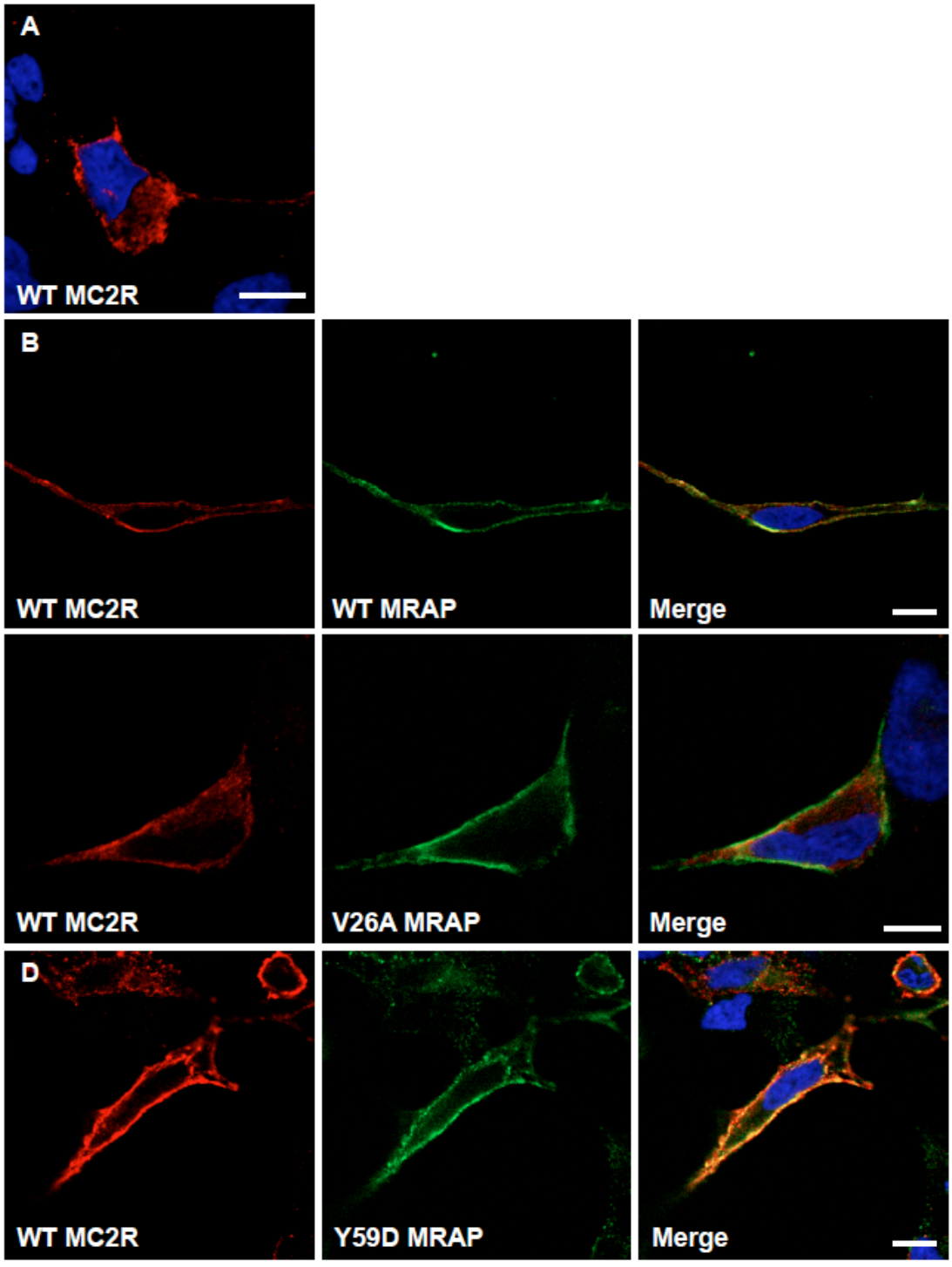

Figure 3.6. Immunofluorescent staining using both HA and FLAG antibodies detected HA-MC2R at the cell surface of transiently transfected HEK293 cells when co-expressed with wild type, mutant Y59D and V26A FLAG-tagged MRAP. Wild type MRAP, mutant Y59D and mutant V26A MRAP interact with and promote trafficking of MC2R to the cell surface; in contrast, cells transfected with MC2R and empty vector (no MRAP) show intracellular accumulation of MC2R. A: MC2R and Empty Vector (no MRAP). B: Wild type MC2R and

wild type MRAP. C: Wild type MC2R and mutant V26A MRAP. D: Wild type MC2R and Mutant Y59D MRAP.

3.6 Discussion

This is the first report of missense mutations in MRAP. These mutations resulted in a much later onset phenotype compared to FGD2 due to truncation mutants. In family I however there is a very wide range of clinical phenotypes with both a likely death secondary to adrenal insufficiency (sibling II:3) and survival to 15 years with no evident consequences (sibling II:2). This phenomenon has also been seen with MC2R mutations, in particular S74I [91]. The reasons for this remain unclear; however it seems likely that other genetic and environmental factors will influence the cortisol response to a suboptimal ACTH stimulus. We recently reported a child with FGD but without hyperpigmentation [87]. Excessive skin pigmentation related to elevated proopiomelancortin products acting on MC1R causes hyperpigmentation which is an important clinical finding suggestive of adrenal insufficiency. This child's diagnosis was delayed because of the absence of hyperpigmentation due to coexistent MC2R and MC1R mutations, genes located on different chromosomes but belonging to the same family, the melanocortin receptors. This case illustrates how more than one genetic defect can modify the clinical phenotype. Similarly, the patient who died, presumably due to adrenal insufficiency, may have had genetic defects in other genes affecting adrenal function, for example the oxidative stress pathway (discussed further in chapter 7), rendering her more susceptible to adrenal crisis when stressed.

The functional significance of the mutations identified in this study were investigated by transfecting MC2R in a heterologous cell line along with wild type or mutant forms of MRAP. These cells were then stimulated with ACTH and the cAMP

response was calculated using a cAMP-responsive luciferase reporter gene. Other assays are available which can also be used to evaluate MC2R function *in vitro*. ACTH binding to MC2R causes a conformational change in the receptor which leads to the exchange of GDP by GTP on the α-subunit. The GTP bound Gα-subunit stimulates adenylyl cyclase which stimulates conversion of ATP to cyclic AMP. cAMP subsequently activates Protein Kinase A (PKA) leading to phosphorylation of cAMP response element binding protein (CREB). The ideal assay would measure the primary receptor response following stimulation with ACTH ie formation of the GTP bound Gα-subunit. This can be assayed using a radioactive immunoassay.

cAMP production can also be measured directly using the cAMP competitive binding assay. This is based on the competition between cAMP in the samples and [^{3}H] cAMP, for the binding protein extracted from bovine adrenal glands. It is a sensitive assay that allows detection of cAMP over a broad range of concentrations. The gold standard cAMP assay is the cAMP ELISA assay however this is very expensive which can prohibit its use in the laboratory for experiments which require analysis of multiple samples.

cAMP imaging techniques have also been developed based on dissociation of PKA. Luciferase and YFP can be cloned to the regulatory and catalytic subunit of PKA. In the absence of cAMP both subunits form a complex which gives a high BRET signal. When cAMP binds to the regulatory subunits the catalytic subunits dissociate which eliminates the BRET signal. The change in the BRET signal allows cAMP concentrations via PKA dissociation to be measured [110].

However Luciferase is now the most widely used genetic reporter in studies on gene expression due to its high sensitivity and its absence from mammalian cells. Firefly luciferase is a 61kDa monomeric protein that does not require post-translational processing for enzymatic activity and therefore functions as a genetic reporter immediately upon translation [111]. Both reporters yield linear assays with sub attomole sensitivities; the linear range of luciferase detection for both firefly and *Renilla* luciferases extends over 7 logs of enzyme concentration [112]. Also, the absence of endogenous luciferase activity results in very low background activity. This leads to a higher sensitivity compared to other reporters eg CAT and beta-Gal assays.

The dual luciferase assay is convenient as both firefly and *Renilla* luciferase activity can be measured sequentially from a single sample and the method requires no incubations or pre-treatment. In contrast, the cAMP competitive binding assay requires radioactive buffers, generation of a standard curve, sample pre-treatment and lengthy incubations; generating dose response curves for multiple samples would be very time consuming.

Experimental accuracy is improved by using an internal control. In this case the "experimental" reporter, firefly luciferase, reflects the effect of the experimental conditions (mutant versus wild type MRAP) on the level of cAMP production. The second "control" reporter, *Renilla* luciferase, is used to provide an internal control to which the activity of the experimental reporter is normalized. Normalizing the activity of the experimental reporter to the activity of the internal control eliminates inherent assay-to-assay variability, such as differences in the number and health of cultured

cells and the efficiencies of transfection and cell lysis, which can undermine experimental accuracy.

Dose response curves were generated which showed ACTH stimulated the production of cAMP in a concentration dependent manner. Experiments were repeated a minumum of 3 times with most experiments repeated 6 times; a similar pattern was seen in all experiments. Furthermore the functional characterisation of the 2 mutant MRAPs compared to wild type fits with the clinical picture in that the patients with the Y59D mutation were more severely affected than the patient with the V26A mutation. Two negative controls were employed, the first consisted of HEK293 cells transfected with wild type MC2R in conjunction with empty vector pcDNA 3.1. When stimulated with ACTH the luciferase activity was minimal (<1% of wildtype) indicating that MRAP is required together with MC2R for a normal response to ACTH. As the only difference in these cells compared to those transfected with MC2R and wild type MRAP was the absence of MRAP it can be assumed that the absence of luciferase activity is secondary to the absence of MRAP, therefore verifying the assay. As a second negative control cells were transfected with both wild type MC2R and wildtype MRAP but not stimulated with ACTH. These cells showed minimal luciferase activity (<1% wild type), again indicating the assay was robust.

This assay, like all *in vitro* assays, can only give information about total cAMP concentrations rather than free cAMP concentrations ie second messenger pools that are not sequestered or bound to proteins. Also the concept of cAMP compartmentalisation that assumes different cAMP concentrations in different

cellular compartments can not be tested in this assay [113]. In addition the luciferase assay measures cAMP production indirectly using the luciferase reporter assay, assuming luciferase transcription and translation is directly related to cAMP production. However the dose response curves do demonstrate increasing amounts of luciferase activity and finally bioluminescence detected by the luminometer. This is almost certainly due to increasing cAMP responses as the negative controls demonstrate that cAMP production is not generated when cells are unstimulated or when MC2R or MRAP are absent, and indicate that the assay is a good way of characterising these mutants *in vitro*.

Previous work has shown that the transmembrane domain of MRAP (amino acids 36-62) is the domain that is required for MC2R–MRAP interaction and cell surface expression of MC2R. The substitution of the tyrosine residue for an aspartic acid in family I is therefore likely to interfere with MC2R interaction or trafficking. In addition, given that tyrosine has an uncharged polar structure but aspartic acid has a charged polar structure it is conceivable that this substitution would indeed affect MC2R interaction and trafficking to the cell surface. However confocal immunofluorescent studies did not support this. These studies indicated that the Y59D and V26A mutant were both able to successfully traffic MC2R to the cell surface suggesting that decreased function was secondary to a signaling defect at the cell surface. There is increasing evidence that MRAP has both a trafficking and a ligand binding/signal transduction function. A region between residues 19 and 21 seems to be specifically required for receptor signaling; deletion of this region results in a trafficking competent but signaling defective MRAP. Binding data suggests that this region influences ACTH binding by MC2R [106-108].

When tyrosine is substituted with phenylalanine at position 59 there is no significant difference in function compared to wild type indicating that the negative charge associated with aspartic acid may be interfering with function, potentially because of the likely conformational change of the transmembrane domain resulting from the charged residue at this position. As tyrosine is a target for phosphorylation by certain intracellular kinases this observation raises the possibility that phosphorylation of this residue modulates the function of MRAP. Given aspartic acid is negatively charged this may mimic a continually phosphorylated tyrosine, potentially leading to continual downregulation of MRAP and reduced function *in vitro* as well as *in vivo.* Alternatively post translational modification of MRAP through this tyrosine residue may be affected by the aspartic acid substitution giving rise to reduced function.

In Family II, the index patient had only a mild abnormality of adrenal function, leading to a suboptimal cortisol response to ACTH stimulation. However he also had considerable elevations in ACTH levels up to 3359pg/ml leading to hyperpigmentation. Adrenal failure secondary to autoimmune disease, tuberculosis or adrenoleucodystrophy was thought to be unlikely as it is probable that in this case mineralocorticoid deficiency would have evolved over time. It is likely that his non-specific symptoms including fatigue, weight loss and depression were secondary to his mild cortisol deficiency.

Consistent with the observation of a mild phenotype in this patient the characterisation of V26A mutant MRAP demonstrates impaired rather than absent function evidenced by a right shift in the dose response curve. Furthermore this shift

was very small for V26A and correlates with the patient's mild clinical picture. This small reduction in function is unsurprising given that this is a very conservative change as both valine and alanine are nonpolar hydrophobic amino acids only differing in that valine has an additional carbon and methyl group.

In summary, these missense mutations illustrate that *MRAP* mutations can present late in life leading to a variable phenotype of ACTH resistance. Consistent with the phenotype, characterisation of these mutations confirms reduced rather than absent function. These results, describing late onset disease resulting from missense *MRAP* mutations, further substantiate the hypothesis that disease severity in FGD patients reflects the functional significance of the underlying mutation. Furthermore, these results have significant clinical implications as it is clearly important to screen late presenting patients with unexplained glucocorticoid deficiency for mutations in *MRAP*.

Chapter 4: Identification of the gene causing FGD in the Irish traveller population

4.1 Patients

4.1.1 The Irish travelling community

The Irish travelling community was estimated to have a population of 36,224 at the 2008 Republic of Ireland traveller census and a further 3,905 were estimated to live in Northern Ireland [114]. Irish travellers are an indigenous nomadic minority who have been documented as being part of Irish society for centuries. Although they have much in common with European travellers and Roma gypsies they are ethnically and genetically distinct. Irish travellers have a long shared history, identity, language and value system and are recognised as a cultural minority in Ireland.

Travellers experience considerably higher mortality than the general Irish population across all age ranges; overall traveller mortality is 3.5 times higher [115]. This is due to all cause mortality, both external causes of death (including accidents, suicides and poisonings) and also illness, with respiratory illness and heart disease considerably higher than expected. Cancer deaths are also increased; 21.9 observed deaths in males (compared to 9.0 expected deaths) and 14 observed deaths in females (compared to 8.0 expected deaths). Infant mortality is 3.6 times higher than the general population; traveller infant mortality rate is 14.1 per 1000 live births comparing to 3.9 per 1000 live births in the general population. Infant mortality rates are strongly associated with the socio-economic status of the mother which is clearly a contributing factor to the Irish traveller infant mortality rate [116]. However additionally there is a genetic contribution which is harder to define. Irish travellers nearly always marry within the community and often marry a relative which has created a genetically isolated

population with high levels of consanguinity. There is a significantly increased incidence of autosomal recessive disorders within this population, one of which is Familial Glucocorticoid Deficiency. A recent paper describing the phenotype of nine Irish travellers with FGD estimated the disease prevalence to be one in 2506 compared to an overall prevalence of one in 201,898 in the general Irish population [4].

4.1.2 Clinical Presentation

I studied 7 children with adrenal failure from 3 kindreds within the Irish travelling population; all children are the product of first cousin marriages (Figure 4.1). Patients had been referred to the tertiary paediatric endocrine clinic in Our Lady's Children's Hospital in Dublin with typical clinical and biochemical features of Familial Glucocorticoid deficiency (FGD). They had isolated glucocorticoid deficiency, raised ACTH and normal renin and aldosterone levels. Patient 1, 3 and 7 presented with failure to thrive and hyperpigmentation; ACTH, cortisol levels and ACTH stimulation testing confirmed cortisol deficiency (Table 4.1). Patients 5 and 6 presented with hypoglycaemia, patient 5 with a hypoglycaemic seizure, both during an intercurrent illness. Hypoglycaemia together with hyperpigmentation on clinical examination led to positive screening for adrenal insufficiency. Patients 2 and 4 were screened due to positive family history; initially they had normal biochemistry but subsequently developed adrenal insufficiency. Unlike other forms of FGD, cortisol deficiency is often not as severe and onset is usually in childhood following a period of normal adrenal function, verifying development of disease during childhood. This potentially suggests a degenerative process that is in contrast to FGD 1 and 2, which can usually be detected from birth. All children were maintained on replacement hydrocortisone

10-12mg/m^2/day. Age of presentation of adrenal failure, presenting complaints and biochemical data supporting adrenal insufficiency are presented in Table 4.1. Patient 8 has not yet developed adrenal failure but does show evidence of other features (described in detail below) including short stature, increased chromosomal fragility and Natural Killer (NK) cell deficiency.

Figure 4.1

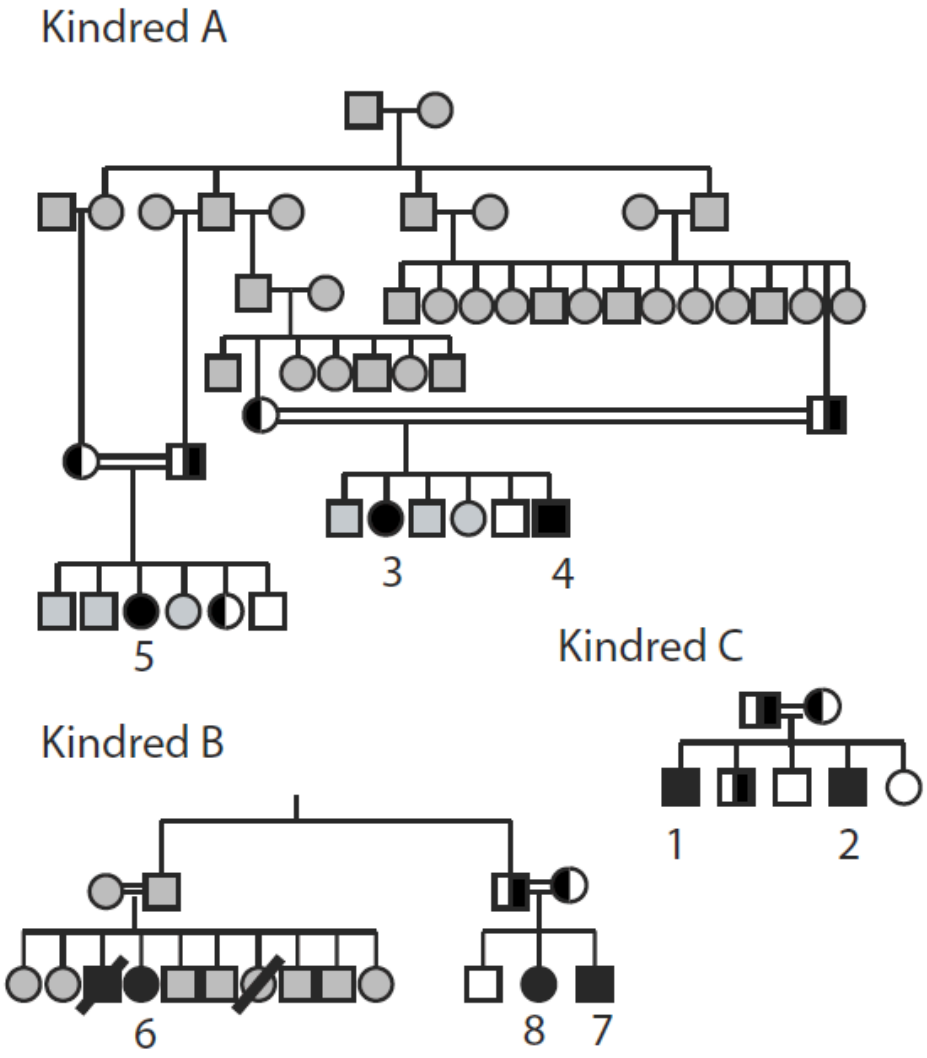

Figure 4.1 Pedigree of 3 affected kindreds. Shaded black, affected; shaded half black and half white, unaffected and heterozygous genotype; shaded white, unaffected and wild sequence type; shaded grey, unknown genotype and disease state.

Table 4.1

Patient	Age at diagnosis of adrenal insufficiency (yrs)	9am cortisol (nmol/L) NR>200	ACTH at diagnosis (ng/l) NR 9-52	Maximum cortisol with ACTH stimulation NR>550	Renin nmol/l/h NR 0.5-3.5	Aldosterone pmol/l NR 100-850
1	2.5	112	265	314	3.5	130
2	12	167	50	356	3.3	435
3	7.9	114	259	-	0.8	75
4	0.5*	244	156	325	3.2	165
5	5	<20	439	-	2.5	<55 / 126
6	4.5	308	195	308	2.6	105
7	0.5*	229	126	364	8.2	1125
8	-*	210	27	577	4.3	285

Table 4.1 Adrenal phenotype of patients included in the study. Patient 8 (aged 4 years) was included because she has short stature, increased chromosomal fragility and NK cell deficiency however she has not yet developed adrenal insufficiency. FTT: failure to thrive * Screened due to positive family history

Adrenal imaging in one child was available and showed small atrophic adrenal glands on CT. Known causes of adrenal insufficiency were excluded including adrenoleucodystrophy, congenital adrenal hyperplasia, Triple A syndrome and Addison's disease. Patients had normal long chain fatty acids, normal 17-hydroxy-progesterone levels and adrenal autoantibodies were negative. Patients also had normal tear formation, normal swallow and no evidence of neurological disease, clinically excluding Triple A syndrome.

Children had a low birth weight and are currently notably short compared to their mid-parental height standard deviation score (SDS) despite a normal growth hormone/insulin-like growth factor 1 (IGF-1) axis (Table 4.2 and Figure 4.2). Boys had a persistently delayed bone age throughout childhood but most girls (except

patient 8) had a normal bone age. Due to their failure to thrive in infancy, failure to show any catch up growth in childhood, and resultant short stature, many of these children were screened for additional pathologies. Cystic fibrosis screening, coeliac antibodies and inflammatory markers were all negative and thyroid function tests were normal in all patients.

Table 4.2

Patient	Gestation (weeks)	Birth Weight SDS	Current Height SDS	Bone age	IGF1 nmol/l	IGFBP3 mg/l NR 1.3-5
1	36	-3.0	-3.3	Delayed	40 (20-85)	2.9/4.2
2	39	-1.8	-2.1	Delayed	58 (20-85)	-
3	40	-2.1	-1.4	Normal	53 (20-85)	3.8
4	39	-2.3	-2.3	Delayed	38 (20-85)	-
5	-	-	-1.1	Normal	24 (7-40)	4.3
6	37	-2.2	-1.3	Normal	23 (4-37)	4.1/5.4/4.3
7	38	-2.0	-3.4	Delayed	13 (4-20)	-
8	39	-1.9	-2.6	Delayed	6 (4-20)	1.7

Table 4.2. Growth phenotype of all patients. SDS, standard deviation score; IGF1, Insulin growth factor 1; IGFBP3, Insulin growth factor binding protein 3; NR; normal range.

Four children, patients 1 (male), 3, 5 and 6 (female) were of pubertal age. The boy had evidence of delayed puberty with no clinical signs of puberty or adrenarche. Biochemistry showed low gonadotrophins (eg LH 0.1 IU/l, FSH 0.4 IU/l) and undetectable testosterone levels consistent with hypogonadotrophic hypogonadism or constitutional delay of growth and puberty. Aged 14 years his pubertal staging was G1, P1, A1 with testes 3ml and no pubertal growth spurt. He was commenced on

testosterone injections for 6 months. These were subsequently stopped and over the following 5 years his puberty advanced to A2 P5 G5 but his testes remained only 12 ml bilaterally aged 20 years. At this time his gonadotrophins are normal (LH 2.2IU/l, FSH 4.1 IU/l) with 9am testosterone 13.3nmol/l. Clinically he has evidence of absent adrenarche, this is confirmed biochemically; DHEAS 1.6 µmol/l (2.1-15.2) and androstendione 3.1 nmol/l (2.8-10.5), indicating poor adrenal androgen synthesis.

Figure 4.2

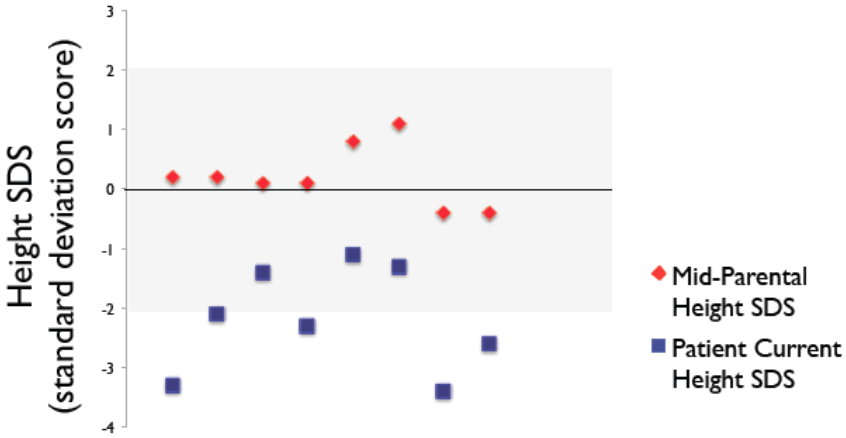

Figure 4.2 Graph showing patient and paired mid-parental height standard deviation scores.

The 3 girls progressed into puberty at a normal age with menarche at ages 12.5 years, 14 years and 14.1 years. All girls currently report regular monthly menses. All girls also clinically demonstrate lack of adrenarche, and although they had normal breast development, pubic hair and axillary hair development was delayed and pubertal staging continues to remain abnormal with staging B5, P3, A1, M1. Lack of adrenal androgens was also confirmed biochemically in the girls with androstendione (A4) and especially DHEAS levels low or undetectable (Table 4.3).

Table 4.3

Patient	Current age (years)	Puberty	A4 nmol/l 2.8-10.5	DHEAS µmol/l 2.1-15.2
1 (male)	20	Delayed	3.1	1.6
3 (female)	18	Normal	3.6	<0.4
5 (female)	17	Normal	1.9	<0.4
6 (female)	22	Normal	2.3	<0.4

Table 4.3 Pubertal status and adrenal androgen levels in those children who have reached puberty. A4, androstendione.

Fanconi's anaemia is another autosomal recessive disorder common in the Irish travelling community due to the high levels of consanguinity [117]. It is a genetically heterogeneous disorder, however a common homozygous deletion of exons 11-14 in the FANCA gene has been identified in the Irish traveling population. Fanconi's anaemia has three cardinal features; elevated chromosomal breakage, pancytopaenia and congenital anomalies, including dysmorphic features such as radial ray abnormalities, micropthalmia (usually unilateral) and growth retardation. The children reported here had failure to thrive and growth retardation but did not have any of the other congenital abnormalities and did not develop pancytopaenia or bone marrow failure. However, given the family history, a number of children were screened for Fanconi's anaemia using a chromosomal breakage screen. This is a screening test that involves culturing peripheral lymphocytes with an alkylating agent such as diepoxybutane or mitomycin C and looking for chromosomal breakage, for example abnormal chromosomal exchanges. Fanconi anaemia cells show increased chromosomal breakage compared to normal cells. These tests were carried out in a

laboratory in Bristol that is accredited to perform these investigations and to provide results for clinical care. Four children (patients 4, 5, 7, 8) had evidence of increased chromosomal breakage on screening with diepoxybutane (Table 4.4) but not always at levels high enough to be consistent with Fanconi's anaemia (patients 4, 5 and 7). All children screened negative for the known genetic defect in the FANCA gene and displayed no other clinical characteristics suggestive of any other DNA repair disorder, and so the chromosomal fragility remained unexplained.

Table 4.4

Patient	Normal cells out of 80 screened	Chromosomal breakage	Chromosomal exchanges
1	70	7 breaks	1 exchange
2	69	3 breaks	2 exchanges
3	73	8 breaks	none
4	56	13 breaks	4 exchanges
5	64	22 breaks	8 exchanges
6	pending	pending	pending
7	20	21 breaks	5 exchanges
8	69	152 breaks	54 exchanges

Table 4.4 Chromosomal breakage. Lymphocytes treated with 0.1μg/ml diepoxybutane for the duration of culture, normal background < 8 breaks/2 exchanges per test (80 cells quantified)

In 2006 Eidenschenk *et al*. reported four children from the Irish travelling community with a primary immunodeficiency consisting of a specific natural killer (NK) cell deficiency and susceptibility to viral infections [118]. One child had developed an Epstein Barr virus-driven lymphoproliferative disorder and two others developed

severe respiratory illness of probable viral etiology. The fourth child was well with no history of recurrent infections or lung disease but was screened for NK cell deficiency due to the family history. The group identified a single 12 Mb region on chromosome 8p11.23-q11.21 that was linked to the immunodeficiency but were unable to identify the causative gene within this region. None of the children were described as having adrenal insufficiency or increased chromosomal fragility. However, two of my patient cohort (patients 7 and 8) are related to the kindred described and had had immunological investigations performed that identified a similar degree of NK cell deficiency (Table 4.5). On screening of the remainder of the cohort all children showed low but not absent NK cells with normal T and B cell lymphocyte subsets (Table 4.5).

Table 4.5

	Total lymphs	T cells CD3+	T helper CD3/CD4	T supp CD3/8	B cells CD19	NK cells NR 200-300 /9-16%
1	3586	75/2892	41/1478	34/1252	20/808	210/5%
2	Unavailable					
3	2278	85/1934	57/1205	24/515	10/245	60/2%
4	2597	81.2/2110	40.1/1043	34.6/898	14.1/365	78/3%
5	2151	84.9/1825	47.3/1016	36.6/787	12.8/274	29/1.4%
6	1719	76/1309	51/861	23/389	19/327	27/2%
7	2515	60/1512	49/1206	10/239	33/842	18/1.1%
8	1816	73.9/1337	55.1/1001	17.9/325	17.5/319	141/3%

Table 4.5. Percentage and absolute numbers of T and B cell subsets in the first whole-blood sample analyzed are indicated for each individual tested. The absolute NK cell count (measured in cells/ml of whole blood) and the percentage of lymphocytes that were NK cells are also indicated.

NK cells are circulating cytotoxic lymphocytes that lack antigen specific T-cell and B-cell receptors. They belong to the innate immune system and are derived from CD34+ haematopoietic progenitor cells. They are defined by the expression of the cell surface marker CD56 and the lack of CD3 (thereby excluding T cells). NK cells are thought to mature in both bone marrow and secondary lymphoid tissue such as lymph nodes and tonsils. Although the maturation pathway has not been fully elucidated, it has been postulated that CD56 bright NK cells terminally differentiate into active CD56 dim NK cells. CD56 bright NK cells are named for their high-density surface expression of CD56 compared to CD56 dim NK cells which have a low density CD56 cell surface expression. It has been postulated that the CD56 dim NK cell population is more mature than the CD56 bright population, and is derived directly from this population. Interestingly the CD56 molecule itself has been found to be important in promoting this terminal maturation step [119]. The function of NK cells remains unclear, however a few very rare cases of complete NK cell deficiency in humans have been reported and result in overwhelming fatal infection during childhood [120, 121]. NK cells can secrete cytokines and chemokines that influence the host's immune response. They can also kill certain infected or transformed cells and have anti-proliferative effects on viral and malignant transformed cells. CD56 dim NK cells can efficiently lyse target cells in the absence of prior stimulation and without the need for antibody recognition [122]. The lack of well defined inherited disorders associated with a deficiency in NK cell development has led to lack of understanding regarding definitive NK cell function in humans.

Only one patient in our cohort clearly demonstrated increased susceptibility to infection; patient 6 had recurrent pneumonitis and had evidence of bronchiectasis on

CT chest. However on closer questioning it was apparent that patient 1, 3 and 7 also complained of recurrent chest infections requiring multiple courses of antibiotics and also required regular steroid and Ventolin inhalers. On routine examination, patients 1 and 3 had abnormal chest X-rays with evidence of pneumonia but no evidence of bronchiectasis or interstitial lung disease, however this would usually require CT examination for diagnosis. Otherwise the patients did not display any increased susceptibility to infection and specifically did not have increased rates of viral infections eg. Herpes virus 1 and 2, Epstein Barr virus or molluscum contagiosum infection.

It was apparent that these features (adrenal insufficiency, chromosomal fragility and NK cell deficiency) co-segregated in many individuals, and as inheritance patterns were suggestive of autosomal recessive mechanisms, it was hypothesized that a single genetic disorder might underlie all features. Ethics approval was obtained in April 2008 (application number SAC-110-08) from Our Lady's Children's Hospital, Dublin Ethics Committee to investigate this group of patients to try to identify the genetic basis for their disease. This involved completing an Ethics Approval form together with providing an information sheet to provide details on the study for patients and parents (Appendix 1). Parental consent and an assent for children forms were drawn up. Once these were in place homozygosity mapping was used to identify common areas of homozygosity between affected patients in order to subsequently interrogate these areas in an attempt to identify the causative gene.

Patients had already been screened for mutations in *MC2R* and *MRAP*. In addition I sequenced *STAR* and P450 Side Chain Cleavage Enyzme (*CYP11A1*) and found normal gene sequences.

4.2 Gene identification

The technique of homozygosity mapping in consanguineous families utilises the concept that affected individuals will be homozygous by descent for a mutation and polymorphic markers nearby. The disease locus is therefore identified by seeking regions of homozygosity that are common between affected members of a consanguineous family and not seen in the unaffected ones. This technique has already proven very successful in identifying new genes in highly consanguineous families [79]. However the clinical presentation of FGD in these kindreds was variable, as discussed previously a number of patients have been shown to have entirely normal adrenal biochemistry before later presenting with adrenal insufficiency. In addition chromosomal fragility and NK cell deficiency are not always present. It is therefore difficult to confidently assign a relative as unaffected. For that reason only affected individuals were genotyped and regions of homozygosity common to all affected patients were identified.

SNP array genotyping was performed with the GeneChip® mapping 10K microarray containing approximately 11,500 SNPs from The SNP Consortium database. The median physical distance between SNPs was approximately 105 kb, the average distance between SNPs was 210 kb and the mean genetic gap difference was 0.32cM. Briefly total genomic DNA was digested using a specific restriction enzyme, *Xba*I, and ligated to adapters. A generic primer that recognised the adapter sequence was

used to preferentially amplify fragments of DNA from 250 to 1000 base pairs long. Each SNP was located within one of these amplified fragments. The amplified DNA was then fragmented, labeled and hybridized to the GeneChip Mapping 10K Array. Allele specific hybridization was performed by synthesizing two 25 base-pair oligonucleotide probes each with the two possible alleles in the centre of the probe, one probe a perfect match for the "A" allele and one probe a perfect match for the "B" allele. The DNA was hybridized to the array and it could then be determined whether the SNP was AA AB or BB by analyzing the resulting signal from the allele specific probes.

Hybridized arrays were processed with an Affymetrix Fluidics station 450 and fluorescence signals were detected using the Affymetrix GeneChip Scanner 3000 by colleagues in the Genome Centre at Barts and the London. Signal intensity data was analysed by the GeneChip DNA analysis software based on a model algorithm to generate SNP calls [95].

Formal linkage analysis requires high quality genotyping, correct pedigree structure and accurate computational analysis [96]. Within an inbred population, when there are multiple loops of consanguinity it is recommended practice to simplify the pedigree structure for LOD score calculations. However this then raises the concern regarding the actual significance of the LOD score [96]. Furthermore, formal linkage analysis assumes the pedigree structure is correct but in inbred populations, including the Irish traveller population, there are often unknown or undisclosed inbreeding loops. These will have an unpredictable effect on the formal LOD score and IBD analysis. In addition, the limited number of individuals available for analysis (4 patients) reduced

the potential power, therefore formal linkage analysis was not performed. Instead, the IBDfinder program was used to identify regions of autozygosity [96]. This program takes a qualitative approach to the identification of regions of identity by descent (IBD) in affected individuals from consanguineous unions. It ignores linkage disequilibrium and pedigree structure, thereby allowing the analysis of singletons and groups of related or unrelated individuals. Formal linkage probabilities were not calculated but a graphical user interface was used to identify regions of homozygosity. IBD finder generates a graphical display of a numerical score that changes as the genotype data are scanned. The program uses the presence of rare SNP alleles as well as heterozygous markers to identify regions. Each homozygous SNP is scored by counting the number of homozygous SNPs between it and the nearest heterozygous SNP, and the average number of homozygous SNPs between it and the nearest centromeric and teleromeric heterozygous SNPs. These scores are plotted against the chromosome map coordinates to give a read out of the size of the region of homozygosity and also the number of SNPs that lie in that region. An allowance can be made for genotyping errors. Significant regions were therefore determined by including all regions where >10 consecutive SNPs were identical in all patients and allowing for a genotyping error of 1 in 50.

This led to the discovery of 3 IBD regions common to all 4 genotyped affected patients; 4:96.3-100.3, 8:36.8-51.9 and 8:62.1-64.5 (table 2), totaling 21.5Mb (Table 4.6).

Examination of ENSEMBL and similar databases (eg UCSC) revealed 319 known and predicted genes at these loci. Ideally, genes would have been prioritised for

sequencing based on known function and by determining their expression patterns in human tissues either *in silico* or *in vitro*. Expression patterns could be investigated *in silico*, using databases based on EST and RT-PCR data such as the Gene Expression Omnibus (http://www.ncbi.nlm.nih.gov/geo/) and the GNF SymAtlas (http://symatlas.gnf.org/SymAtlas/) as well as mouse in situ hybridization maps such as Genepaint (http://www.genepaint.org/). Genes with little or no evidence of adrenal expression using any of these tools would be considered less likely to be candidates for FGD genes. Genes showing highly adrenal-specific expression would be considered good candidates for further study by sequencing and/or knockdown analysis.

However, given the number of potential candidate genes discovered it was decided to prioritise genes for sequencing on the basis of their known functions. Based on known function and expression patterns only 2 genes appeared to be good candidates for FGD. These included the Steroidogenic Acute Regulatory Protein (StAR) and also Voltage Dependent Anion Channel 3 (VDAC3). The 7 exons in StAR together with the intron/exon junctions in 3 patients (from 3 different families) had previously been analysed and no potential disease causing mutation was identified. Therefore although it was possible that an intronic mutation or a mutation in the promoter region of StAR could be present leading to the FGD phenotype, this was considered to be unlikely and StAR was therefore excluded as a potential disease-causing gene.

VDAC3 on chromosome 8:42,249142-42263415 has 2 annotated transcripts which are known to be protein coding, VDAC3-002 (ENST00000521158) and VDAC3-003 (ENST00000022615). VDAC3 is an outer mitochondrial membrane protein porin that

forms a channel through the mitochondrial outer membrane and allows diffusion of small hydrophilic molecules through the mitochondrial membrane.

VDAC3 is thought to be specifically involved in translocation of adenine nucleotides through the outer membrane. Although VDAC3 is ubquitously expressed it shows relatively high expression in the adrenal gland and testes (www.proteinatlas.org) and therefore may play a role in steroidogenesis. Primers were designed to amplify all the protein coding exons in this gene and these were sequenced. This revealed wild type sequences with no potential disease-causing mutations indentified.

4.2.2 Targeted Exome Sequencing

Homozygosity mapping identified 21.5 Megabases (Mb) of genome in which the disease-causing gene was most likely located. The remainder of the genes in these intervals were not obvious candidates based on their known or suspected functions. Targeted massively parallel sequencing was then used to sequence all the protein coding regions within this 21.5 Mb region, which totaled approximately 1.1 Mb. The coordinates of the regions of homozygosity (Table 4.6) were supplied as well as the co-ordinates of the total genomic sequence of MC2R, MRAP and StAR to ensure no variants in these genes, known to be associated with FGD, had been missed. First, a custom sequence capture array targeting the exons, 50bp up- and downstream, plus 1Kb upstream of the transcription start site for each REFSEQ gene within these regions, was designed and manufactured by Roche NimbleGen. This was a Titanium Optimized Sequence 385K Capture Array that allows capture and enrichment of contiguous or non-contiguous genomic regions. Briefly, 5μg of genomic DNA was required, this was fragmented and hybridized to the custom designed capture array.

Unbound fragments were removed and the target-enriched pool was eluted and amplified. The enriched sample was then ready for high-throughput sequencing.

A 472-fold enrichment of the targeted regions was achieved and sequencing was performed for one patient sample on one lane of an Ilumina platform using Solexa technology. SNPs, with a threshold coverage of at least 10 reads, were called and the results were checked against the Ensembl SNP database, release 54.

This identified 680 variants from the 2009 human reference sequence (GRCh37/hg19) within the disease-linked loci only. It was hypothesized that the disease causing mutation would be novel so all variants with a minor allele frequency (MAF) > 0.01 in any SNP database were removed. This reduced the number of potential variants to 41 (Table 4.7). The mechanism of inheritance is almost certainly autosomal recessive given the inheritance pattern illustrated in the family tree (Figure 4.1). In addition, these patients are born within a genetically isolated population from highly consanguineous marriages. Therefore, heterozygous variants were excluded, leaving 9 homozygous variants for further analysis (Table 4.8). This included 3 variants in MRAP; 1 in the 5' untranslated region (UTR) in exon 2 (variant 7, Table 4.8), 1 intronic variant (variant 9, Table 4.8) and 1 intergenic variant (variant 8, Table 4.8). Variant 9 was subsequently identified as a SNP (rs67001164) and variant 8 was located 3145 bases before exon 3, not near any putative promoter site of MRAP, and therefore both were deprioritised. Variant 7 in the 5' UTR was sequenced but this variant did not segregate with disease in the families.

Table 4.6 Regions of homozygosity according to SNP genotyping.

SNP name	Position	Patient 4	Patient 3	Patient 5	Patient 7
Chrm 8					
rs725680	36800000	AB	AB	AB	AA
rs1455362	40200000	AB	AB	AB	AA
rs724322	40200000	AB	AB	AB	AA
rs726922	40200000	AB	AB	AB	BB
rs725401	40400000	AB	AB	AB	AA
rs721176	40500000	BB	BB	BB	BB
rs1073640	40600000	AA	AA	AA	AA
rs2127705	43200000	AA	AA	AA	AA
rs1603681	47400000	AA	AA	AA	AA
rs1384217	49700000	AA	AA	AA	AA
rs1383279	50300000	AA	AA	AA	AA
rs723497	50500000	BB	BB	BB	BB
rs2385545	50900000	AA	AA	AA	AA
rs1385982	50900000	AA	AA	AA	AA
rs1074385	50900000	AA	AA	AA	AA
rs1450127	51300000	AA	AA	AA	AA
rs310575	51600000	BB	BB	BB	BB
rs723597	51900000	AA	AA	AA	BB
rs723595	51900000	AA	AA	AA	BB
rs663747	61700000	AB	AB	BB	AA
rs1808634	62100000	AA	AA	AA	AA
rs745101	62100000	AA	AA	AA	AA
rs1367972	62200000	AB	AB	BB	AA
rs344288	63000000	BB	BB	BB	BB
rs344285	63000000	BB	BB	BB	BB
rs684872	63000000	AA	AA	AA	AA
rs622576	63000000	BB	BB	BB	BB
rs344214	63100000	BB	BB	BB	BB
rs1825310	63200000	BB		BB	BB
rs931130	63800000	AA	AA	AA	AA
rs2127561	63800000	BB	BB	BB	BB
rs965894	63800000	BB	BB	BB	BB
rs725329	63900000	AB	AB	AB	BB
rs1431587	64500000	AA	AA	AA	BB
rs1452488	64600000	AB	AB	AB	AA
chrm 4					
rs1073308	96200000	BB	BB	BB	BB
rs723367	96200000	AA	AB	AA	
rs965823	96300000	AA	AB	AA	AB
rs5003029	96400000				
rs1986598	96400000	AA	AA	AA	AA
rs1118570	96800000	AA	AA	AA	AA
rs1369980	97000000	BB	BB	BB	BB
rs1436532	97000000	BB	BB	BB	BB
rs1073690	97000000	BB	BB	BB	BB
rs997076	97200000	BB	BB	BB	BB
rs1911792	98700000	BB	BB	BB	AB
rs1111541	99300000	BB	?	BB	BB
rs1881450	99700000	AA	AA	AA	AA
rs951299	99800000	BB	BB	BB	BB
rs1230151	100000000	AA	AA	AA	AA
rs1540053	100301200	AB	AA	BB	AA

There were 6 additional variants in 6 different genes, with 3 of these variants in intergenic regions and 3 in intronic regions. There was no obvious coding variant that was most likely to cause disease, for example, a non-synonymous coding variant, coding insertion or deletion.

Table 4.7

VAR ID	CHRM	VAR FROM	REF NUC	VAR NUC	VAR DEPTH	VAR FREQ	GENE	CONSEQUENCE TYPE
408347	4	100229019	G	A	255	127	ADH5	INTRONIC
409185	8	37773181	T	C	255	127	PROSC	INTERGENIC
409194	8	38006687	A	C	54	27	ADRB3	INTERGENIC
409199	8	38120162	A	G	12	6	STAR	UTR
409199	8	38120162	A	G	12	6	STAR	UTR
409205	8	38125491	A	C	68	34	STAR	INTRONIC
409213	8	38445203	G	A	208	104	FGFR1	UTR
409213	8	38445203	G	A	208	104	FGFR1	UTR
409213	8	38445203	G	A	208	104	FGFR1	UTR
409213	8	38445203	G	A	208	104	FGFR1	UTR
409213	8	38445203	G	A	208	104	FGFR1	UTR
409213	8	38445203	G	A	208	104	FGFR1	UTR
409213	8	38445203	G	A	208	104	FGFR1	UTR
409215	8	38445420	C	G	113	56	FGFR1	UTR
409215	8	38445420	C	G	113	56	FGFR1	UTR
409236	8	38946344	C	T	32	16	PLEKHA2	SYNONYMOUS_CODING
409237	8	38946345	T	C	40	20	PLEKHA2	NON_SYNONYMOUS_CODING
409245	8	38964795	A	C	147	73	HTRA4	UTR
409264	8	39261615	T	C	255	127	ADAM32	INTERGENIC
409268	8	39369387	A	G	93	93	ADAM5P	INTRONIC
409274	8	39560326	C	A	58	58	ADAM19	INTERGENIC
409323	8	41873633	T	G	31	31	ANK1	INTERGENIC
409344	8	42997668	T	C	255	255	HOOK3	INTERGENIC
409348	8	43076807	T	G	255	127	AC113191	UTR
409351	8	43133390	G	T	223	223	HGSNAT	INTRONIC
409357	8	49036627	A	G	255	255	MCM4	INTRONIC
409364	8	50986687	A	G	58	29	7SK	INTERGENIC
409365	8	50986688	G	A	62	31	7SK	INTERGENIC
409372	8	62651834	A	G	255	127	ASPH	INTRONIC
409373	8	62699494	C	T	132	66	ASPH	INTRONIC
409388	8	64055354	G	A	127	63	AC120042	UTR
409400	8	64065989	C	G	232	116	AC120042	INTERGENIC
409401	8	64066222	T	C	255	127	AC120042	INTERGENIC
409416	8	64141220	A	T	83	41	TTPA	INTRONIC
409417	8	64141221	T	A	76	38	TTPA	INTRONIC
409418	8	64161480	C	T	153	76	GGH	INTERGENIC
411160	18	13877416	G	A	232	116	MC2R	INTRONIC
411191	18	13899483	C	T	255	127	MC2R	INTRONIC
411219	21	32587235	G	A	199	199	MRAP	UTR
411221	21	32590002	A	G	24	24	MRAP	INTERGENIC
411226	21	32595042	C	T	255	255	MRAP	INTRONIC

Table 4.7 All novel variants identified using targeted exome sequencing. Variant ID (Var ID), Chromosome number (chrm), location of variant (var from), reference and variant nucleotide (ref nuc and var nuc) are detailed. Variant depth (var depth) describes the number of times the variant was sequenced and variant frequency (var freq) is the number of times the variant

nucleotide was called, determining if the variant is homozygous or heterozygous. The gene and consequence of the variant is also described. Those variants shaded in gray are homozygous variants.

Table 4.8

	Chrm	Location	Ref base	Variant base	Total depth	Variant freq	Gene	Variant type
1	8	39369387	A	G	93	93	ADAM5P	Intronic
2	8	39560326	C	A	58	58	ADAM19	Intergenic
3	8	41873633	T	G	31	31	ANK1	Intergenic
4	8	42997668	T	C	255	255	HOOK3	Intergenic
5	8	42014233	G	T	223	223	HGSNAT	Intronic
6	8	49036627	A	G	255	255	MCM4	Splice site
7	21	32587235	G	A	199	199	MRAP	UTR
8	21	32590002	A	G	24	24	MRAP	Intergenic
9	21	32595042	C	T	255	255	MRAP	Intronic

Table 4.8 Novel homozygous variants identified in patient 4 by targeted exome sequencing. Chrm – chromosome; Ref base – reference base; Variant freq – variant frequence.

However when the 3 intronic variants were analysed, 1 variant in mini chromosome maintenance-deficient 4 homologue *(MCM4)* was in the consensus splice site of exon 2 of *MCM4*. Of the other intronic variants, 1 in *ADAM5P* at nucleotide 39369387 (variant 1, Table 4.8) lies 50 bases downstream of exon 10 and was subsequently identified as a SNP (rs73612404); MAF 0.456), and the variant (variant 5, Table 4.8)

in *HGSNAT* was 45 bases 5' to exon 4 and was also subsequently identified as a SNP (rs72647302;MAF 0.02) when the 1000 genome project database was examined.

Therefore the only potential variant to be further examined was variant 6, c.71-1insG, a homozygous splice site mutation in the acceptor splice site of exon 2 of *MCM4*. This variant was within the region of homozygosity, in the pericentric region of chromosome 8 (Figure 4.3).

Exon 2 of *MCM4* including the intron/exon regions, was amplified by PCR and sequenced (Figure 4.4). This variant was also sequenced in the other 8 affected patients from the Irish Travelling community, their parents and unaffected siblings and demonstrated to segregate with disease (Figure 4.1). In kindreds A and C parents were heterozygous for the *MCM4* variant and all siblings tested had either heterozygous or homozygous wildtype sequences, (parental and sibling samples were not available for kindred B). This variant was not present in SNP databases and was not seen in The 1000 Genomes Project (www.1000genomes.org) the NHLBI Exome sequencing Project (>10700 alleles sequenced; http://evs.gs.washington.edu/EVS/). 300 Caucasian control chromosomes were also screened using a genotyping approach. PCR products for *MCM4* exon 2 were digested by *Alu*1 restriction digest. *Alu*1 cleaves the PCR product from a wild-type sequence once but does not cut the mutant sequence. Control samples gave rise to 2 bands following digestion, PCR products from DNA with c.71-1insG were not digested and remained as 1 band, and heterozygotes resulted in 3 bands. All control samples had homozygous wild type sequences.

Figure 4.3

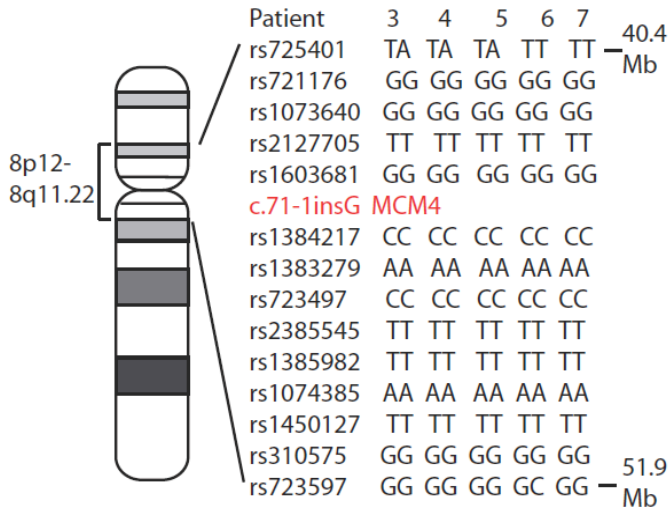

Figure 4.3 SNP genotyping of chromosome 8p12.2-q12.3 locus surrounding MCM4

Figure 4.4

A

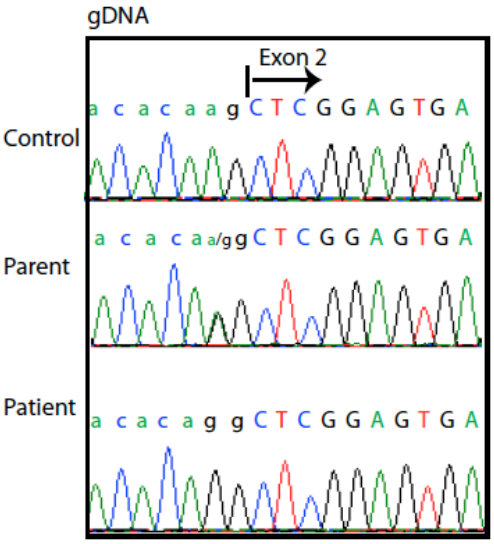

B

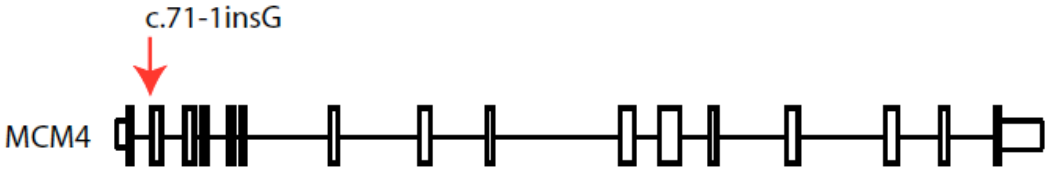

Figure 4.3 A. Partial sequence chromatograms showing; the intron2/exon2 junction in genomic DNA from control, parent and patient samples (intronic bases in lowercase, exonic in uppercase). An arrow indicates the start of exon 2 of MCM4. B. The location of the mutation, c.71-1insG, prior to exon 2 (red arrow).

4.2.3 cDNA Sequencing

This mutation was present in the 3' splice site of intron 1, altering the consensus sequence, and would thus be predicted to disrupt splicing of exon 2, potentially by shifting the splice acceptor site upstream by 1 nucleotide and leading to a frameshift and a foreshortened open reading frame encoding a prematurely terminated translation product (p.Pro24ArgfsX4). However, the true significance of the mutation cannot be established from DNA sequencing or prediction websites. To identify the consequences of this mutation, blood was taken from patient 1, patient 2, and an unaffected sibling control in kindred 3 (Figure 4.1) and RNA was extracted. Briefly, total RNA from patient and control leucocytes was purified and cDNA synthesised using reverse transcription as described in Methods, Section 2.5. The cDNA was used as a template for PCR amplification and sequencing of MCM4 exons 2-4.

Sequencing confirmed that this mutation did affect splicing by shifting the splice acceptor site by one base and incorporating an extra guanine into the mRNA transcript (Figure 4.5A). This results in a foreshortened open reading frame and a predicted prematurely terminated translation product (p.Pro24ArgfsX4) (Figure 4.5 B, C and D) of only 27 amino acids. Parents had a mixed cDNA sequence with evidence of both wild type and mutant sequences present. This verified that the splice site mutation identified in *MCM4* was pathological, leading to a truncated protein and confirming this variant in *MCM4* as the disease-causing mutation.

Figure 4.4

A

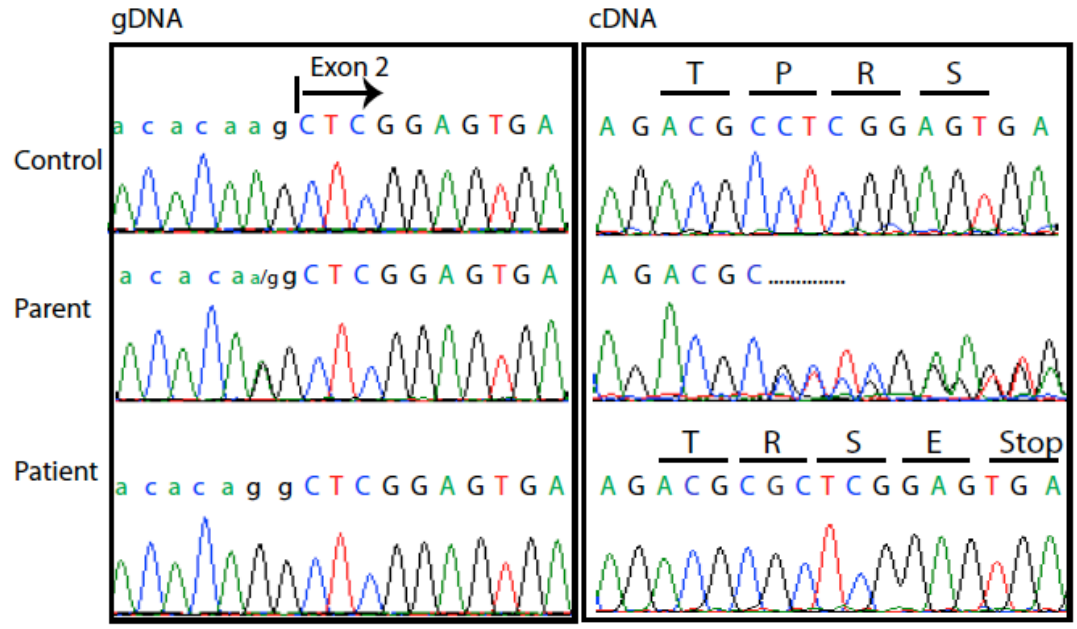
gDNA
cDNA
Exon 2
Control
Parent
Patient
a c a c a a g C T C G G A G T G A
T P R S
A G A C G C C T C G G A G T G A
a c a c a a/g g C T C G G A G T G A
A G A C G C .....
a c a c a g g C T C G G A G T G A
T R S E Stop
A G A C G C G C T C G G A G T G A

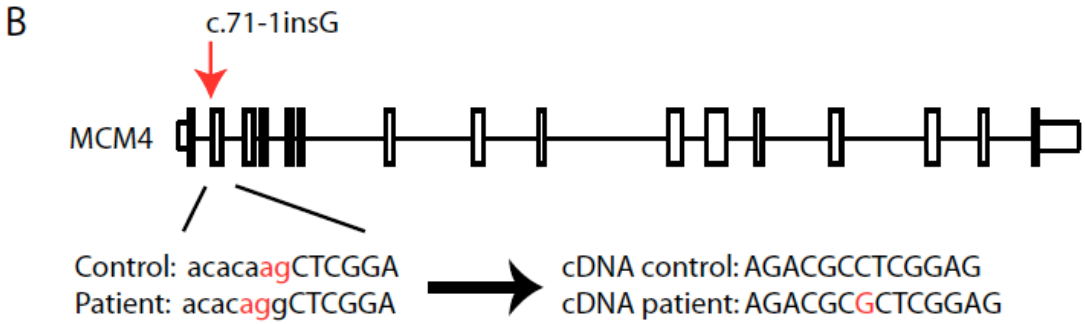
B
c.71-1insG
MCM4
Control: acacagCTCGGA
Patient: acacaggCTCGGA
cDNA control: AGACGCCTCGGAG
cDNA patient: AGACGCGCTCGGAG

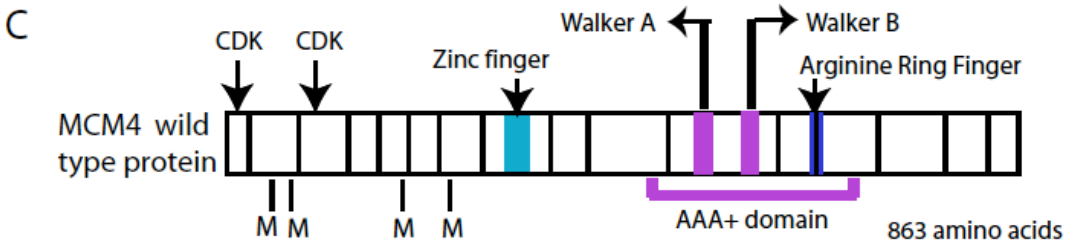
C
CDK
CDK
Zinc finger
Walker A
Walker B
Arginine Ring Finger
MCM4 wild type protein
M M
M M
AAA+ domain
863 amino acids

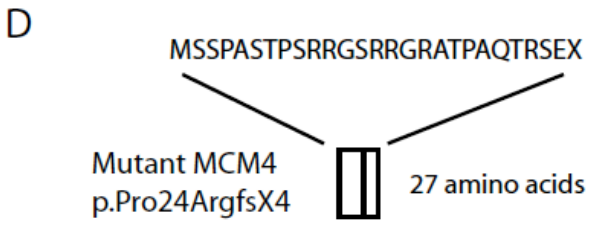
D
MSSPASTPSRRGSRRGRATPAQTRSEX
Mutant MCM4
p.Pro24ArgfsX4
27 amino acids

Figure 4.4 A. Partial sequence chromatograms showing; the intron2/exon2 junction in genomic DNA from control, parent and patient samples (as above). Arrows indicate the base change from A to G and (right) cDNA from control, parent and patient indicating wild-type, mixed and mutant cDNA sequences respectively, the latter resulting in a premature stop codon. B. The location of the mutation, c.71-1insG, prior to exon 2 (red arrow) which leads to a shift in the consensus splice site (nucleotides ag in red) and the introduction of an extra G into patient mRNA/cDNA is indicated. C. Protein structure of MCM4 indicating (top) the positions of the two CDK (cyclin dependent kinase) binding domains, zinc finger (turquoise), Walker A&B motifs (purple) and an arginine ring finger (dark blue), these motifs are conserved across all MCMs and are essential for MCM4 functionality. Also indicated are 4 in-frame methionines (M). D. The predicted consequence of the c.71-1insG mutation leading to premature truncation of the protein at amino acid 27 (p.Pro24ArgfsX4) is shown.

4.3 Discussion

Homozygosity mapping identified three regions of homozygosity common to all genotyped patients totalling 21.5 Mb. Genes were prioritised for sequencing by selecting those that appeared to be good candidates for FGD based on known gene function. These criteria identified only two potential genes, *STAR* and *VDAC3*, which both had normal sequences. The original plan was then to select those genes that showed highly adrenal specific expression and use a novel screening approach based on siRNA knockdown of candidates in adrenal cells. However candidates could not be filtered further as no genes showed adrenal specificity. This approach was therefore not feasible given the large number of potential candidate genes identified within the loci. In addition it was possible that some candidate genes may not influence the immediate ACTH signaling response and would therefore resist identification using the proposed knockdown screen.

In 2009 massively parallel sequencing was being successfully applied to discover genes for rare Mendelian disorders. In a milestone proof-of-concept paper, Ng *et al.*

showed that targeted whole exome sequencing, followed by a filtering approach (Figure 4.6), correctly identified the known disease gene involved in Freeman Sheldon syndrome [123]. The same group then went on to show that exome sequencing could identify the gene underlying an uncharacterised Mendelian disorder, Miller syndrome, using the same strategy [124].

This approach uses targeted exome capture through enrichment by array hydridization to 164,000 targets used to define the exome followed by sequencing using massively parallel platforms. There are a number of different technologies available including 454, Solexa and SOLiD technology [125, 126].

454 technology with pyrosequencing utilizes adapters which are ligated to fragments of DNA and facilitate their capture on a bead (one fragment per bead). A water-in-oil emulsion is created to amplify each fragment individually in its droplet, after amplification the emulsion is broken, the DNA denatured and the beads containing one amplified DNA fragment each are distributed into the wells of a fiber optic slide. The wells are loaded with sequencing enzymes and primer (complementary to the adapter on the fragment ends), then exposed to a flow of one unlabeled nucleotide at a time, allowing synthesis of the complementary strand of DNA. When a nucleotide is incorporated pyrophosphate is released and converted to ATP, which drives a luciferase-based reporter. The read length is between 100-150 nucleotides long.

Solid technology (ABI) also involves ligation of adapters to fragments of DNA followed by amplification on beads by emulsion PCR. The DNA is denatured and

beads deposited onto a glass slide. A sequencing primer is hybridized to the adapter and reads of 30-35 nucleotides are created using a sequencing-by-ligation technique.

Figure 4.5

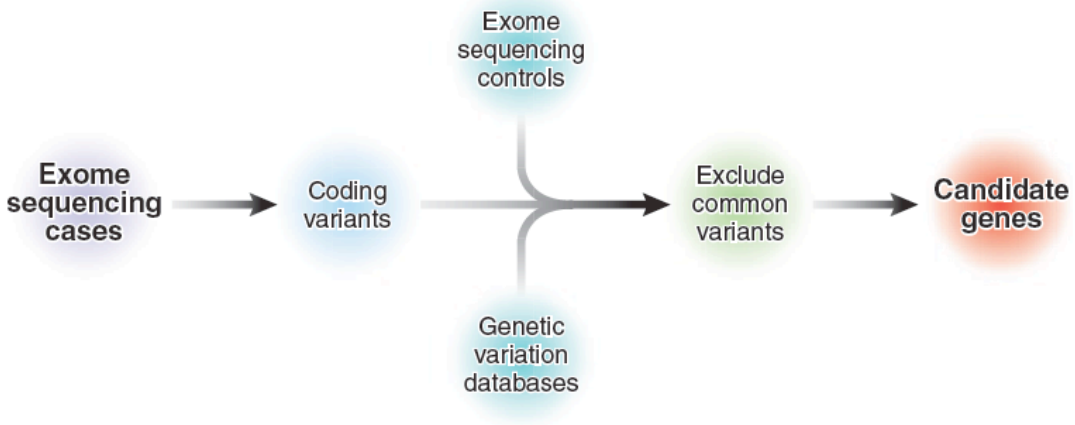

Figure 4.5 Filtering strategy applied in exome sequencing. (Taken from Nature Genetics *Biesecker*, *January 2010* [126])

For our sequencing Solexa technology from Ilumina was employed. For this fragments of DNA are ligated to end adapters, denatured and bound at one end to a solid surface that has been coated in a dense layer of adapters. Each single stranded fragment is immobilized at one end while its free end hybridizes to a complementary adapter on the surface. This adapter initiates synthesis of the complementary strand in the presence of amplification reagents. Multiple cycles of this solid phase amplification followed by denaturation create clusters of approximately 1000 copies of single stranded DNA molecules on the surface. Synthesis reagents, primers, DNA polymerase and four differently labeled reversible terminator nucleotides are added to the flow cell. Synthesis of the complementary strands involves incorporation of each nucleotide in sequence and identification by its colour before the 3' terminator and

fluorophore are removed. The cycle is continually repeated giving a read length of approximately 30-35 bases [125, 127]

This technology allowed us to sequence all the protein coding regions in the associated areas of homozygosity and identified a splice site mutation in *MCM4* as the only potential disease causing mutation. This mutation segregated with disease within three kindreds and was not present in over 11,000 control chromosomes sequenced. I confirmed that this splice site mutation was pathological giving rise to an abnormal mRNA sequence that is predicted to be translated into a truncated protein with potentially significant functional effects.

MCM4 is one part of the MCM2-7 complex that is essential for normal DNA replication and genome stability (Figure 4.7). It has recently been confirmed as the replicative helicase and therefore plays an essential role in cell division. The MCM (mini chromosome maintenance) proteins were originally identified and subsequently named from a screen for *Saccharomyces cerevisiae* (budding yeast) mutants that led to defects in maintaining a simple minichromosome. The MCM genes MCM2, MCM3 and MCM5 were first identified as causing defective plasmid segregation. MCM4 (originally CDC54), along with MCM7, were isolated as cell cycle division mutants and MCM6 was isolated as a chromosome segregation mutant in *Schizosaccharomyces pombe* (fission yeast) [128, 129]. Each MCM gene is essential for viability and many experiments have demonstrated the key involvement each protein plays in DNA replication. MCMs are found in both eukaryotes and archea but have not been identified in bacteria, although many bacteriophage genomes do contain MCM orthologues [130].

MCMs are a distinct subgroup of the large AAA ATPase family, these generally form large ATP-dependent complexes, often heterohexamers, and have many cellular functions. MCM2-7 are defined by a characteristic version of the ATPase domain which spans approximately 200 residues and is named the MCM box. This MCM box is highly conserved throughout the MCM family and includes 2 ATPase consensus motifs, the Walker A and Walker B motifs (Figure 4.5C). The Walker A motif GDPxx(S/A)KS, is involved in ATP binding. The Walker B motif, D(D/E), is part of the sequence IDEFDKM which is conserved throughout all MCMs and is required for ATP hydrolysis. All MCMs also contain an "arginine finger" (SRFD) and a "zinc finger" which is thought to contribute to complex assembly and ATPase activity [131]. MCM2-7 show less homology outside this MCM box; MCM4 from humans is more similar to MCM4 in yeast than MCM2 in humans [132]

The heterohexameric complex of minichromosome maintenance proteins MCM2-7 plays an essential role in origin licensing in all eukaryotes. Origin licensing builds a fundamental basis for genome stability in DNA replication. MCM2-7 is recruited to replication origins by Cdt1 as an essential component of the pre-replication complex, which is assembled from late M to early G1 phase of the cell cycle (Figure 4.7). This complex also includes the origin recognition complex (Orc1-6) and Cdc6, additional AAA ATPase proteins. These origins are then licensed for DNA synthesis, ensuring a single initiation of DNA synthesis from MCM bound origins in the subsequent S phase thus restricting genome replication to once per cell cycle. Once the MCM proteins are loaded onto the DNA, Orc1-6 and Cdc6 are no longer required and are released for subsequent cycles of DNA replication [130].

DNA unwinding is an active process that requires coupling the conformational changes caused by nucleotide binding and hydrolysis to the physical manipulation of nucleic acids. In the event of DNA damage, insufficient dNTPs or an unusual DNA sequence, DNA replication forks can be damaged leading to DNA double strand breaks and chromosome rearrangements. This activates checkpoints that block further DNA replication, cause cell cycle arrest which leads to stabilisation of DNA – protein interactions until the problem is rectified. This stabilisation of the replication fork requires interaction with Mrc1, Tof1 and Csm3 (the M/T/C complex) [130].

MCM2-7 has also recently been identified as the replicative helicase activated by S phase promoting kinases such as cyclin dependent kinases (CDKs) and Dbf4-dependent kinase (DDK) (Figure 4.7 C). CDK and DDK both control origin firing but CDK appears to provide the link to the cell cycle. Following activation additional proteins are loaded onto DNA at the sites of replication, these include Cdc45, the GINS complex and MCM10 [133-135]. The function of these replication factors remains unknown. Finally DNA polymerase is loaded and bidirectional DNA synthesis can commence. All 6 MCMs colocalise with DNA polymerase during elongation. Inactivation of any of the MCMs during S phase rapidly blocks DNA replication [136].

Figure 4.6

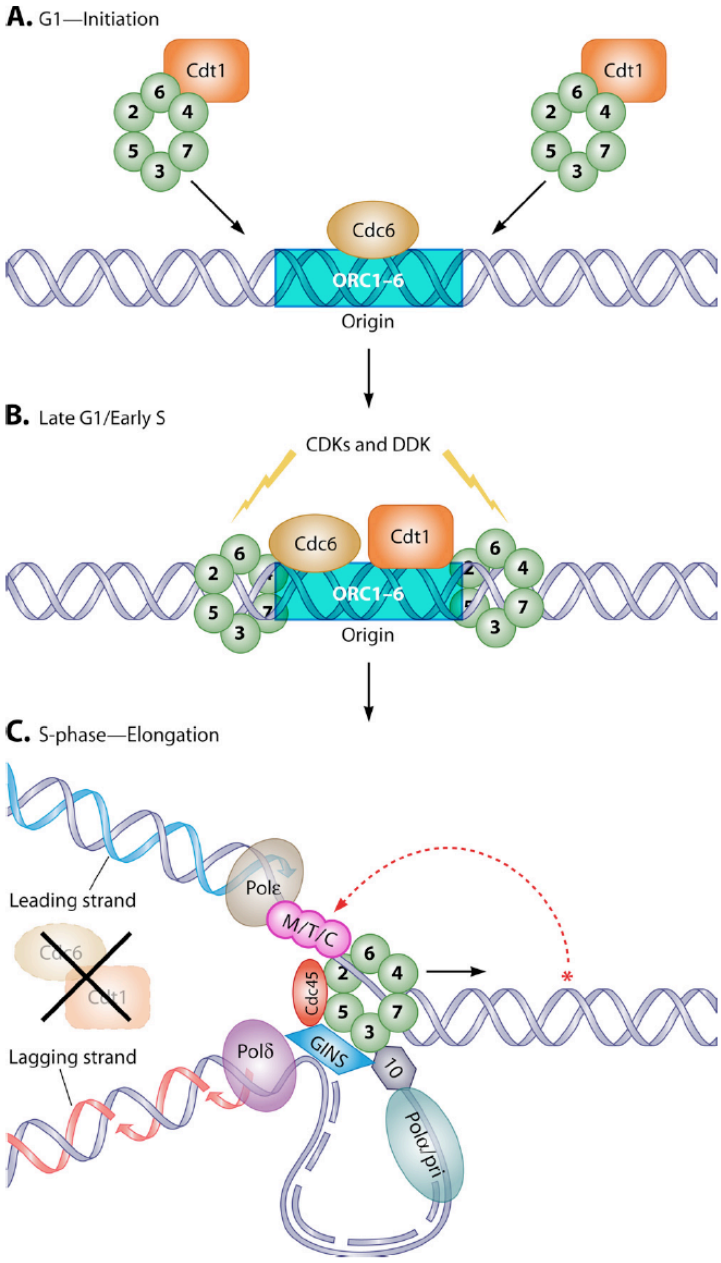

Figure 4.6 (Taken from Bochman et al. Microbiology and molecular biology reviews dec 2009) MCM involvement in eukaryotic DNA replication initiation and elongation.

The eukaryotic helicase MCM2-7 is a heterohexamer containing 6 distinct and essential subunits. The heterohexameric complex is completely conserved among all eukaryotes implying the 6 subunits are all of functional importance. There are different hypotheses to explain this, firstly that the active AAA ATPase sites are biochemically equivalent but the divergent N and C termini in each subunit have different functions. Alternatively the 6 subunits may be catalytically distinct and contribute differentially to the DNA unwinding. This latter hypothesis is currently favoured as the same mutation within the active site in different subunits leads to different phenotypes [130]. However it is now apparent that MCMs do have many functions beyond replication. There is an abundance of MCMs over and above the quantity required to licence DNA replication origins and function as the replicative helicase. They are also widely distributed in regions outside of replicating DNA. This has lead to the suggestion that MCMs may affect transcription and influence the epigenetic code by modifying chromatin remodeling.

Although the heterohexamer MCM2-7 has been identified as the replicative helicase, the dimeric heterotrimer MCM4/6/7 has been shown to exist as a subcomplex that exhibits helicase activity *in vitro* which is inhibited by the addition of MCM2 or the MCM5/3 dimer. This suggests that MCM4, MCM6 and MCM7 are needed for helicase activity but MCM2, MCM3 and MCM5 act as negative regulators *in vitro*. However *in vivo* it appears that active sites contributed by MCM4, MCM6 and MCM7 are largely required for ATP hydrolysis, ssDNA binding and helicase activity while MCM2, MCM3 and MCM5 play a secondary role possibly involving the coordination of ATP hydrolysis with DNA unwinding [131].

MCM4 has been shown to have a number of independent functions within the MCM2-7 complex. DDK phosphorylation of MCM4 has been shown to assist Cdc45 loading [137]. Consensus sites for CDKs are found in most MCM4 families and CDK phosphorylation of MCM4 is required for S-phase initiation however MCM4 phosphorylation appears to have many different functions and effects. Phosphorylation of human MCM4 occurs at numerous N-terminal serines and threonines including Ser-3, -32, -54 and -88 and Thr-7, -19 and -110. Phosphorylation by CDK1 and CDK2 at these sites in HeLa cells has been shown to vary with the cell cycle [138]. Phosphorylation is greatly enhanced in the G2 and M phases at sites Thr-7, -19, Ser-32, -54, -88 and Thr-110 whereas phosphorylation of Ser-3 is detected only during the interphase. Phosphorylated MCM4 exhibits different affinities for chromatin; MCM4 phosphorylated at sites 3 and 32 was not generally colocalized with replicating DNA; MCM4 phosphorylated at site 32 was enriched in the nucleolus throughout the cell cycle. In general, hypophosphorylation of MCM2, MCM3 and MCM4 correlates with MCM chromatin binding, however mutation of CDK sites in a single MCM, at least in yeasts, is not sufficient to disrupt replication control, indicating the presence of multiple levels of redundant control [131]. *In vitro* studies indicate that CDK-dependent phosphorylation of MCM4 also disrupts the helicase activity of the MCM2-7 complex. MCM4 has also been postulated to be the target of the checkpoint kinase pathway in response to replication arrest [139]. Taken together these data suggest that phosphorylation of MCM4 may have several distinct and site-specific roles in the function of DNA replication during the mammalian cell cycle.

A viable mutant allele of *Mcm4*, Chaos 3 (chromosome aberrations occurring spontaneously 3), was identified in a forward genetic screen used to discover potential

novel genes involved in chromosomal instability and therefore potentially associated with cancer risk. This screen utilizes chemical mutagenesis using N-ethyl-N-nitrosourea (ENU), an alkylating agent that acts by transferring the ethyl group of ENU to nucleobases (usually thymine) in nucleic acids. This agent is a highly potent mutagen and can produce a mutation rate as high as $1.5x10^{-3}$ in mouse spermatagonial cells [140]. ENU produces point mutations and can be used to isolate both dominant and recessive mutations that lead to chromosomal instability. Micronuclei can arise from acentric chromosome fragments or whole chromosomes that have not been incorporated in the main nuclei at cell division and therefore act as a measure of *in vivo* chromosomal damage [101]. Flow cytometry is a high-throughput assay that measures micronucleus formation by exposing cells to anti-CD71, which specifically labels micronucleated reticulocytes allowing their detection, and therefore is a proxy measure of chromosomal instability induced by potential mutagens. This screen identified Chaos 3 as a mouse chromosome instability mutation [101]

Mcm4 Chaos 3 encodes a mutation in an evolutionarily invariant amino acid (F345I). Heterozygote mice show mildly elevated (2 - 5 fold) micronucleus frequencies compared to wild type animals. Homozygotes show a significant increase with over 7% of erythrocytes containing micronuclei. The authors created the corresponding allele in budding yeast and showed a minichromosome loss phenotype. *Mcm4* null mutations are lethal; homozygosity for a disrupted *Mcm4* allele ($MCM4^{-}$) results in pre-implantation lethality. However, $Mcm4^{Chaos3/-}$ embryos died late in gestation indicating $Mcm4^{Chaos\ 3}$ is hypomorphic. Initially, $Mcm4^{Chaos3/Chaos3}$ mice were fertile and overtly indistinguishable from wild type littermates apart from the increased

micronucleus formation. However, more than 80% of females subsequently died due to mammary adenocarcinomas, with a mean latency of 12 months [141].

It is clear that any mutation in *MCM4* is likely to have significant phenotypic consequences given its essential role in DNA replication and genome stability. The mutation identified in the patient cohort was predicted to give rise to a foreshortened open reading frame and a prematurely terminated protein of only 27 amino acids, effectively abolishing all MCM4 function. Loss of function *MCM4* mutations been shown to be incompatabile with survival in eukaryotes and therefore if the *MCM4* mutation identified here is indeed the causative mutation then the patients must be able to adapt in some way, possibly utilising an alternative transcriptional or translational start site down stream of the mutation. The results from experiments designed to investigate this are described in Chapter 5.

Chapter 5: Investigation of MCM4 protein production in patients

5.1 Introduction

MCM4, as part of the heterohexameric complex MCM2-7, is a fundamental contributor to the integrity of the eukaryotic genome. A mutation that effectively abolishes MCM4 function would be predicted to be lethal in every eukaryotic system, therefore raising the intriguing question as to how these patients are able to survive.

5.2 *MCM4* transcripts

Ensembl and UCSC were examined for alternative transcripts that may be unaffected by this mutation. There are 9 protein coding transcripts but only 3 MCM transcripts that include all functional domains of MCM4, MCM4-004 (ENST00000523944), -001 (ENST00000262105) and -003 (ENST00000396826) (Figure 5.1). Two of these transcripts are merged Ensembl/Havana (Sanger) transcripts that are also consensus coding sequences (CCDS); MCM4-004 (CCDS6143) and -001 (CCDS6143). This database is a collaborative effort to identify a core set of human and mouse protein coding regions that are consistently annotated and of high quality.

All three transcripts would be similarly affected by the splice site mutation identified, producing a prematurely terminated protein (illustrated in Figure 4.5). Transcripts MCM4-004 and -001 have slightly different N-terminal untranslated regions but start from the same initiating methionine and have the same protein sequence. Transcript MCM4-003 has a different mRNA sequence with 39 bases noted as intronic rather than exonic giving rise to an in-frame deletion of 13 amino acids (Figure 5.2 A and B). However this protein would be affected similarly to transcript -004 and -003 with

the mutation leading to a prematurely terminated protein. I could not detect any cDNA sequence consistent with MCM4-003 in patient or control samples (Figure 5.2C)

Figure 5.1

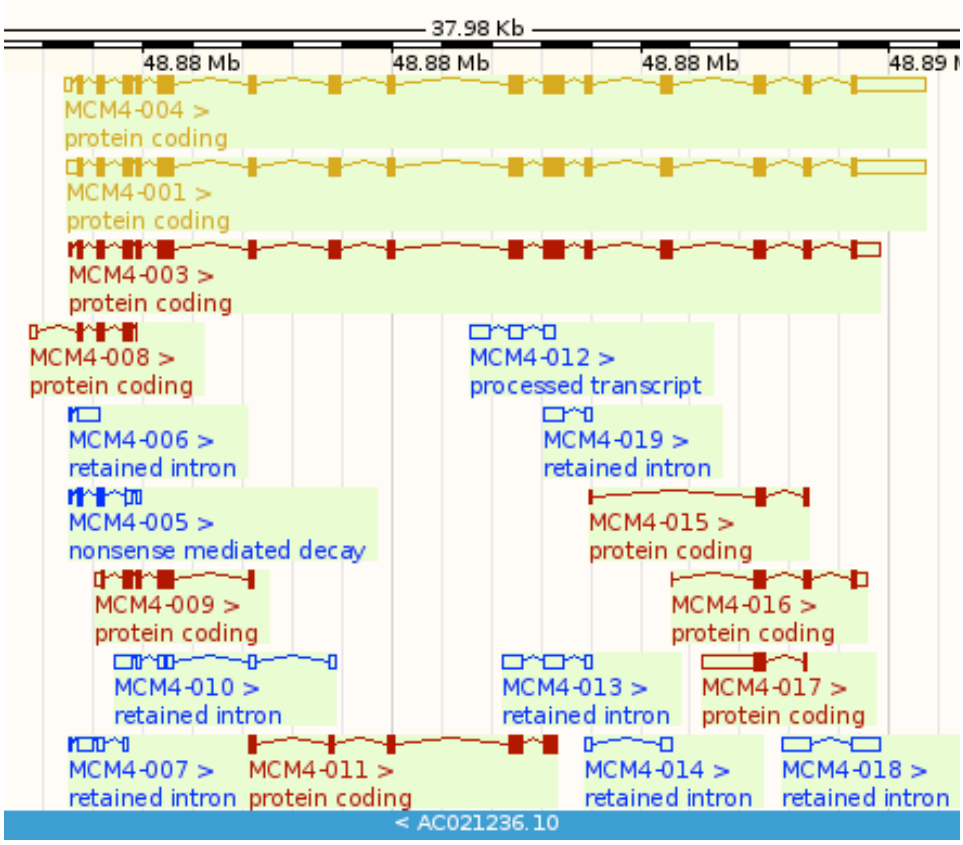

Figure 5.1 Schematic diagram showing all annotated MCM4 transcripts from the Ensembl database (www.ensembl.org). Red; protein coding, yellow; merged Ensembl/Havana, Blue; processed transcript.

Figure 5.2

A. MCM4-001/MCM4-004

...GTACTCCGAGCACTATGTCGTCCCCGGCGTCGACCCCGAGCCGCCGCGGCAGCCGGCGTG
GAAGGGCCACCCCCGCCCAGACGC
gtgagtcccccgagccgggcccactacagcccccggcgccgccccgtctgccctctcgcc
.............................aatccaggaaggccggccctgaaagttaat
ggctgtcttttctgttttgtgtgacacaag
CTCGGAGTGAGGATGCCAGGTCATCTCCCTCTCAGAGACGTAGAGGCGAGGATTCCACCT
CCACGGGGGAGTTGCAGCCGATGCCAACCTCGCCTGGAGTGGACCTGCAGAGCCCTGCTG
CGCAGGACGTGCTGTTTTCCAGCCCTCCCCAAATGCATTCTTCAG
gtgcgtgtctgaagatcttggttttgctgtgcttgatacacagctgatgctttatctgct
.............................caacatgctgtaatttcaggtttgatatgc
caccagaatttcctaattttgtttttatag
CTATCCCTCTTGACTTTGATGTTAGTTCACCACTGACATACGGCACTCCCAGCTCTCGGG
TAGAGGGAACCCCAAGAAGTGGTGTTAGGGGCACACCTGTGAGACAGAGGCCTGACCTGG
GCTCTGCACAGAAGGGCCTGCAAGTGGATCTGCAGTCTGACGGG
gtgagtatgcagtctcctgaaaccatcttatggcgggtatcatgtgggtaactctgtttt
catgattctgtcatgtttttctgtgtag

B. MCM4-003

...GTACTCCGAGCACTATGTCGTCCCCGGCGTCGACCCCGAGCCGCCGCGGCAGCCGGCGTG
GAAGGGCCACCCCCGCCCAGACGC
gtgagtcccccgagccgggcccactacagcccccggcgccgccccgtctgccctctcgcc
.............................aatccaggaaggccggccctgaaagttaat
ggctgtcttttctgttttgtgtgacacaag
CTCGGAGTGAGGATGCCAGGTCATCTCCCTCTCAGAGACGTAGAGGCGAGGATTCCACCT
CCACGGGGGAGTTGCAGCCGATGCCAACCTCGCCTGGAGTGGACCTGCAGAGCCCTGCTG
CGCAGGACGTGCTGTTTTCCAGCCCTCCCCAAATGCATTCTTCAG
gtgcgtgtctgaagatcttggttttgctgtgcttgatacacagctgatgctttatctgct
.............................caacatgctgtaatttcaggtttgatatgc
caccagaatttcctaattttgtttttatag
CTATCCCTCTTGACTTTGATGTTAgttcaccactgacatacggcactcccagctctcgggtag
AGGGAACCCCAAGAAGTGGTGTTAGGGGCACACCTGTGAGACAGAGGCCTGACCTGGGCT
CTGCACAGAAGGGCCTGCAAGTGGATCTGCAGTCTGACGGG
gtgagtatgcagtctcctgaaaccatcttatggcgggtatcatgtgggtaactctgtttt
catgattctgtcatgtttttctgtgtag

C.

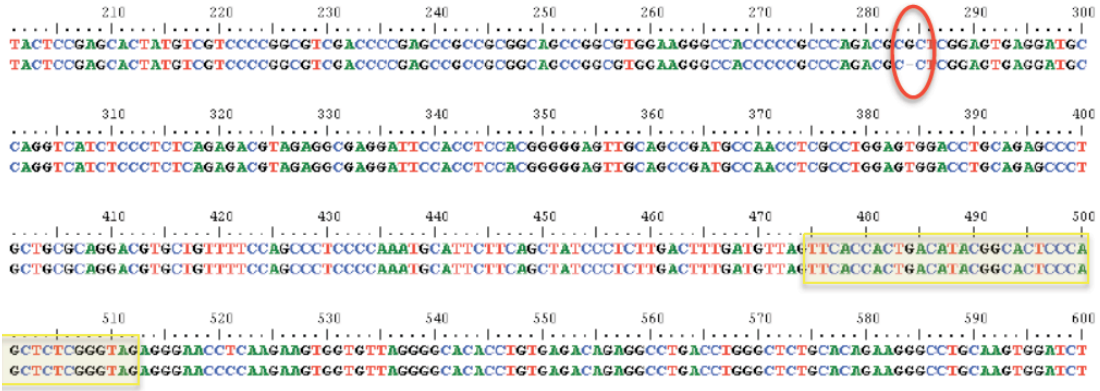

Figure 5.2 A. Transcript MCM4-001/-004. B. Transcript MCM4-003. Bases noted as intronic in MCM4-003 but exonic in MCM4-004 and -001 are highlighted in yellow. Upper case; exons, lower case; introns, purple; untranslated. C. Sequencing of patient cDNA confirming

transcript -001 /-004 is identified in patient sample – exonic region not present in transcript 003 highlighted.

5.3 MCM4 protein in patient and control lymphocytes and human cell lines

Cell lysates from control and patient populations were then examined to try to identify if MCM4 protein was absent from patient cells. Peripheral mononuclear cells were extracted from whole blood using a gradient density centrifugation technique as described in detail (section 2.6 materials and methods). These cells, including lymphocytes (T cells, B cells and NK cells), monocytes and macrophages, were washed, lysed and the supernatant added to an equal volume of loading buffer.

Cell lysates from patients and unaffected human controls were immunoblotted for MCM4, using a polyclonal C-terminal anti-MCM4 antibody (Abcam) that was raised against the exon 14 peptide sequence. This identified two major proteins migrating at approximately 96kDa and 90kDa, the smaller 90 kDA protein appearing to run as a doublet in some samples (Figure 5.3). Patient samples showed only one major MCM4 species at 90kDa (Figure 5.3A and B). Cell lysates from the human cell lines, HEK293 (human kidney cell line), H295R (human cancer adrenal cell line) and SHSY5Y (human neuroblastoma cell line) were also immunoblotted using the same MCM4 antibody. In these images it is easier to visualise the 2 separate smaller MCM4 isoforms present (Figure 5.3C).

To confirm that the faster migrating bands seen on immunoblotting with MCM4 antibody were MCM4 isoforms and not non-specific bands a different MCM4 antibody was used but unfortunately this gave rise to multiple non-specific bands and so was not helpful. Therefore small interfering RNAs (siRNAs) designed against

MCM4 were used in an effort to cause depletion of both wild type full length MCM4 and also the smaller putative MCM4 isoforms. siRNAs s69687 and s8592 (Applied Biosystems) that specifically target *MCM4* at exon 5 and exon 12 respectively were transfected at concentrations of 50nM into HEK293T cells, as a control a scrambled siRNA was transfected into HEK293T cells. After 48 hours the cells were harvested and cell lysates were immunoblotted for MCM4. The MCM4 specific siRNA leads to reduced expression of both full length wild type MCM4 and also the smaller MCM4 isoforms suggesting that this band is indeed MCM4 and not a non-specific artefact (Figure 5.4). Cell lysates were also immunoblotted for β-Actin as a loading control.

Figure 5.3

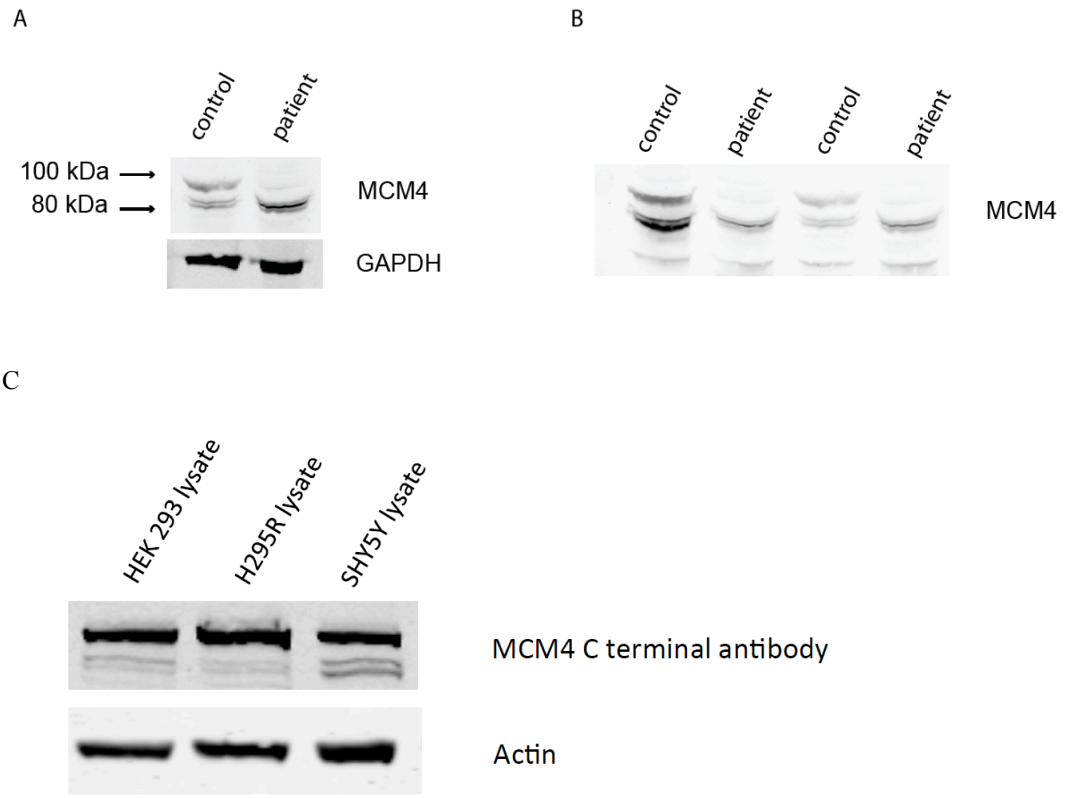

Figure 5.3 Cell lysates from both control and patient lymphocytes show evidence of MCM4 protein. A and B. Lysates from patient and control human lymphocytes were immunoblotted with an anti- MCM4 antibody. Whilst control subjects have two main protein species of approximately 96 and 90kDa, the predicted full-length 96kD product is missing in the

patients. There is also a faster migrating band present in some control and patient samples that is approximately 75kDa. C. Lysates from human cell lines show evidence of 3 MCM4 species, with 2 smaller MCM4 isoforms present.

Figure 5.4

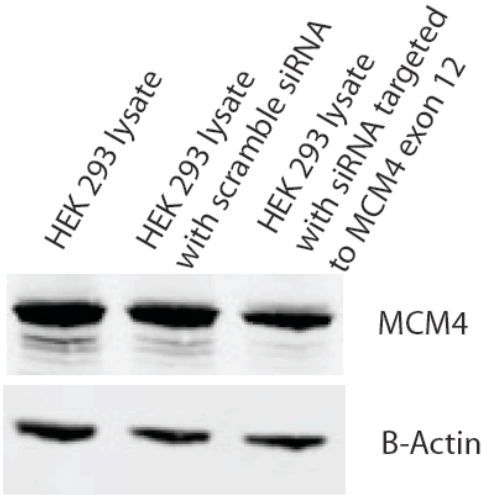

Figure 5.4 siRNA targeted to exon 12 of *MCM4* shows depletion of both 96kDa isoform and the smaller MCM4 isoforms at approximately 90kDa.

5.4 Translation of MCM4 can occur from an alternative downstream methionine

As discussed above there is no alternative splice variant reported that would explain these smaller MCM4 species. I hypothesized that alternative translational start sites may be present to explain the 2 smaller isoforms of MCM4 present in patient samples. Expression vectors for C-terminally HA-tagged full length MCM4 and MCM4 in which the initiating methionine codon was abolished by site-directed mutagenesis (M1X) were transiently transfected into HEK293 cells and the cell lysates were immunoblotted with both HA and MCM4 antibodies. M1X expression resulted in a smaller MCM4 species of approximately 90kDa that also appeared to be a doublet and that corresponded in size to that seen in control samples indicating that the shorter

forms seen could arise by alternative initiation of translation from a downstream initiating methionine codon (Figure 5.5).

Figure 5.5

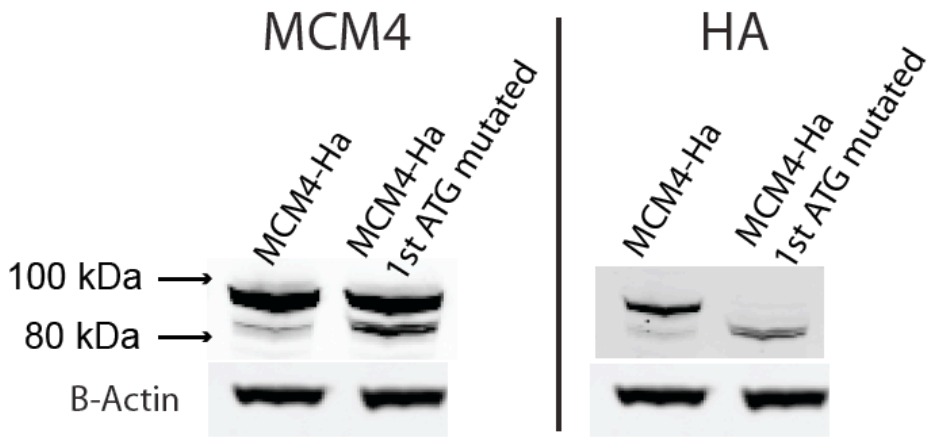

Figure 5.5 HEK293 cells were transfected with full length MCM4 or MCM4 with the first methionine mutated, both of which were tagged with a C-terminal HA tag. The lysates were then blotted with both MCM4 antibody (left panel) and HA antibody (right panel). Abolition of the initiating methionine of MCM4 leads to expression of a smaller MCM4 species of approximately 90kDa detected using the HA antibody (right panel). In the left panel please note the full length MCM4 at 96kDa detected in cells that have been transfected with MCM4 with the first methionine mutated (M1X) is endogenous MCM4.

There are multiple in-frame methionines down stream of the initiating methionine (M1); the first 2 down stream methionines would produce 2 proteins of approximately the correct size. The protein from the second methionine (M2) at amino acid position 51 (exon 2) has a predicted molecular weight of 91 kDa, the protein from the third methionine (M3) at amino acid position 75 (exon 2) has a predicted molecular weight of 89 kDa. This small difference in size correlates to the small difference in size seen in all blots. Both M2 and M3 are also C-terminal to the mutation and would therefore be unaffected by the insertion (Figure 4.5). The third downstream in-frame

methionine at position 194 (exon 5) produces a protein of approximately 75 kDa, which is too small to be either of the isoforms seen consistently in patient and control samples but may explain the smaller MCM4 protein seen intermittently in patient and control lymphocytes (Figure 5.3B).

5.5 MCM4 isoforms identified in cell lysates correspond in size to MCM4 constructs beginning from the 1st, 2nd, 3rd and 4th in-frame methionines.

cDNAs encoding MCM4 isoforms beginning at the 1st (described above), 2nd, 3rd and 4th in-frame methionines were generated by PCR and then inserted into the triple FLAG expression vector. These constructs were transiently expressed in HEK293 cells, the cell lysates collected and immunoblotted. The 1st 2nd and 3rd in-frame methionines produced proteins corresponding in size to those seen *in vivo* suggesting that the faster migrating proteins observed in patients may result from internal initiation from the second and third in frame ATG (Figure 5.6A). The 4th in-frame methionine gives rise to a much smaller protein of approximately 75kDa as expected, however this isoform may be present in some patient and control samples (Figure 5.3B and 5.6B).

Figure 5.6

A.

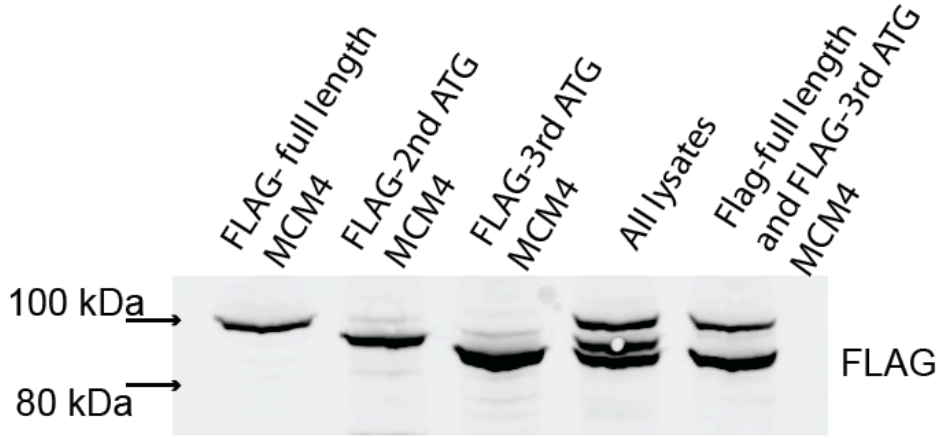

B

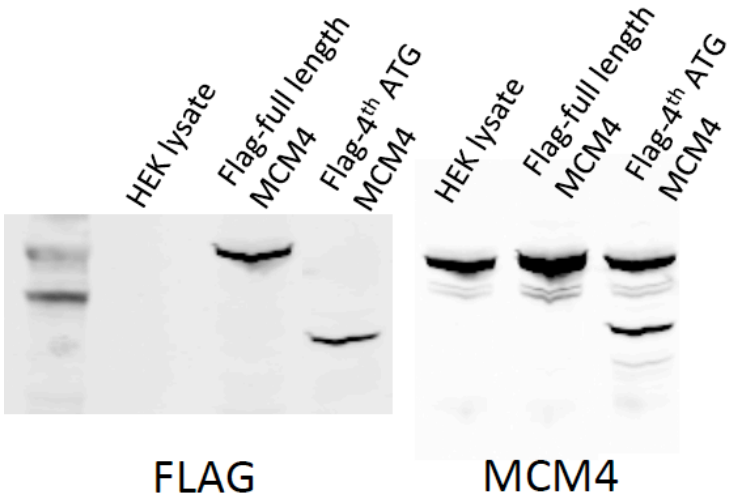

Figure 5.6 A. Flag-tagged full length MCM4 and constructs beginning at the second and third in frame ATGs were expressed in HEK293 cells. Lysates from each were run individually (lanes1-3), altogether (lane 4) or in combination with the full length and 3rd ATG (lane 5) and immunoblotted using an anti-FLAG antibody. The relative mobility of the different species indicates that the smaller MCM4 species may be produced by translation from the 2nd and 3rd in frame ATG.

B. Flag-tagged full length MCM4 and constructs beginning at the 4th in frame ATG were expressed in HEK293 cells. Lysates from wild type cells, cells with FLAG-full length MCM4 and FLAG-4th ATG MCM4 were each run individually (lanes1-3), and immunoblotted using an anti-FLAG and anti-MCM4 antibody. The relative mobility of the different species indicates that the smaller MCM4 species is too small to be due to internal initiation from the 4th in-frame ATG. Similarly to Figure 5.5, the right hand panel immunoblotted with MCM4

identifies endogenous MCM4 in cells that are transfected with an MCM4 construct beginning at the 4th in frame ATG but this is not identified when immunoblotting with the FLAG antibody.

5.6 Smaller MCM4 isoforms lack the N-terminus

The smaller protein isoforms were also seen in a number of human cell lines (Figure 5.3B) but was not detected by immunoblotting with an N-terminal antibody for MCM4 suggesting this smaller MCM4 protein lacks the N-terminus (Figure 5.7). The N–terminal antibody (Santa Cruz) is targeted to the first 300 amino acids of MCM4.

Figure 5.7

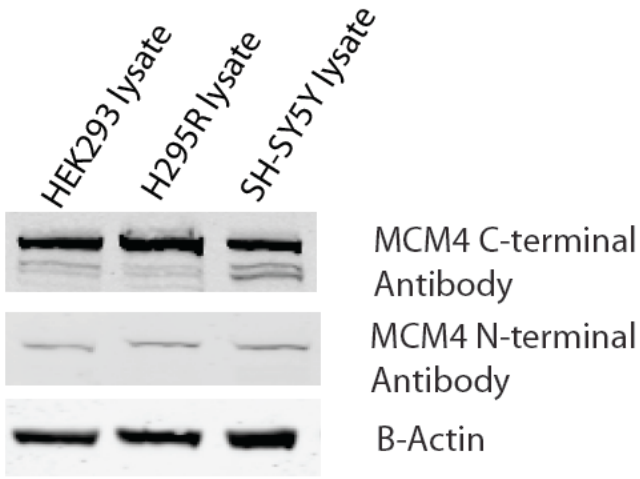

Figure 5.7 Different cell lysates show evidence of both the major full length and smaller MCM4 isoforms when immunoblotted with the MCM4 C-terminal antibody. However when the same lysates are immunoblotted with the N-terminal antibody the smaller MCM4 isoforms are no longer seen suggesting that the smaller isoforms lack the N-terminus of MCM4.

5.7 Discussion

These experiments demonstrate the loss of the 96kDa MCM4 isoform in patients confirming the loss of translation of full length, wild type MCM4 protein. This is likely to be due to the frameshift introduced by the extra guanine incorporated into the

mutant mRNA (c.71-1insG). As predicted, given the essential requirement of MCM4 in DNA replication, the patients show evidence of alternative translation and slightly smaller MCM4 isoforms are present in cell lysates. Additional smaller isoforms have been reported in some previous work on MCM4 [142] but in other MCM4 papers the western blots are cropped to show only the full length MCM4. In one paper by Chuang *et al.* it is apparent there are additional bands below the wild type (Figure 1 A of their paper) but this is not completely clear as again the blot is cut just at this point [102]. Although I could not use alternative MCM4 antibodies to confirm these proteins were MCM4 specific, siRNA targeted to exon 12 of MCM4 shows depletion of wild type 96 kDa isoforms as well as the smaller isoforms indicating that these are indeed MCM4 and not nonspecific artefacts.

There are no alternative cDNA transcripts present that could explain these proteins and so alternative translational start sites downstream of the mutation were examined. When the initiating methionine in MCM4 is mutated alternative translation can occur giving rise to two slightly smaller MCM4 isoforms of approximately the same size as those seen in patients and control cell lines. This suggests that these smaller isoforms are indeed from internal initiation from downstream methionines.

Initially it was felt that the MCM4 doublet observed in the immunoblot of patient and control leukocytes may be due to a post translational modification of one MCM4 isoform, for example phosphorylation, as there is evidence for multiple phosphorylation sites on MCM4 [131, 142]. However the FLAG-tag experiment illustrates that the difference in size between MCM4 from the first methionine and MCM4 from the 2nd and 3rd methionine is similar to the difference in size between

the 3 isoforms seen in control samples therefore suggesting that the MCM4 isoforms seen in patient samples may be due to internal initiation from the second and third in-frame methionines. Furthermore an N-terminal MCM4 monoclonal antibody that was raised against the first 300 amino acids of MCM4 does not detect the smaller isoforms indicating that they are missing this N-terminal epitope of MCM4. This is consistent with the location of the mutation and the alternative translational start site downstream, producing proteins missing the N-terminus. Taken together, these studies strongly suggest that the smaller MCM4 species arise from internal initiation.

As *Mcm4* knockout in animals is lethal it is likely that the smaller MCM4 isoform rescues the patients from a lethal phenotype, ie the full length isoform is required for adrenal cortisol production but alternative isoforms are sufficient for alternate functions and to be compatible with life. In this regard it is important to note that both proposed proteins starting from amino acids 51 and 75 contain all the essential conserved C-terminal domains required for canonical MCM4 function including the 200 residue "MCM box" which includes the Walker A and B domains and the zinc and arginine fingers.

Single missense mutations in MCM4, eg Chaos 3 homozygous mice, in eukaryotic systems can lead to a severe phenotype. It is therefore surprising that a protein missing 51 or 71 amino acids is compatible with survival. However the mutations studied are generally in conserved areas that are functionally essential. The N-terminus of MCM4 is not well conserved. It is defined as the first 198 amino acids and studies have revealed that deletion of the first 130 amino acids is not lethal in eukaryotic cells [143]. Masai *et al.* investigated the function of N-terminally truncated

MCM4 mutants. They generated truncation mutants lacking the first 67, 130, 150 or 200 amino acids of MCM4 protein in fission yeast cells. The -67 and -130 truncated mutants were able to function normally but the -150 mutant showed a reduced growth rate and the -200 mutant was not viable. The residues conserved in MCM4 start at position 158 suggesting that the -200 mutant is lacking some essential conserved residues required for MCM4 function.

This group also investigated the function of the N-terminal domain of MCM4. The initiation of DNA replication is strictly controlled by G1 cell cycle signals that are activated or suppressed by extracellular growth or differentiation signals respectively. The G1 cell cycle signals regulate Cdk-cyclins and ultimately protein kinases. Cdc7-Dbf4 is among those activated by G1 signals and is known to play a critical role in the activation of DNA replication origins. The N-terminal region of MCM4 is highly enriched for serine/threonine residues including specific (S/T)(S/T)P clusters. Masai *et al*. showed that specific residues in the MCM4 N-terminal segment can be phosphorylated by Cdc7 kinase *in vivo* and *in vitro*. They showed that both Cdc7 and Cdk phosphorylate MCM4 and that Cdc7 stimulates loading of Cdc45 onto the chromatin through phosphorylation of the N-terminus of MCM4. Although the N-terminus is not well conserved throughout species, multiple (S/T)(S/T)P clusters are found in many species suggesting that Cdc7-phosphorylation of the MCM4 N-terminal domain and its role in recruitment of Cdc45 may be conserved throughout evolution. Cdc45 plays a crucial role in the initiation of DNA replication suggesting that phosphorylation of MCM4 is a key event for activation of replication origins.

MCM2 and MCM6 also contain putative phosphorylation sites in their N-terminal domains. Mutation or deletion of these sites in just one MCM has no effect, but deletion in all 3 MCMs results in loss of viability. Taken together this suggests that phosphorylation of MCM2, MCM4 or MCM6 plays functionally important but potentially redundant roles in recruitment of replication factors including Cdc45 onto the chromatin. In contrast it has been reported that Cdc2 phosphorylates the chromatin free forms of MCM4 through its N-terminus during the G2/M stages of the cell cycle to prevent re-association with chromatin [144]. This role, which has not been shown to be replicated by MCM2 or MCM6, is a potentially important method of regulation, limiting DNA replication to once per cell cycle and preventing abnormal re-replication.

This provides a hypothesis that patients expressing only N-terminally truncated MCM4 isoforms lacking either the first 51 or 75 amino acids may be able to survive by utilising usually redundant phosphorylation sites on MCM2 and MCM6. However, the loss of the optimum phosphorylation sites on MCM4 would clearly have an effect on cell cycle regulation and most likely initiation of DNA replication. Patients could also have potentially lost an important mechanism of regulation that helps to limit initiation of DNA replication to once per cell cycle. Together these defects are likely to have substantial effects on patient cells including interfering with origin licensing, causing cell cycle defects and chromosomal damage such as breaks and gaps, all simultaneously leading to replication stress and genomic instability. This is evident in patients; lymphocytes treated with diepoxybutane show increased levels of chromosomal fragility compared to wild type controls. This is clearly of concern for the patients future health as genomic instability has been shown to lead to increased

incidence of cancer both in animal models with MCM4 defects and in humans who have other disorders of DNA replication [141, 145, 146].

Chapter 6: Adrenal histology in a MCM4 depleted mouse model, *Mcm4*$^{Chaos3/-}$ *Mcm3*$^{-/+}$

6.1 Introduction

MCM4 is a ubiquitously expressed protein that forms the pre-replication complex together with MCM2-7, the origin recognition complex proteins ORC 1-6, CDT1 and CDC6. It is surprising that a mutation in *MCM4* would give rise to specific developmental defects such as adrenal failure although this phenomenon has been previously reported with defects in other subunits of the replication complex, for example Meier Gorlin Syndrome [147]. This syndrome is caused by mutations in ORC1-6 and is associated with distinct defects including absent or hypoplastic patella and markedly small ears as well as pre- and postnatal growth failure and microcephaly.

Adrenal glands from affected patients were not available for study. In an attempt to elucidate the mechanism of adrenal failure caused by a defect in MCM4 a collaboration was established with a group from Cornell University, Ithaca, New York, USA who had already reported a Mcm4 depleted mouse model. The mice have previously been reported in detail and are described in the methods section [101, 102, 141]. Briefly, to generate the mice analyzed here, mice of the genotypes *Mcm4*$^{Chaos3/Chaos3}$ (chromosome aberrations occurring spontaneously 3) and *Mcm4*$^{+/-}$ *Mcm3*$^{+/-}$ were crossed to generate the control (*Mcm4*$^{Chaos3/+}$ *Mcm3*$^{+/-}$) and test (*Mcm4*$^{Chaos3/-}$ *Mcm3*$^{+/-}$) animals.

6.2 Test *Mcm4*$^{Chaos3/-}$ *Mcm3*$^{+/-}$ animals

A mutant hypomorphic allele of *Mcm4*, *Chaos3*, leads to genomic instability and cancer in mice [141]. Chaos 3 is a point mutation changing phenyalanine to isoleucine at residue 345, an amino acid conserved across diverse eukaryotes and important for interaction between MCM4 and other MCMs. As previously discussed in chapter 4 (section 4.3) micronucleus frequencies act as a measure of *in vivo* chromosomal damage and *Mcm4*$^{Chaos3/+}$ heterozygote mice show mildly increased micronuclei frequency compared to wild type (2 to 5 fold) whereas homozygotes show a marked (approximately 20 fold) increase over wild type. Young Chaos 3 heterozygotes and homozygote mice are overtly indistinguishable from wild type littermates but greater than 80% of female homozygotes die with mammary adenocarcinomas within 12 months [141].

The same group generated *Mcm4*$^{+/-}$ heterozygote mice using a gene trap vector inserted between exons 12 and 13 of *Mcm4* disrupting the highly conserved MCM domain (Figure 6.1). *Mcm4*$^{+/-}$ heterozygote mice appeared normal and did not have higher levels of spontaneous micronuclei. Homozygosity for a disrupted *Mcm4* allele (*Mcm4*$^{-/-}$) caused pre-implantation lethality. *Mcm4*$^{Chaos3/-}$ embryos died late in gestation at approximately 14.5 days post coitum and most were growth retarded [141].

Mouse embryonic fibroblasts from *Mcm4*$^{+/-}$ heterozygote mice show normal levels of MCM4 but *Mcm4*$^{Chaos3/Chaos3}$ mice have reduced levels of MCM4. *Mcm4*$^{Chaos3/-}$ have markedly reduced levels MCM4 indicating the F345I mutation appears to destabilise the MCM4 protein [141]. Genetic reduction of MCM3 (*Mcm3* heterozygosity)

surprisingly rescued the near 100% lethality of *Mcm4*$^{Chaos3/-}$ mice giving nearly 6 fold increased viability [102]. MCM3 mediates nuclear export of MCM2-7 suggesting that it is the reduced export and therefore increased levels of chromatin bound MCM that rescues the embryos. *Mcm4*$^{Chaos3/-}$ *Mcm3*$^{+/-}$ mice also have high levels of genomic instability, indicated by elevated micronuclei in red blood cells. Furthermore they exhibit severe growth failure and increased susceptibility to the development of, primarily, mammary tumours, histiocytic sarcomas, and lymphomas, depending on genetic background. These animals provide the closest viable animal model to our patient cohort, in that MCM4 levels were reduced to the lowest levels compatible with life.

Figure 6.1

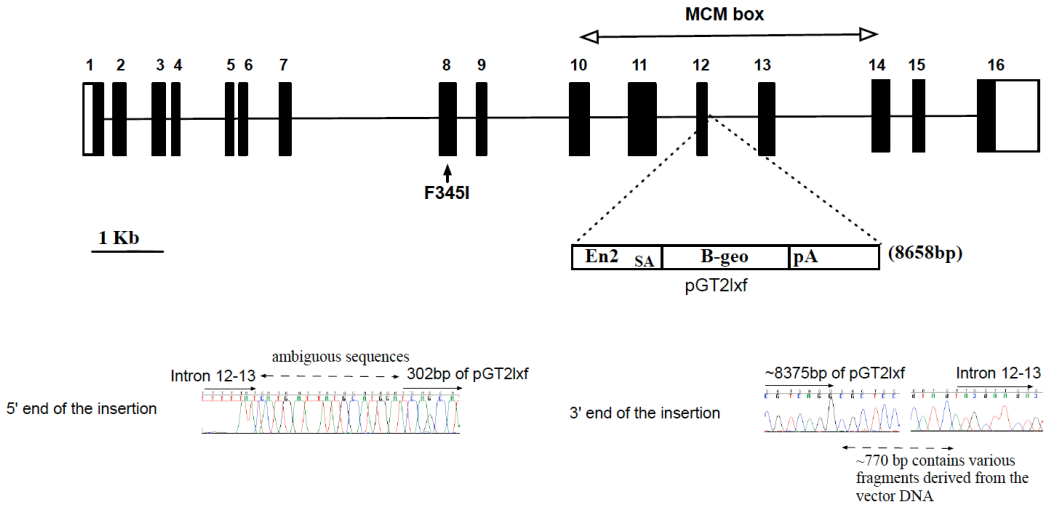

Figure 6.1 (Taken from *Shima et al*.[141]; supplementary Figure 1) "Structure of the Mcm4 gene-trap allele. Mcm4 exons are shown with filled rectangles (5' and 3' YTR regions are left blank). The highly conserved MCM box is shown spanning exons 10-14. The gene trap vector contains En2 (engrailed 2) intron and subsequent splice acceptor (SA), and beta-geo (B-geo) reporter gene along with SV40 polyadenylation signal (pA). B-geo is a fusion gene of beta-galactosidase and neomycin resistant gene. The pGT21xf vector is inserted right after exon 12, thus efficient splicing of transcripts from exon 12 to the splice acceptor in the gene trap vector disrupts the MCM box. Both 5' and 3' ends of the insertion were confirmed by

genomic PCR as shown with the sequence traces. There were insertions of some ambiguous sequences at both ends of the insertion site. However there was no evidence for deletions that may be caused by the insertion. The F345I mutation is also indicated."

6.3 Analysis of adrenals from Mcm4 mutant mouse models

Adrenals from 3.5 month old wild type littermates and also *Mcm4*$^{Chaos3/+}$*Mcm3*$^{-/+}$ mice were of normal size. Haematoxylin and eosin (H and E) staining revealed a normal morphology in both control animals, illustrated in figure 6.2 A, a', a'' and D, E, e'. In contrast H and E staining of adrenals from 2 different *Mcm4*$^{Chaos3/-}$ *Mcm3*$^{-/+}$ 3.5 month old animals revealed an abnormal adrenal histology characterised by small, tightly packed, intensely stained spindle-shaped cells in the cortex just beneath the capsule which appeared to be migrating into the cortex (figure 6.2 B, b', b'' and C, c',c'').

By 12 months of age these cells were abundant and in some areas spanned the cortex from the capsule to the medulla (Figure 6.3). Such changes were not observed in wild type littermate controls (not shown). The normal adrenal morphology in *Mcm4*$^{Chaos3/+}$*Mcm3*$^{-/+}$ control mice demonstrates that it is neither the Mcm3 heterozygosity nor the single Chaos 3 allele that leads to an abnormal adrenal morphology but the additional reduction in Mcm4 levels that leads to adrenal disease.

Figure 6.2

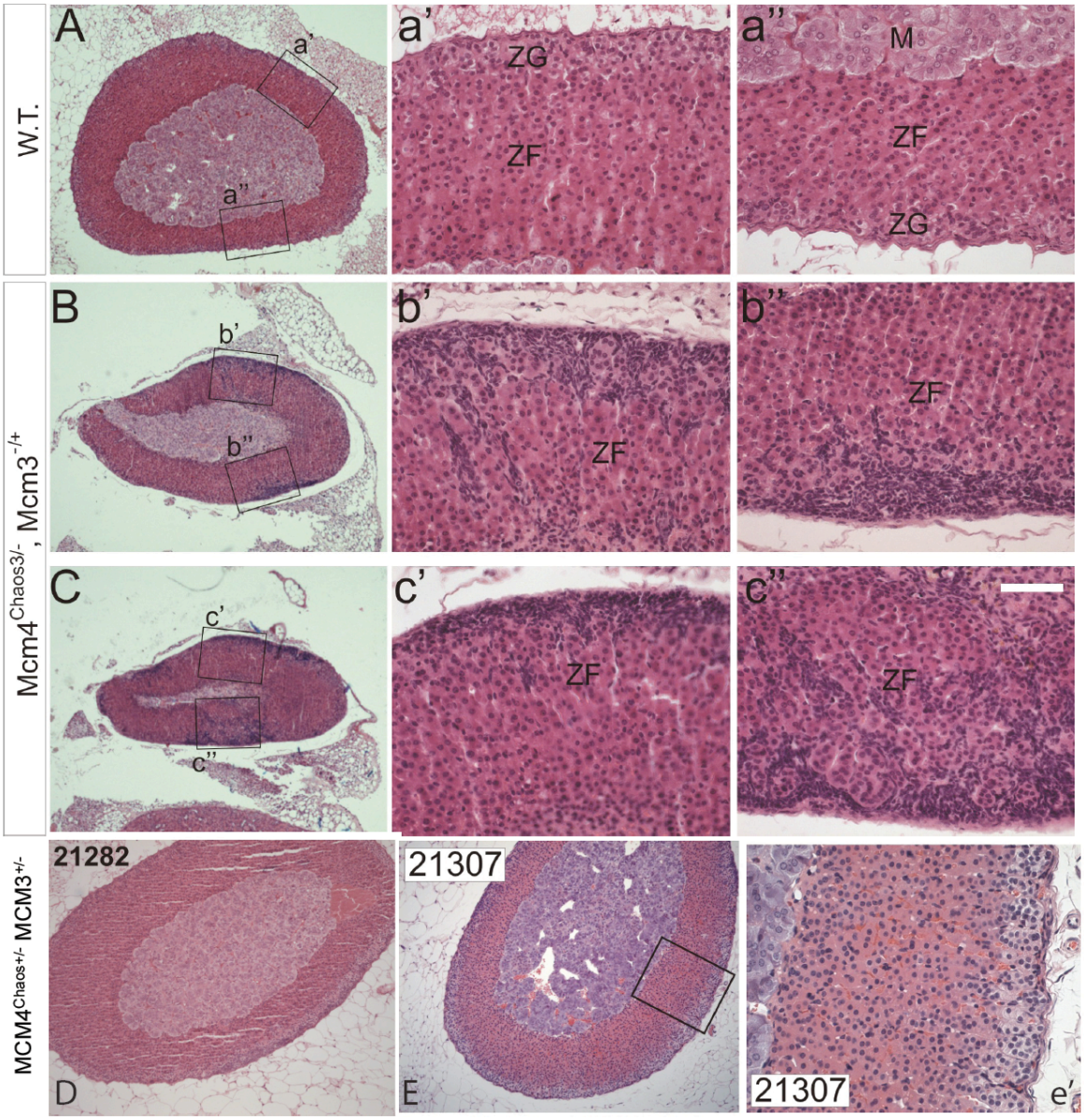

Figure 6.2 Analysis of adrenals from Mcm4 mutant mouse models. A, D and E. Adrenal cortices of wild type and *Mcm4*$^{Chaos3/+}$*Mcm3*$^{-/+}$ mice have a normal morphology. B, C. H/E staining of mutant *Mcm4*$^{Chaos3/-}$ *Mcm3*$^{-/+}$ mouse adrenals (B and C) shows they have an abnormal morphology with atypical spindle-shaped cells observed within the cortex. Abbreviations: ZG, Zona Glomerulosa; ZF, Zona Fasciculata; M, Medulla. Scale bar; 100 microns (numbers eg 21282 relate to individual mice identification numbers)

Figure 6.3

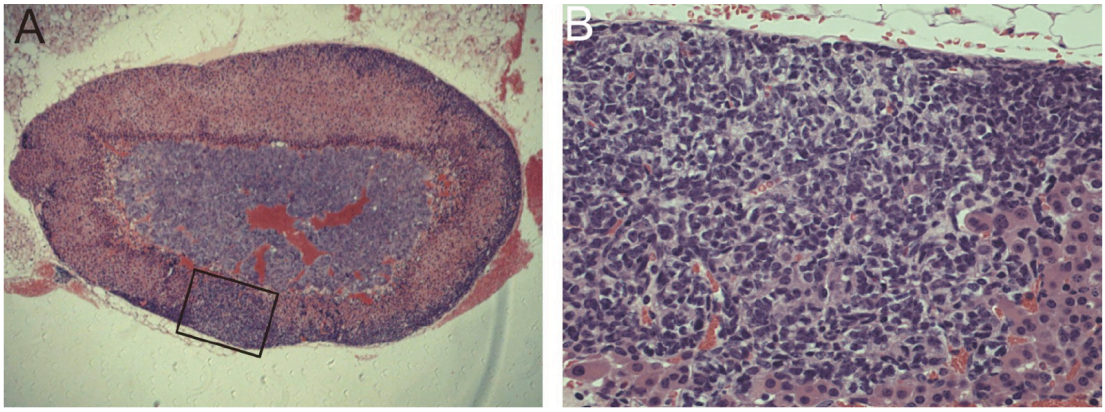

Figure 6.3 H/E staining of adrenals from *Mcm4*$^{Chaos3/-}$ *Mcm3*$^{-/+}$ mice show a more severe phenotype at 12 months. Image representative of findings in n=2 mice studied

Figure 6.4

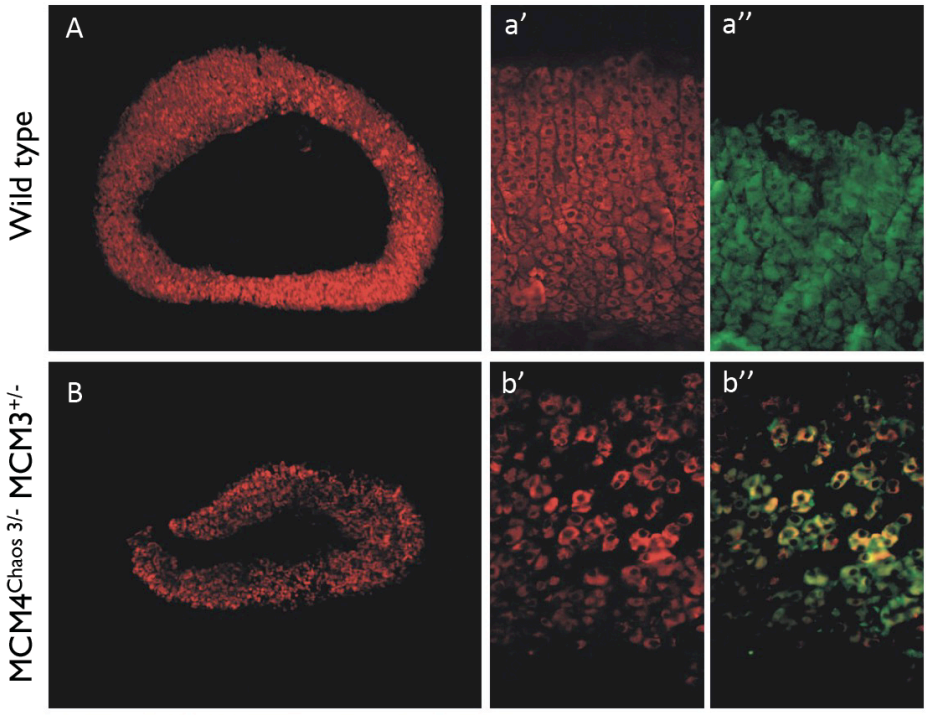

Figure 6.4 Atypical cells in the cortex are not steroidogenic. 3.5 month old wild type (A) and *Mcm4*$^{Chaos3/-}$ *Mcm3*$^{-/+}$ mice adrenals (B) were stained for CYP11A1 (A, a', B, b'), CYP11B1 (a'') and merged CYP11A1-B1 (b''). The atypical cells populating the ZF in *Mcm4*$^{Chaos3/-}$ *Mcm3*$^{-/+}$ adrenals are negative for both CYP11A1 and CYP11B1 (b'').

The expression of steroidogenic enzymes CYP11A1 and CYP11B1 was analysed in both control and mutant *Mcm4*$^{Chaos3/-}$ *Mcm3*$^{-/+}$ mice. This indicated that many cells in the mutants were negative for CYP11A1 (P450 side chain cleavage) (Figure 6.4B), in contrast to the wildtype (Figure 6.4A). Co-staining with the zona fasciculata marker CYP11B1 (P450 11β-hydroxylase) showed that these CYP11A1 negative cells were also CYP11B1 negative (Figure 6.4b'') implying they were not capable of producing glucocorticoid. Sections were also stained with the nuclear stain DAPI. This demonstrated that the cells not expressing CYP11A1 were morphologically identical to the spindle shaped cells seen in H and E staining confirming that the spindle-shaped cells are non-steroidogenic cells (Figure 6.2 and 6.5b').

Figure 6.5

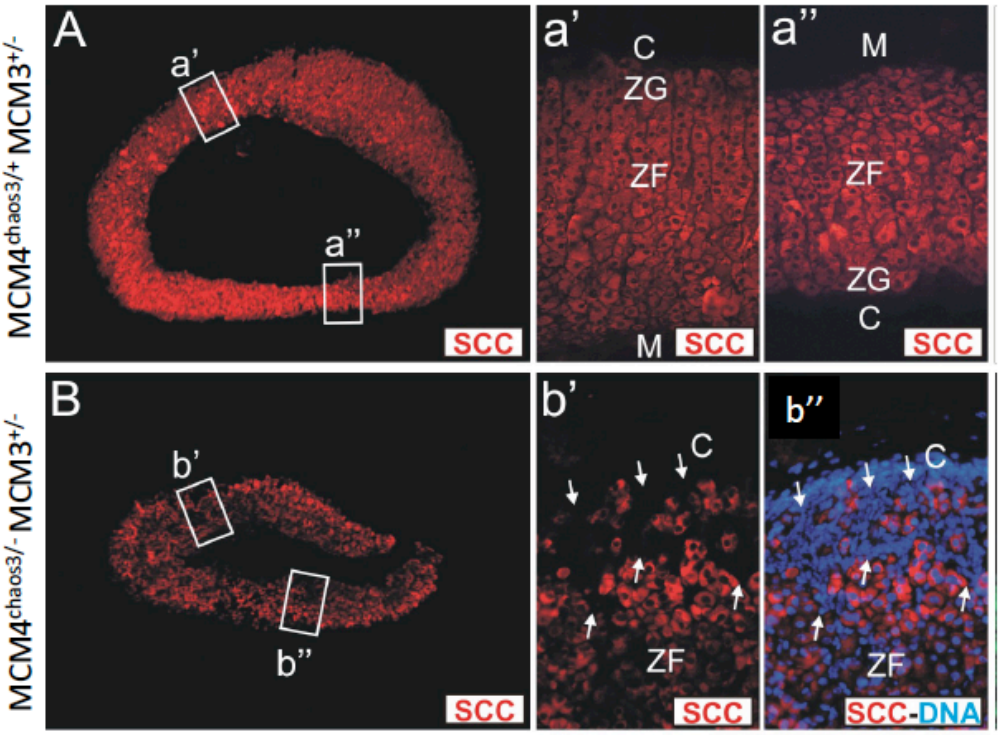

Figure 6.5 Spindle shaped cells are non-steroidogenic. 3.5 month wild type (A, a' and a'') and mutant *Mcm4*$^{Chaos3/-}$ *Mcm3*$^{-/+}$ adrenals were stained for CYP11A1 (SCC). Mutant *Mcm4*$^{Chaos3/-}$ *Mcm3*$^{-/+}$ adrenals were also stained with DAPI showing that the cells that stained negative for

CYP11A1 had the same morphology as the spindle shaped cells seen in previous H and E staining. Abbreviations: ZG, Zona Glomerulosa; ZF, Zona Fasciculata; M, Medulla; C. Capsule.

The adrenal capsule adjacent to these abnormal cells appeared to be much thinner in the adrenals from mutant *Mcm4*$^{Chaos3/-}$ *Mcm3*$^{-/+}$ mice compared to the adrenal capsule from wild type mice. This is particularly obvious in the higher power H and E images in Figure 6.6 where the wild type adrenals (A-H) have capsules showing the usual architecture, being two to three cell layers thick with thin, elongated nuclei arranged in the plane of the capsule, but the mutant adrenals have either a very thin capsule (P) or appear to have completely lost it (J, K) adjacent to the abnormal cells. Interestingly, the capsule adjacent to regions lacking the spindle cell phenotype appears to be relatively normal (O, Q). The juxtaposition of the thinning capsule and the non-steroidogenic cells in the mutant adrenals suggested that these cells might be capsular in origin.

To explore this further, expression of the mesenchymal capsule marker Gli1 was analysed by *in situ* hybridisation and indicated that the abnormal cells were Gli1 positive (Figure 6.7 provided by Dr Leo Guasti). Gli1 expression is dependent on hedgehog signaling and should only be seen in the capsule and a few subcapsular cells [21, 45]. No steroidogenic cells in wild type adrenals stain positive for Gli1 expression and the presence of many Gli1 positive cells within the adrenal cortex in the *Mcm4*$^{Chaos3/-}$ *Mcm3*$^{-/+}$ mutant mice is very abnormal.

Figure 6.6

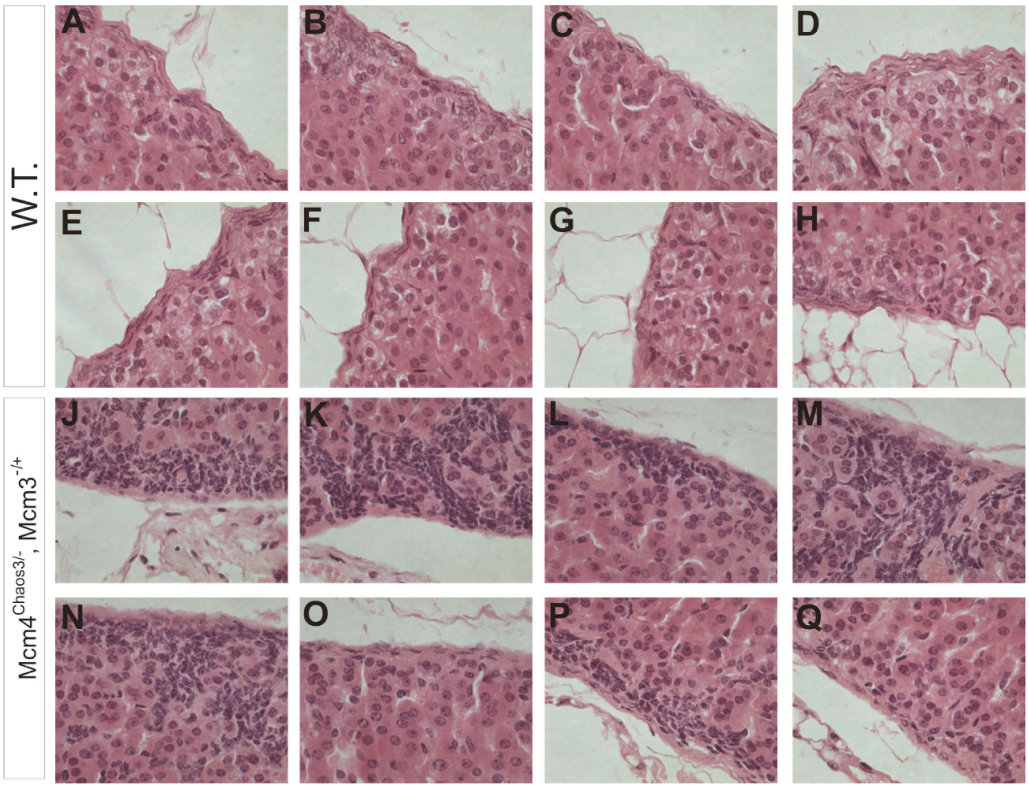

Figure 6.6 H/E staining of adrenals from normal and mutant mice. The normal capsule architecture in the wild type (A-H) is lost adjacent to the abnormal cells in *Mcm4*$^{Chaos3/-}$ *Mcm3*$^{-/+}$ mice adrenals (J-Q).

GATA-4 and GATA-6 are zinc finger transcription factors that are expressed in human and mouse adrenals and regulate cellular proliferation, differentiation and apoptosis within the adrenal cortex, with null mutations for GATA-4 and GATA-6 being embryonic lethal in mice. GATA-4 is expressed in the foetal adrenal but not the adult adrenal and up-regulates inhibin-α, CYP17 and StAR expression predominantly in less differentiated proliferating cells [55]. Up-regulation of GATA-4 expression has been seen pathologically in adult adrenals in some adrenocortical tumours and has been associated with more aggressive behavior. Immunohistochemistry showed that the abnormal spindle shaped cells also stained positive for GATA-4 expression (Figure 6.7) in contrast to the wild type adrenal cortex which showed typically very

few GATA-4 positive cells. As GATA-4 stains the nucleus it is clear that the morphology of the nuclei in these cells is identical to that seen in the spindle shaped cells and those cells identified as non-steroidogenic in figure 6.5b''. In addition the distribution is very similar to the spindle shaped cells identified in Figure 6.2 and 6.3. Taken together this strongly suggests that the GATA-4 staining is marking the spindle shaped, non-steroidogenic cells.

Figure 6.7

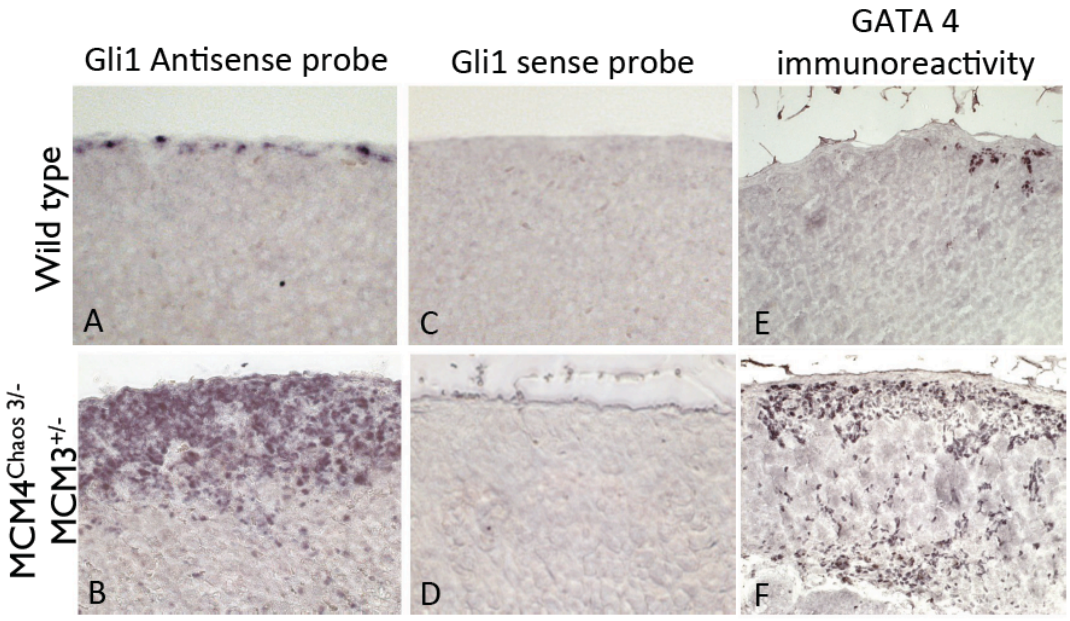

Figure 6.7 A-D. *In situ* hybridisation on 12 month old adrenals showed that Gli1 expression is restricted to the capsule in the wild type (A) but detected in the cortex in the atypical cells in *Mcm4*$^{Chaos3/-}$ *Mcm3*$^{-/+}$ mice (B). C and D are sense probe controls. E-F. GATA-4 immunoreactivity was rarely observed in the wild type adrenals and always in cells close to the capsule; a few darkly stained cells are visible in E. In *Mcm4*$^{Chaos3/-}$ *Mcm3*$^{-/+}$ mice, the atypical cells are GATA-4 positive (darkly stained cells in F). Scale bars; a'-d' 100 microns, E-F 40 microns.

It is thought that hedgehog and Wnt /β-catenin signaling may regulate adrenocortical progenitor populations in concert as β-catenin expression has been shown to be required for SF1 positive cell proliferation and survival [48]. β-catenin expression

was therefore analysed in wild type and mutant *Mcm4*$^{Chaos3/-}$ *Mcm3*$^{-/+}$ mice. This revealed a very abnormal morphology with evidence of increased β-catenin expression throughout the zona fasciculata in contrast to wild type when only a small number of cells in the zona glomerulosa stain positive (Figure 6.8B).

Figure 6.8

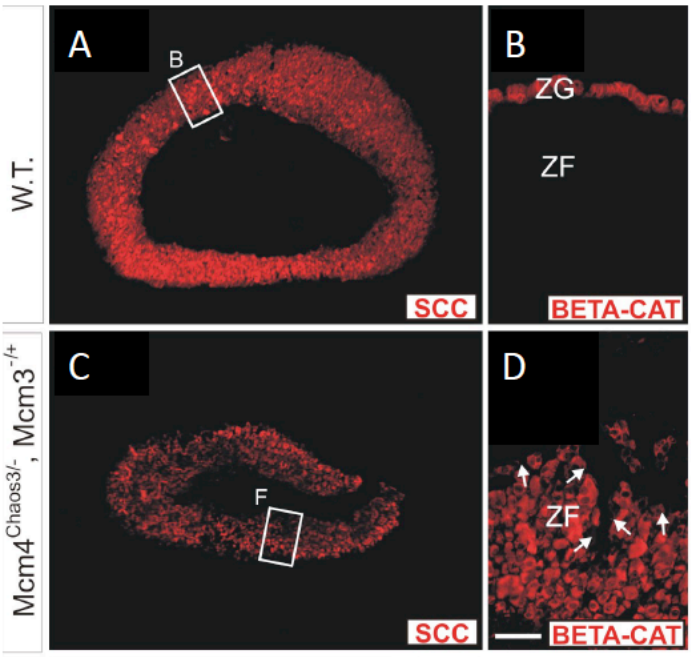

Figure 6.8 Abnormally increased β-catenin in mutant mice. 3.5 month old wild type (A and B) and *Mcm4*$^{Chaos3/-}$ *Mcm3*$^{-/+}$ mice adrenals (C and D) were stained for P450 side chain cleavage (SCC) and β-catenin (BETA-CAT). There is significantly increased expression of β-catenin in the mutant mice throughout the zona fasciculata (D) compared to wildtype (B).

6.4 Discussion

This chapter has analysed a mouse model in which MCM4 levels have been reduced to the lowest levels compatible with life, in order to study the effect this has on adrenal development and histology.

Adrenals from 3.5 month old *Mcm4*$^{Chaos3/-}$ *Mcm3*$^{-/+}$ mice revealed an abnormal morphology characterised by small, tightly packed, spindle-shaped cells infiltrating the cortex from just beneath the capsule. By 12 months of age these cells were abundant throughout the cortex and in some areas spanned the cortex from the capsule to the medulla indicating that this is a progressive phenotype. They were not observed in the wild type or in *Mcm4*$^{Chaos3/+}$*Mcm3*$^{-/+}$ adrenals. Analysis of the expression of steroidogenic enzymes indicated many cells in the mutants were negative for Cyp11a1 (P450 side chain cleavage) in contrast to the wild type. Co-staining with the zona fasciculata marker Cyp11b1 (P450 11-beta-hydroxylase) showed that these Cyp11a1 negative cells were also Cyp11b1 negative indicating they were not steroidogenic. These cells were also GATA-4 and Gli1 positive. Taken together these data indicate that the adrenal morphology in this MCM4 depletion mouse model is grossly abnormal with steroidogenic cells displaced by non-steroidogenic, GATA-4 and Gli1 positive cells that are likely to compromise steroidogenic output.

A similar morphological picture has been seen in certain in-bred mouse strains post gonadectomy [148, 149]. Both female and male mice of the DBA/2J strain develop spindle shaped cells, termed A cells, with limited steroidogenic capacity, post gonadectomy. Similarly to the mutant *Mcm4*$^{Chaos3/-}$ *Mcm3*$^{-/+}$ mice these cells appear initially in the subcapsular region of the adrenal gland and were shown to stain positive for GATA-4 both by immunohistochemistry and *in situ* hybridisation. As the mice age these animals also develop sex steroid producing cells known as B cells presumably in response to unopposed gonadotrophin production by the pituitary gland [149]. These are large lipid laden cells and were not identified in adrenal glands from the MCM4 depleted mice. In addition, luteinizing hormone receptor (LHR) mRNA

was detected in both A and B cells. Although antibodies to test for LH receptor positivity in the mutant *Mcm4*$^{Chaos3/-}$ *Mcm3*$^{-/+}$ mice were not available it is unlikely this would have been positive as there is presumably no additional stimulus in the MCM4 depleted animals to push the undifferentiated spindle shaped cells towards a gonadal phenotype in contast to the gonadectomised animals. The gonadectomized mice subsequently develop adrenocortical tumours and the severity of tumorigenesis correlated with the level of GATA-4 and LHR expression. In addition to these mouse studies, GATA-4 has also been shown to be associated with adrenal tumourogenesis in human studies [58]. Wooley *et al.* have also demonstrated that gonadectomy in female mice causes undifferentiated cells in the subcapsular region of the adrenal gland to differentiate into sex steroid producing cells that are histologically and functionally similar to ovarian tissue.

GATA-4 and GATA-6 are thought to have important but distinct roles in adrenocortical and gonadal cell differentiation and function. Both have been implicated in the regulation of gene expression and differentiation in steroidogenic cells in the testes and ovary [56, 57]. GATA-4 expression is high during periods of active cell proliferation in sertoli and granulosa cells. GATA-4 expression is expressed transiently in the foetal mouse and foetal human adrenal gland but not the adult adrenal. In the foetal human adrenal GATA-4 expression was patchy and not isolated to any specific adrenal zone at gestational week 19, however it was mainly localized to the foetal zone. In contrast GATA-6 is expressed in both foetal and adult adrenal. In the foetal adrenal GATA-6 was abundant and localized to both foetal and definitive zones but was more prominent in the definitive zone [55].

In the mutant *Mcm4*$^{Chaos3/-}$ *Mcm3*$^{-/+}$ mice there was no evidence of sex hormone producing cells and no evidence of either adrenocortical adenomas or adrenocortical tumours. However the appearance of the spindle shaped cells in the MCM4 deficient animals suggests that these cells are potentially undifferentiated subcapsular cells that are unable to differentiate into steroidogenic cells. These cells are positive for the capsular marker Gli1, and at least during embryogenesis these cells appear to be a stem cell population for growth of the cortex [21]. The juxtaposition of these Gli1 positive spindle cells with the capsule would suggest that they are inappropriately proliferating stem/progenitor cells that are unable to convert to a steroidogenic phenotype. The depletion of the capsule adjacent to these regions further suggests that the normal control of this niche has been perturbed with the balance between self-renewal and division disrupted, leading to a loss of these cells. Instead they abnormally activate GATA-4 expression, perhaps in a response to try to force differentiation or in an attempt to recapitulate foetal adrenal conditions again to try to promote differentiation. Alternatively these cells may originate from the foetal adrenal and are unable to extinguish GATA-4 expression as normal in post-natal life leading to an abnormal accumulation of GATA-4 positive cells.

This hypothesis does not explain why cortisol production in humans is specifically affected by an MCM4 defect whereas there appears to be no deficit in aldosterone production. Perhaps the absolute volumes produced (cortisol approximately 15mg/m^2/day versus aldosterone 150 micrograms/day) means that cortisol production is primarily affected and patients may go on to develop mineralocorticoid deficiency with further degeneration of the adrenal cortex. Figure 6.5b'' indicates that the spindle shaped cells are infiltrating the cortex at 3.5 months by growing between the

glomeruli which can be observed expressing CYP11A1, suggesting that, at least at that age, aldosterone production is not compromised. Alternatively, progenitor cells may be able to differentiate into glomerulosa cells but are unable to further differentiate into fasciculata cells, supporting the cell migration model of adrenal development/regeneration [21].

Many cells in the mutant *Mcm4*$^{Chaos3/-}$ *Mcm3*$^{-/+}$ mice express abnormally high levels of β-catenin compared to wild type. Interestingly, transgenic mice with constitutive activation of β-catenin in the adrenal cortex also show evidence of subcapsular adrenal spindle cells [150]. However, as well as spindle cell hyperplasia these animals also developed steroidogenic cell hyperplasia and dysplasia of the cortex and medulla. In addition they developed adrenocortical tumours with ectopic differentiation of the zona glomerulosa at the expense of the fasciculata cells leading to primary hyperaldosteronism. This group showed centripetal invasion of the adrenal cortex by spindle shaped cells originating from outer cortical areas, and similarly to the mutant *Mcm4*$^{Chaos3/-}$ *Mcm3*$^{-/+}$ mice, these spindle cells expressed GATA-4 but no steroidogenic enzymes. In addition rats placed on a low sodium diet show evidence of increased β-catenin expression, increased CYP11B2 expression and expansion of the zona glomerulosa ([21] personal communication). Indeed if the increased β-catenin expression seen in the MCM4 depleted animals is replicated in human patients and similarly cells are preferentially differentiated into zona glomerulosa cells rather than zona fasciculata cells, this is a possible explanation for the patients aldosterone sufficiency.

β-catenin is required for progenitor cell renewal and differentiation in numerous cell lines [23] and adrenocortical cell renewal is impaired in mice with reduced β-catenin levels [48]. However the putative progenitor cells do not express β-catenin and therefore the authors speculate that hedgehog signaling, which is known to frequently cooperate with Wnt signaling, is implicated in the accumulation of spindle shaped cells in the mutant adrenals. King *et al.* also suggested that progenitor cell proliferation and differentiation may be regulated by both β-catenin and hedgehog signaling as these are frequently regulated reciprocally [21]. This suggests that MCM4 regulation of hedgehog and β-catenin signaling may act to control adrenal stem cell differentiation. However the mechanism by which MCM4 regulates β-catenin expression requires additional study.

In contrast, it is interesting to note that a spontaneous autosomal recessive mutation in *Tpp1*, a component of the shelterin complex that maintains telomere integrity, causes telomere dysfunction and genomic instability but also a disordered morphogenesis of the adrenal cortex in mice (the *acd* mouse) [151]. This suggests that chromosomal instability *per se* can cause adrenal disease. However the mechanism of adrenal disease has not been fully elucidated in these animals and is thought to be due to a fundamental defect in cellular proliferation within the adrenal cortex. In contrast to the $Mcm4^{Chaos3/-}$ $Mcm3^{-/+}$ mice *acd* mutant mice had markedly increased cortical cells, with up to a sevenfold increase in volume, and with nuclei often showing a variety of inclusions. These changes were not seen in $Mcm4^{Chaos3/-}$ $Mcm3^{-/+}$ mice. Given the morphological differences between the two mutant mice it seems unlikely that the chromosomal instability that is undoubtedly present in the $Mcm4^{Chaos3/-}$ $Mcm3^{-/+}$ mice is the sole cause of the adrenal failure.

The significant morphological changes seen in the *Mcm4*$^{Chaos3/-}$ *Mcm3*$^{-/+}$ mouse adrenals demonstrate that MCM4 deficiency causes adrenal defects in mice as well as humans. However, it would be important to demonstrate that these changes cause biochemical abnormalities such as low corticosterone levels or elevated ACTH levels. Unfortunately as we did not have direct access to the mice it proved difficult to carry out these experiments, but this is something that should be investigated in the future.

Replacement of steroidogenic cells with spindle cells cannot be demonstrated in patients with MCM4 deficiency as there are no human adrenal glands to study. However the adrenal phenotype seen in mice suggests that MCM4 may have a role in adrenal development, possibly in the control of adrenal stem cell differentiation, and it is likely that this is recapitulated in humans.

Chapter 7: Discussion

7.1 Introduction

FGD is a rare autosomal recessive disorder that is characterized by isolated glucocorticoid deficiency. A number of genetic causes have been described including mutations in the Melanocortin 2 receptor (MC2R), the Melanocortin 2 receptor accessory protein (MRAP), the steroidogenic acute regulatory protein (StAR) and most recently nicotinamide nucleotide transhydrogenase (NNT) [73, 75, 79, 153]. Patients typically present in infancy or early childhood however there is significant variability in the age of presentation with age of onset reported from birth to late childhood. There is variability in onset within patients with mutations in the same gene, for example, *MC2R,* and even within patients with the same mutation, for example the S74I mutation in MC2R [91]. In contrast patients with mutations in *MRAP* usually present in the neonatal period [79]. It was postulated that this difference was due to the nature of the mutations as most MC2R mutations are missense mutations but all MRAP mutations result in either an absent or severely truncated protein.

I identified two populations who presented with late onset FGD. Firstly two families of Turkish ethnicity who presented with delayed onset FGD and secondly eight patients from the Irish travelling community. This second cohort demonstrated late onset glucocorticoid deficiency that was associated with a number of additional features including chromosomal fragility, NK cell deficiency and short stature.

I investigated these patients and discovered firstly that missense mutations in *MRAP* can lead to later onset FGD and secondly I discovered a novel pathogenetic mechanism in Irish traveller patients with FGD.

7.2 Missense *MRAP* mutations

I identified the first two missense mutations in MRAP; Y59D and V26A in the Turkish families. I generated ACTH dose response curves for MC2R when transfected with wild-type or mutant MRAP and showed that both mutant MRAPs demonstrate impaired rather than absent function evidenced by a right shift in the dose response curve. Immunocytochemistry showed normal trafficking indicating a probable signaling defect. The characterisation of these mutations confirming reduced rather than absent function is consistent with the phenotype and further substantiates the hypothesis that disease severity in FGD patients reflects the functional significance of the underlying mutation.

7.3 Novel pathogenetic mechanism of adrenal failure – *MCM4* mutations

I studied eight children from a genetically isolated Irish population who had an interesting variant of adrenal failure. Patients had typical biochemical features of FGD with isolated glucocorticoid deficiency, raised ACTH and normal renin and aldosterone levels. Unlike other forms of FGD, cortisol deficiency was often not as severe and onset was usually in childhood following a period of normal adrenal function. Affected children develop hypocortisolaemia but also growth failure, increased chromosomal breakage and natural killer (NK) cell deficiency.

Targeted exome sequencing in patients identified a variant (c.71-1insG) in mini chromosome maintenance-deficient 4 homologue (*MCM4*) that is predicted to result in a severely truncated protein (p.Pro24ArgfsX4). Given the essential role MCM4 plays in cell division it is surprising that this mutation, causing early termination of the reading frame, should produce such a mild phenotype when gene knockout in mice is embryonic lethal. However although I confirmed patient lymphocytes show loss of the full-length 96kDa MCM4 protein as predicted from RNA analysis, they do show evidence of two smaller MCM4 isoforms that likely rescue the patients from a lethal phenotype.

Given the location of the mutation and the fact that the antibody I used detects the C-terminus of MCM4, it is probable that this smaller isoform has a disrupted N-terminal domain in these patients, but the essential conserved C-terminal domains remain intact. This protein was not detected by immunoblotting with an N-terminal antibody for MCM4 providing further evidence this smaller MCM4 protein lacks the N-terminus. The N-terminus is not well conserved, and studies have revealed that deletion of the first 130 amino acids is not deleterious in eukaryotic cells [144]. Further work has also suggested that although the eukaryotic N-terminal domain is non-essential it is involved in protein kinase regulation of cell cycle progression [154].

Given the known function of MCM4 together with the ubiquitous requirement of this protein it is not surprising that patients would have chromosomal instability or growth failure. However it could not have been predicted that defects in this gene could specifically lead to adrenal failure and NK cell deficiency. Nevertheless I believe that

I have identified the correct disease causing mutation for a number of reasons. First I performed homozygosity mapping on 4 individuals from 3 different families and all individuals had adrenal failure and NK cell deficiency. Because of the variability especially in timing of onset of the disease 'unaffected' family members were not included in the analysis and therefore formal linkage studies were not carried out. All areas of homozygosity common to these three individuals were included in the areas for targeted exome sequencing. Candidate gene sequencing proved inconclusive and I therefore used exome sequencing to sequence all protein coding regions within these areas of homozygosity to ensure no coding sequence variants were missed. I cannot however rule out the possibility that a variant outside the coding regions could be contributing to the phenotype.

It is also possible that the disease causing mutation lies in a small area of homozygosity that was not identified by genome wide scanning using 10K Arrays. To help prove that the MCM4 mutation I identified was causing adrenal disease I examined a *Mcm4* depletion mouse model. I found that these mice have grossly abnormal adrenal morphology, characterized by non-steroidogenic GATA-4 and Gli1 positive cells within the steroidogenic cortex significantly reducing the number of steroidogenic cells in the zona fasciculata. Some features similar to this mutant adrenal histology have been described in murine adrenal hyperplasia [149, 151, 155]. The hyperplastic cells in these mouse models are morphologically very similar to those I observed, and are also GATA-4 positive and non-steroidogenic. The presence of these non-steroidogenic cells in the cortex reduces the number of steroidogenic CYP11B1 expressing cells and hence presumably the glucocorticoid output of the zona fasciculata. The adrenal cortex is a dynamic organ that is constantly remodeling

to maintain homeostasis. It is proposed that it does this by recruiting differentiated steroidogenic cells into the zona fasciculata or zona glomerulosa from stem/progenitor cell populations [21, 156]. One such population has been characterised in the mesenchymal adrenal capsule with, at least during development, Gli1 expressing cells delaminating from the capsule and entering the cortex, concomitantly extinguishing Gli1 expression and activating SF-1 and CYP11A1 expression to become steroidogenic [21]. In light of this it is interesting to note that the GATA-4 positive, non-steroidogenic, cells also express Gli1, suggesting that they may be capsule cells that enter the cortex but fail to differentiate into a steroidogenic identity, instead activating GATA-4 expression. This is supported by the observation that the capsule appears to be thin adjacent to the regions of infiltration, further suggesting that over time the rate of infiltration exceeds the ability of the capsule to self renew. Depletion of MCMs has been proposed to lead to stem cell defects in mice [102, 157], with lower MCM2 levels associated with reduced numbers of stem cells in the subventricular zone, skeletal muscle and intestinal crypts in adult mice. Similarly, the relatively specific impingement of the MCM4 defect on adrenal function may be a consequence of its effect on the growth of these mesenchymal stem/progenitor cells and their differentiation into steroidogenic cells. This suggests MCM4 may have additional functionality beyond DNA replication.

This study did not, as expected, provide further information on the essential components of the ACTH signaling pathway however it has identified a surprising and novel mechanism of adrenal failure that had not previously been recognised. Exome sequencing has also identified mutations in nicotinamide nucleotide transhydrogenase as another cause of FGD, highlighting another novel unexpected

mechanism of adrenal failure [73]. Further exome sequencing projects are likely to identify more novel genes involved in adrenal development and function in the near future.

Complete NK cell deficiency in humans is very rare, with the few cases reported resulting in overwhelming and fatal infection during childhood [122]. The children in our cohort clearly have low but not absent NK cell levels and only one patient demonstrates increased susceptibility to infection. I have not characterised the NK defect however a second group also investigated children from the Irish travelling community with primarily NK cell deficiency and increased susceptibility to viral infections. This group used linkage analysis and fine mapping to identify the same mutation that I identified in MCM4 as the disease causing mutation in these patients [158]. On further examination these patients also had evidence of adrenal insufficiency and intrauterine and postnatal growth failure. The patients had more severe immune defects than the patients I studied; one patient developed an Epstein Barr virus-driven lymphoproliferative disorder and two others developed severe respiratory illnesses that were probably of viral origin. One patient died from progressive lung disease. This group further characterized this mutation by creating EBV-transformed B-cell lines from patients and controls. In agreement with my results they showed that the patient cell lines had no evidence of full length MCM4 protein but did have evidence of two smaller MCM4 isoforms, both missing the N-terminus. In addition they showed that the mutation did not destabilize the mRNA and that the smaller MCM4 isoforms formed a normal MCM2-7 complex with the other MCM proteins and this complex was able to bind DNA normally. However they also showed that the smaller MCM4 isoforms led to a cell cycle defect by affecting DNA

replication and disrupting the normal control of the prevention of re-replication therefore impacting the mitotic phase of the cell cycle. They confirmed that the MCM4 mutation causes genomic instability specifically in response to aphidicolin treatment but not diepoxybutane (DEB). This may explain the differences in chromosomal instability seen in our patients as we used lymphocyte culture in DEB to look for chromatid breaks and chromosomal exchanges.

Gineau and colleagues further investigated the impact of MCM4 deficiency on NK cell terminal differentiation. NK cell classification in humans is based on the surface density of CD56, an N-CAM isoform. It has been shown that $CD56^{bright}$ cells account for 10% of peripheral blood NK cells and can proliferate and produce IFN-γ in response to stimulation with cytokines such as IL-2 and IL-18. $CD56^{bright}$ NK cells differentiate into $CD56^{dim}$ NK cells; these account for 90% of peripheral blood NK cells and are cytolytic and produce cytokines when they encounter target cells. They showed that the patients had very small numbers of NK cells due to selective loss of the $CD56^{dim}$ NK cell subset and that the $CD56^{bright}$ NK cells did not proliferate in response to IL-2 or IL-15. They concluded that the MCM4 deficit selectively affects the ability of $CD56^{bright}$ NK cells to terminally differentiate into $CD56^{dim}$ NK cells [158]. This further corroborates my hypothesis that MCM4 may have additional functionality beyond DNA replication for example in differentiation of adrenal stem cells into steroidogenic cells.

MCM4, as part of the MCM 2-7 complex, is part of the pre-replicative complex, which licenses origins for DNA synthesis in the S phase [132, 159]. Recently 5 genes that encode different components of the pre-replicative complex have been implicated

in Meier-Gorlin syndrome [148], which includes pre- and post-natal growth failure. The growth phenotype illustrated by our patients is also recapitulated in *Mcm4*$^{Chaos3/-}$ *Mcm3*$^{+/-}$ mice [142]. It is possible that this growth failure is explained by the ubiquitous requirement of the MCM complex for DNA replication and cell proliferation. Taken together this indicates that defects in replication licensing might lead to disorders with similar growth retardation phenotypes but distinct developmental abnormalities.

In addition to the abnormal adrenal and growth phenotype *Mcm4*$^{Chaos3/-}$ *Mcm3*$^{+/-}$ mice also have high levels of genomic instability, indicated by elevated micronuclei in red blood cells, which correlates with the chromosomal fragility seen in our patients. Furthermore they exhibit increased susceptibility to the development of, primarily, mammary tumours, histiocytic sarcomas, and lymphomas, depending on genetic background [102]. None of the patients have as yet developed any form of cancer but given the protein is essential for normal DNA replication and the phenotype observed in the mice, the patients may have an increased risk of neoplastic change. Increased cancer risk is associated with many other chromosomal instability syndromes for example Bloom syndrome, Fanconi anaemia, ataxia telangiectasia and Nijmegen breakage syndrome [146]. It is possible that impaired DNA replication in this syndrome due to dysregulation of the MCM2-7 complex and intrinsic genome instability may overwhelm DNA damage, repair and response systems allowing the occurrence of mutations in critical housekeeping genes, for example p53. Our patient cohort will have to be followed carefully but a formal screening process to identify malignancy early has not yet been put in place.

In conclusion I have identified a mutation in *MCM4* characterising a new DNA replication disorder. Patients demonstrate many similarities to other DNA repair and replication disorders including increased chromosomal fragility, pre- and post-natal growth retardation and variable immune deficiency, and in addition this disorder includes adrenal insufficiency. Patients exhibit variability not only in disease susceptibility but also in the other features of the syndrome including age of onset of adrenal insufficiency, NK deficiency and levels of chromosome breakage. The other components of the MCM complex therefore represent prime potential candidates for other undiagnosed cases of chromosomal instability or adrenal failure.

7.4 Future work

In collaboration with our colleagues in Cornell I plan to perform ACTH stimulation tests on $Mcm4^{Chaos3/-}$ $Mcm3^{+/-}$ and wild type mice using a similar protocol to that published previously by Coll *et al.* [160]. I will assay basal and stimulated corticosterone levels using a corticosterone radioimmunoassay to reveal whether these mice have reduced corticosterone output as Nnt mutant mice do [73].

Also in collaboration with Cornell I plan to study ovarian and testicular tissue from $Mcm4^{Chaos3/-}$ $Mcm3^{+/-}$ mice compared to wild type. It is possible that these tissues may share some of the same abnormal features seen in adrenal cortex given both are steroidogenic and are derived from the same mesenchymal origins. This may be clinically relevant to the patients and if appropriate their ovarian or testicular reserve can be monitored using anti-mullerian hormone and inhibin B levels. I plan to investigate adrenal expression of MCM4 in wild type mouse and human embryos at

different ages of development to try to further characterise the role of MCM4 in adrenal development.

I believe the interpatient variability in chromosomal fragility is potentially attributable to the use of a sub optimal screening method, i.e. culturing lymphocytes in diepoxybutane. I propose to screen our patient cohort for evidence of chromosomal fragility by identifying micronucleus frequencies using flow cytometry. Shima *et al.* clearly showed that chromosomal instability in mice can be assessed by using micronucleus levels in erythrocytes [101]. Dertinger *et al.* subsequently designed a flow cytometry based system that identifies the incidence of peripheral blood micronucleated reticulocytes in humans [161]. The analysis of micronucleus formation in newly formed red blood cells is essential for all studies involving species whose spleen effectively sequesters and destroys micronucleus containing erythrocytes. Dertinger used a fluorescent immunological reagent, anti-CD71, to identify newly formed erythrocytes together with an additional fluorescent label to exclude platelets from the micronucleated reticulocytes. I propose to investigate micronucleus frequencies in our patient cohort in collaboration with Professor Owen Smith in Our Lady's Children's Hospital in Dublin using the flow cytometry laboratory based in the hospital. I believe this will give a more accurate and consistent measure of chromosomal fragility in our patient cohort.

It remains unclear why only some of the patients studied showed profound susceptibility to infection while others remain relatively unaffected despite all patients having evidence of low NK cells. This may reflect genetic co-modifiers that are present in these consanguineous families, environmental factors or even epigenetic

modifications. I believe this requires further study and plan to use whole exome sequencing rather than targeted exome sequencing in a number of my patients as a first step to potentially identify any interacting genetic variants.

The mouse model used here is not directly equivalent to the mutation present in the Irish travellers. Although MCM4 levels have been reduced, the putative N-terminally truncated form is not present and there is also a reduction in MCM3, which is not present in patients. I have tried to control for MCM3 heterozygosity by including this in our control animals, nevertheless, even though the data are highly indicative that MCM4 is required for appropriate differentiation of the adrenal cortex, with a presumed resultant impact on steroidogenesis, future studies will attempt to recapitulate the human mutation. I will create appropriate mouse models either by homologous recombination with mutation of the endogenous locus as mouse MCM4 has the same alternative splicing or alternatively a human transgene could be constructed from one of the patients, and introduced into mice that are null for MCM4. This will hopefully generate not only a mouse model of this form of FGD but also provide important insights into adrenal development and the control of adrenal stem cells.

Finally, epigenetic reprogramming of somatic cells to a pluripotent state has been achieved by direct reprogramming by expression of transcription factors. Takahashi and Yamanaka demonstrated that the overexpression of four transcription factors Oct4, Sox2, Klf4, and c-Myc could convert somatic fibroblasts to pluripotent cells (iPSCs) [162]. Subsequently Suga *et al.* demonstrated self formation of functional adenohypophysis in three-dimensional culture from an aggregate culture of mouse

embryonic stem cells [163]. I would like to try to create pluripotent stem cells (iPSCs) from affected patient fibroblasts or lymphocytes as it has been shown that terminally differentiated cells can be reprogrammed to pluripotency in humans [164-166]. Examining the differentiation of patient versus control iPSCs to an adrenal lineage may provide important information about the role of MCM4 in adrenal stem cell differentiation.

References

1. Shepard, T.H., B.H. Landing, and D.G. Mason, *Familial Addison's disease; case reports of two sisters with corticoid deficiency unassociated with hypoaldosteronism.* AMA J Dis Child, 1959. **97**(2): p. 154-62.
2. Stempfel, R.S.E.F.L., *A congenital, familial syndrome of adrenocortical insufficiency without hypoaldosteronism.* The Journal of Pediatrics, 1960: p. 443-451.
3. Migeon, C.J., et al., *The syndrome of congenital adrenocortical unresponsiveness to ACTH. Report of six cases.* Pediatr Res, 1968. **2**(6): p. 501-13.
4. O'Riordan, S.M., et al., *A novel variant of familial glucocorticoid deficiency prevalent among the Irish Traveler population.* J Clin Endocrinol Metab, 2008. **93**(7): p. 2896-9.
5. Kelch, R.P., et al., *Hereditary adrenocortical unresponsiveness to adrenocorticotropic hormone.* J Pediatr, 1972. **81**(4): p. 726-36.
6. Thistlethwaite, D., et al., *Familial glucocorticoid deficiency. Studies of diagnosis and pathogenesis.* Arch Dis Child, 1975. **50**(4): p. 291-7.
7. Cone, R.D., *Studies on the physiological functions of the melanocortin system.* Endocrine reviews, 2006. **27**(7): p. 736-49.
8. Raffin-Sanson, M.L., Y. de Keyzer, and X. Bertagna, *Proopiomelanocortin, a polypeptide precursor with multiple functions: from physiology to pathological conditions.* Eur J Endocrinol, 2003. **149**(2): p. 79-90.

9. Lucki, N. and M. Sewer, *p21-Activated Kinase 6 (PAK6) is a novel regulator of steroidogenic factor 1 (SF-1) and Steroidogenic gene transcription in H295R human adrenocortical cells*, in *SAT-528, poster ENDO 2012*2012.

10. Loriaux, D.L. and J. V, eds. *Adrenal Cortex Physiology*. Comprehensive Clinical Endocrinology2002.

11. Lumbers, *Angiotensin and Aldosterone.* Regul Pept, 1999. **80**(3).

12. Wilburn, L.A., et al., *Ontogeny of enkephalin and catecholamine-synthesizing enzymes in the primate fetal adrenal medulla.* The Journal of clinical endocrinology and metabolism, 1986. **63**(4): p. 974-80.

13. Kempna, P. and C.E. Fluck, *Adrenal gland development and defects.* Best practice & research. Clinical endocrinology & metabolism, 2008. **22**(1): p. 77-93.

14. Hanley, N.A., et al., *Expression profiles of SF-1, DAX1, and CYP17 in the human fetal adrenal gland: potential interactions in gene regulation.* Molecular endocrinology, 2001. **15**(1): p. 57-68.

15. Lalli, E., *Adrenal cortex ontogenesis.* Best practice & research. Clinical endocrinology & metabolism, 2010. **24**(6): p. 853-64.

16. Mesiano, S., C.L. Coulter, and R.B. Jaffe, *Localization of cytochrome P450 cholesterol side-chain cleavage, cytochrome P450 17 alpha-hydroxylase/17, 20-lyase, and 3 beta-hydroxysteroid dehydrogenase isomerase steroidogenic enzymes in human and rhesus monkey fetal adrenal glands: reappraisal of functional zonation.* The Journal of clinical endocrinology and metabolism, 1993. **77**(5): p. 1184-9.

17. Midgley, P.C., et al., *Activity of the adrenal fetal zone in preterm infants continues to term.* Endocrine research, 1996. **22**(4): p. 729-33.

18. Ben-David, S., et al., *Parturition itself is the basis for fetal adrenal involution.* The Journal of clinical endocrinology and metabolism, 2007. **92**(1): p. 93-7.

19. Hatano, O., et al., *Identical origin of adrenal cortex and gonad revealed by expression profiles of Ad4BP/SF-1.* Genes to cells : devoted to molecular & cellular mechanisms, 1996. **1**(7): p. 663-71.

20. Hershkovitz, L., et al., *Adrenal 20alpha-hydroxysteroid dehydrogenase in the mouse catabolizes progesterone and 11-deoxycorticosterone and is restricted to the X-zone.* Endocrinology, 2007. **148**(3): p. 976-88.

21. King, P., A. Paul, and E. Laufer, *Shh signaling regulates adrenocortical development and identifies progenitors of steroidogenic lineages.* Proc Natl Acad Sci U S A, 2009. **106**(50): p. 21185-90.

22. Mitani, F., et al., *A novel cell layer without corticosteroid-synthesizing enzymes in rat adrenal cortex: histochemical detection and possible physiological role.* Endocrinology, 1994. **135**(1): p. 431-8.

23. Kim, A.C., et al., *In search of adrenocortical stem and progenitor cells.* Endocrine reviews, 2009. **30**(3): p. 241-63.

24. Kim, A.C. and G.D. Hammer, *Adrenocortical cells with stem/progenitor cell properties: recent advances.* Molecular and cellular endocrinology, 2007. **265-266**: p. 10-6.

25. Spencer, S.J., et al., *Proliferation and apoptosis in the human adrenal cortex during the fetal and perinatal periods: implications for growth and remodeling.* The Journal of clinical endocrinology and metabolism, 1999. **84**(3): p. 1110-5.

26. Breault, D., *The origins of the Zona Fasciculata*, in *Adrenal Cortex*2012: Texas, USA.

27. Di Blasio, A.M., et al., *Maintenance of cell proliferation and steroidogenesis in cultured human fetal adrenal cells chronically exposed to adrenocorticotropic hormone: rationalization of in vitro and in vivo findings.* Biology of reproduction, 1990. **42**(4): p. 683-91.

28. Clark, A.J. and A. Weber, *Adrenocorticotropin insensitivity syndromes.* Endocr Rev, 1998. **19**(6): p. 828-43.

29. Gray, E.S. and D.R. Abramovich, *Morphologic features of the anencephalic adrenal gland in early pregnancy.* American journal of obstetrics and gynecology, 1980. **137**(4): p. 491-5.

30. Jackson, R.S., et al., *Obesity and impaired prohormone processing associated with mutations in the human prohormone convertase 1 gene.* Nature Genetics, 1997. **16**(3): p. 303-6.

31. Kelberman, D. and M.T. Dattani, *Hypothalamic and pituitary development: novel insights into the aetiology.* European journal of endocrinology / European Federation of Endocrine Societies, 2007. **157 Suppl 1**: p. S3-14.

32. Ishimoto, H., D.G. Ginzinger, and R.B. Jaffe, *Adrenocorticotropin preferentially up-regulates angiopoietin 2 in the human fetal adrenal gland: implications for coordinated adrenal organ growth and angiogenesis.* The Journal of clinical endocrinology and metabolism, 2006. **91**(5): p. 1909-15.

33. Ishimoto, H. and R.B. Jaffe, *Development and function of the human fetal adrenal cortex: a key component in the feto-placental unit.* Endocrine reviews, 2011. **32**(3): p. 317-55.

34. Zubair, M., et al., *Two-step regulation of Ad4BP/SF-1 gene transcription during fetal adrenal development: initiation by a Hox-Pbx1-Prep1 complex*

and maintenance via autoregulation by Ad4BP/SF-1. Molecular and cellular biology, 2006. **26**(11): p. 4111-21.

35. El-Khairi, R., et al., *Role of DAX-1 (NR0B1) and steroidogenic factor-1 (NR5A1) in human adrenal function.* Endocrine development, 2011. **20**: p. 38-46.

36. Ferraz-de-Souza, B., L. Lin, and J.C. Achermann, *Steroidogenic factor-1 (SF-1, NR5A1) and human disease.* Molecular and cellular endocrinology, 2011. **336**(1-2): p. 198-205.

37. Figueiredo, B.C., et al., *Amplification of the steroidogenic factor 1 gene in childhood adrenocortical tumors.* The Journal of clinical endocrinology and metabolism, 2005. **90**(2): p. 615-9.

38. Sbiera, S., et al., *High diagnostic and prognostic value of steroidogenic factor-1 expression in adrenal tumors.* The Journal of clinical endocrinology and metabolism, 2010. **95**(10): p. E161-71.

39. Muscatelli, F., et al., *Mutations in the DAX-1 gene give rise to both X-linked adrenal hypoplasia congenita and hypogonadotropic hypogonadism.* Nature, 1994. **372**(6507): p. 672-6.

40. Zanaria, E., et al., *An unusual member of the nuclear hormone receptor superfamily responsible for X-linked adrenal hypoplasia congenita.* Nature, 1994. **372**(6507): p. 635-41.

41. Babu, P.S., et al., *Interaction between Dax-1 and steroidogenic factor-1 in vivo: increased adrenal responsiveness to ACTH in the absence of Dax-1.* Endocrinology, 2002. **143**(2): p. 665-73.

42. Battista, M.C., et al., *Extracellular matrix and hormones modulate DAX-1 localization in the human fetal adrenal gland.* The Journal of clinical endocrinology and metabolism, 2005. **90**(9): p. 5426-31.

43. Han, Y.G., et al., *Hedgehog signaling and primary cilia are required for the formation of adult neural stem cells.* Nature neuroscience, 2008. **11**(3): p. 277-84.

44. Ingham, P.W. and A.P. McMahon, *Hedgehog signaling in animal development: paradigms and principles.* Genes & development, 2001. **15**(23): p. 3059-87.

45. Huang, C.C., et al., *Progenitor cell expansion and organ size of mouse adrenal is regulated by sonic hedgehog.* Endocrinology, 2010. **151**(3): p. 1119-28.

46. Lee, F.Y., et al., *Eliminating SF-1 (NR5A1) sumoylation in vivo results in ectopic hedgehog signaling and disruption of endocrine development.* Developmental cell, 2011. **21**(2): p. 315-27.

47. Hall, J.G., et al., *Congenital hypothalamic hamartoblastoma, hypopituitarism, imperforate anus and postaxial polydactyly--a new syndrome? Part I: clinical, causal, and pathogenetic considerations.* American journal of medical genetics, 1980. **7**(1): p. 47-74.

48. Kim, A.C., et al., *Targeted disruption of beta-catenin in Sf1-expressing cells impairs development and maintenance of the adrenal cortex.* Development, 2008. **135**(15): p. 2593-602.

49. Kim, A., et al., *Wnt/betacatenin signaling in adrenocortical stem/progenitor cells: implications for adrenocortical carcinoma.* Annales d'endocrinologie, 2009. **70**(3): p. 156.

50. Heikkila, M., et al., *Wnt-4 deficiency alters mouse adrenal cortex function, reducing aldosterone production.* Endocrinology, 2002. **143**(11): p. 4358-65.

51. Beamer, W.G., et al., *Adrenocortical dysplasia: a mouse model system for adrenocortical insufficiency.* The Journal of endocrinology, 1994. **141**(1): p. 33-43.

52. Keegan, C.E., et al., *Urogenital and caudal dysgenesis in adrenocortical dysplasia (acd) mice is caused by a splicing mutation in a novel telomeric regulator.* Human molecular genetics, 2005. **14**(1): p. 113-23.

53. Zantour, B., et al., *[Werner's syndrome and endocrine disorders].* Annales d'endocrinologie, 2003. **64**(3): p. 205-9.

54. McDonald, S., et al., *Acquired monosomy 7 myelodysplastic syndrome in a child with clinical features suggestive of dyskeratosis congenita and IMAGe association.* Pediatric blood & cancer, 2010. **54**(1): p. 154-7.

55. Kiiveri, S., et al., *Differential expression of GATA-4 and GATA-6 in fetal and adult mouse and human adrenal tissue.* Endocrinology, 2002. **143**(8): p. 3136-43.

56. Heikinheimo, M., et al., *Expression and hormonal regulation of transcription factors GATA-4 and GATA-6 in the mouse ovary.* Endocrinology, 1997. **138**(8): p. 3505-14.

57. Ketola, I., et al., *Expression and regulation of transcription factors GATA-4 and GATA-6 in developing mouse testis.* Endocrinology, 1999. **140**(3): p. 1470-80.

58. Kiiveri, S., et al., *Reciprocal changes in the expression of transcription factors GATA-4 and GATA-6 accompany adrenocortical tumorigenesis in mice and humans.* Molecular medicine, 1999. **5**(7): p. 490-501.

59. Mitani, F., et al., *Effects of long term stimulation of ACTH and angiotensin II-secretions on the rat adrenal cortex.* Endocrine research, 1996. **22**(4): p. 421-31.

60. Freedman BD, C.D., Guagliardo NA, Barrett PQ, Majzoub JA, Breault DT, *Zona fasciculata cells arise from the zona glomerulosa (abstract).* Endocrine Reviews, 2011. **32**(OR32).

61. Zeki, S.S., T.A. Graham, and N.A. Wright, *Stem cells and their implications for colorectal cancer.* Nature reviews. Gastroenterology & hepatology, 2011. **8**(2): p. 90-100.

62. Parker, L.N. and W.D. Odell, *Control of adrenal androgen secretion.* Endocrine Reviews, 1980. **1**(4): p. 392-410.

63. Anderson, D.C., *The adrenal androgen-stimulating hormone does not exist.* Lancet, 1980. **2**(8192): p. 454-6.

64. Ibanez, L., et al., *Premature adrenarche--normal variant or forerunner of adult disease?* Endocrine Reviews, 2000. **21**(6): p. 671-96.

65. Campbell, B., *Adrenarche and the evolution of human life history.* American journal of human biology : the official journal of the Human Biology Council, 2006. **18**(5): p. 569-89.

66. Goto, M., et al., *In humans, early cortisol biosynthesis provides a mechanism to safeguard female sexual development.* The Journal of clinical investigation, 2006. **116**(4): p. 953-60.

67. Parker, C.R., Jr., et al., *Immunohistochemical evaluation of the cellular localization and ontogeny of 3 beta-hydroxysteroid dehydrogenase/delta 5-4 isomerase in the human fetal adrenal gland.* Endocrine research, 1995. **21**(1-2): p. 69-80.

68. Kraan, G.P., et al., *The daily cortisol production reinvestigated in healthy men. The serum and urinary cortisol production rates are not significantly different.* The Journal of clinical endocrinology and metabolism, 1998. **83**(4): p. 1247-52.

69. Idkowiak, J., et al., *Premature adrenarche: novel lessons from early onset androgen excess.* European journal of endocrinology / European Federation of Endocrine Societies, 2011. **165**(2): p. 189-207.

70. Arlt, W. and B. Allolio, *Adrenal insufficiency.* Lancet, 2003. **361**(9372): p. 1881-93.

71. Betterle, C., et al., *Autoimmune adrenal insufficiency and autoimmune polyendocrine syndromes: autoantibodies, autoantigens, and their applicability in diagnosis and disease prediction.* Endocrine Reviews, 2002. **23**(3): p. 327-64.

72. Lam, K.Y. and C.Y. Lo, *A critical examination of adrenal tuberculosis and a 28-year autopsy experience of active tuberculosis.* Clinical endocrinology, 2001. **54**(5): p. 633-9.

73. Meimaridou E, K.J., Guasti L, Hughes CR, Wagner F, Frommolt P, Nürnberg P, Mann NP, Banerjee R, Saka HN, Chapple JP, King PJ, Clark AJL, Metherell LA, *Mutations in NNT encoding nicotinamide nucleotide transhydrogenase cause familial glucocorticoid deficiency.* Nature Genetics 2012. **44**: p. 740-742.

74. Mountjoy, K.G., et al., *The cloning of a family of genes that encode the melanocortin receptors.* Science, 1992. **257**(5074): p. 1248-51.

75. Clark, A.J., L. McLoughlin, and A. Grossman, *Familial glucocorticoid deficiency associated with point mutation in the adrenocorticotropin receptor.* Lancet, 1993. **341**(8843): p. 461-2.

76. Tsigos, C., et al., *Hereditary isolated glucocorticoid deficiency is associated with abnormalities of the adrenocorticotropin receptor gene.* J Clin Invest, 1993. **92**(5): p. 2458-61.

77. Clark, A.J., et al., *Inherited ACTH insensitivity illuminates the mechanisms of ACTH action.* Trends Endocrinol Metab, 2005. **16**(10): p. 451-7.

78. Elias, L.L., et al., *Functional characterization of naturally occurring mutations of the human adrenocorticotropin receptor: poor correlation of phenotype and genotype.* J Clin Endocrinol Metab, 1999. **84**(8): p. 2766-70.

79. Metherell, L.A., et al., *Mutations in MRAP, encoding a new interacting partner of the ACTH receptor, cause familial glucocorticoid deficiency type 2.* Nature genetics, 2005. **37**(2): p. 166-70.

80. Chan, L.F., et al., *MRAP and MRAP2 are bidirectional regulators of the melanocortin receptor family.* Proc Natl Acad Sci U S A, 2009.

81. Chung, T.T., et al., *The majority of ACTH receptor (MC2R) mutations found in Familial Glucocorticoid Deficiency type 1 lead to defective trafficking of the receptor to the cell surface.* J Clin Endocrinol Metab, 2008.

82. Metherell, L.A., et al., *Mutations in MRAP, encoding a new interacting partner of the ACTH receptor, cause familial glucocorticoid deficiency type 2.* Nat Genet, 2005. **37**(2): p. 166-70.

83. Metherell, L., *Non-classical lipoid congenital adrenal hyperplasia masquerading as Familial Glucocorticoid Deficiency.* JCEM, 2009.

84. Achermann, J.C., et al., *Molecular and structural analysis of two novel StAR mutations in patients with lipoid congenital adrenal hyperplasia.* Mol Genet Metab, 2001. **73**(4): p. 354-7.

85. Parajes, S., et al., *A novel entity of clinically isolated adrenal insufficiency caused by a partially inactivating mutation of the gene encoding for P450 side chain cleavage enzyme (CYP11A1).* The Journal of clinical endocrinology and metabolism, 2011. **96**(11): p. E1798-806.

86. Lacy, D.E., K.A. Nathavitharana, and M.J. Tarlow, *Neonatal hepatitis and congenital insensitivity to adrenocorticotropin (ACTH).* J Pediatr Gastroenterol Nutr, 1993. **17**(4): p. 438-40.

87. Turan, S., et al., *An atypical case of familial glucocorticoid deficiency without pigmentation caused by coexistent homozygous mutations in MC2R (T152K) and MC1R (R160W).* The Journal of clinical endocrinology and metabolism, 2012. **97**(5): p. E771-4.

88. Elias, L.L., et al., *Tall stature in familial glucocorticoid deficiency.* Clinical endocrinology, 2000. **53**(4): p. 423-30.

89. Evans, J.F., et al., *Adrenocorticotropin evokes transient elevations in intracellular free calcium ([Ca2+]i) and increases basal [Ca2+]i in resting chondrocytes through a phospholipase C-dependent mechanism.* Endocrinology, 2005. **146**(7): p. 3123-32.

90. Gabbitas, B. and E. Canalis, *Cortisol enhances the transcription of insulin-like growth factor-binding protein-6 in cultured osteoblasts.* Endocrinology, 1996. **137**(5): p. 1687-92.

91. Chung, T.T., et al., *Phenotypic characteristics of familial glucocorticoid deficiency (FGD) type 1 and 2.* Clinical endocrinology, 2010. **72**(5): p. 589-94.

92. Weber, A., et al., *Diminished adrenal androgen secretion in familial glucocorticoid deficiency implicates a significant role for ACTH in the induction of adrenarche.* Clin Endocrinol (Oxf), 1997. **46**(4): p. 431-7.

93. Sanger, F., S. Nicklen, and A.R. Coulson, *DNA sequencing with chain-terminating inhibitors.* Proceedings of the National Academy of Sciences of the United States of America, 1977. **74**(12): p. 5463-7.

94. Tippmann, H.F., *Analysis for free: comparing programs for sequence analysis.* Briefings in bioinformatics, 2004. **5**(1): p. 82-7.

95. Kennedy, G.C., et al., *Large-scale genotyping of complex DNA.* Nature biotechnology, 2003. **21**(10): p. 1233-7.

96. Carr, I.M., et al., *IBDfinder and SNPsetter: tools for pedigree-independent identification of autozygous regions in individuals with recessive inherited disease.* Human mutation, 2009. **30**(6): p. 960-7.

97. Li, H., et al., *The Sequence Alignment/Map format and SAMtools.* Bioinformatics, 2009. **25**(16): p. 2078-9.

98. Laemmli, U.K., *Cleavage of structural proteins during the assembly of the head of bacteriophage T4.* Nature, 1970. **227**(5259): p. 680-5.

99. Birnboim, H.C., *A rapid alkaline extraction method for the isolation of plasmid DNA.* Methods in enzymology, 1983. **100**: p. 243-55.

100. Chung, T.T., et al., *The majority of adrenocorticotropin receptor (melanocortin 2 receptor) mutations found in familial glucocorticoid deficiency type 1 lead to defective trafficking of the receptor to the cell surface.* J Clin Endocrinol Metab, 2008. **93**(12): p. 4948-54.

101. Shima, N., T.R. Buske, and J.C. Schimenti, *Genetic screen for chromosome instability in mice: Mcm4 and breast cancer.* Cell Cycle, 2007. **6**(10): p. 1135-40.

102. Chuang, C.H., et al., *Incremental genetic perturbations to MCM2-7 expression and subcellular distribution reveal exquisite sensitivity of mice to DNA replication stress.* PLoS Genet, 2010. **6**(9).

103. Guasti, L., et al., *Localization of Sonic hedgehog secreting and receiving cells in the developing and adult rat adrenal cortex.* Mol Cell Endocrinol, 2011. **336**(1-2): p. 117-22.

104. Guasti, L., et al., *Expression pattern of the ether-a-go-go-related (ERG) family proteins in the adult mouse central nervous system: evidence for coassembly of different subunits.* The Journal of comparative neurology, 2005. **491**(2): p. 157-74.

105. Cooray, S.N., et al., *The melanocortin 2 receptor accessory protein exists as a homodimer and is essential for the function of the melanocortin 2 receptor in the mouse y1 cell line.* Endocrinology, 2008. **149**(4): p. 1935-41.

106. Webb, T.R., et al., *Distinct melanocortin 2 receptor accessory protein domains are required for melanocortin 2 receptor interaction and promotion of receptor trafficking.* Endocrinology, 2009. **150**(2): p. 720-6.

107. Sebag, J.A. and P.M. Hinkle, *Regions of melanocortin 2 (MC2) receptor accessory protein necessary for dual topology and MC2 receptor trafficking and signaling.* J Biol Chem, 2009. **284**(1): p. 610-8.

108. Webb, T.R. and A.J. Clark, *Minireview: The Melanocortin 2 Receptor Accessory Proteins.* Mol Endocrinol, 2009.

109. Cooray, S.N., et al., *Accessory proteins are vital for the functional expression of certain G protein-coupled receptors.* Mol Cell Endocrinol, 2009. **300**(1-2): p. 17-24.

110. Bacskai, B.J., et al., *Spatially resolved dynamics of cAMP and protein kinase A subunits in Aplysia sensory neurons.* Science, 1993. **260**(5105): p. 222-6.

111. de Wet, J.R., et al., *Cloning of firefly luciferase cDNA and the expression of active luciferase in Escherichia coli.* Proc Natl Acad Sci U S A, 1985. **82**(23): p. 7870-3.

112. Sherf, B., *Dual-Luciferase reporter assay: An advanced co-reporter technology integrating firefly and Renilla luciferase assays.*, in *Promega notes*1996. p. 2-9.

113. Antoni, F.A., *Molecular diversity of cyclic AMP signalling.* Front Neuroendocrinol, 2000. **21**(2): p. 103-32.

114. Office, C.S., *Irish Census 2006* C.S. Office, Editor 2006.

115. Kelleher, *All Ireland Traveller health Study*, U.C.D. School of Public Health, Editor 2010.

116. Maher, J. and A. Macfarlane, *Inequalities in infant mortality: trends by social class, registration status, mother's age and birthweight, England and Wales, 1976-2000.* Health statistics quarterly / Office for National Statistics, 2004(24): p. 14-22.

117. Morgan, N.V., et al., *High frequency of large intragenic deletions in the Fanconi anemia group A gene.* American journal of human genetics, 1999. **65**(5): p. 1330-41.

118. Eidenschenk, C., et al., *A novel primary immunodeficiency with specific natural-killer cell deficiency maps to the centromeric region of chromosome 8.* Am J Hum Genet, 2006. **78**(4): p. 721-7.

119. Chan, A., et al., *CD56bright human NK cells differentiate into CD56dim cells: role of contact with peripheral fibroblasts.* Journal of immunology, 2007. **179**(1): p. 89-94.

120. Bernard, F., et al., *A novel developmental and immunodeficiency syndrome associated with intrauterine growth retardation and a lack of natural killer cells.* Pediatrics, 2004. **113**(1 Pt 1): p. 136-41.

121. Eidenschenk, C., et al., *A novel primary immunodeficiency with specific natural-killer cell deficiency maps to the centromeric region of chromosome 8.* American journal of human genetics, 2006. **78**(4): p. 721-7.

122. Orange, J.S., *Human natural killer cell deficiencies.* Curr Opin Allergy Clin Immunol, 2006. **6**(6): p. 399-409.

123. Caligiuri, M.A., *Human natural killer cells.* Blood, 2008. **112**(3): p. 461-9.

124. Ng, S.B., et al., *Targeted capture and massively parallel sequencing of 12 human exomes.* Nature, 2009. **461**(7261): p. 272-6.

125. Ng, S.B., et al., *Exome sequencing identifies the cause of a mendelian disorder.* Nat Genet, 2009.

126. Rusk, N. and V. Kiermer, *Primer: Sequencing--the next generation.* Nature methods, 2008. **5**(1): p. 15.

127. Biesecker, L.G., *Exome sequencing makes medical genomics a reality.* Nature Genetics, 2010. **42**(1): p. 13-4.

128. Bao, S., et al., *Evaluation of next-generation sequencing software in mapping and assembly.* Journal of human genetics, 2011. **56**(6): p. 406-14.

129. Maine, G.T., P. Sinha, and B.K. Tye, *Mutants of S. cerevisiae defective in the maintenance of minichromosomes.* Genetics, 1984. **106**(3): p. 365-85.

130. Hennessy, K.M., et al., *A group of interacting yeast DNA replication genes.* Genes & development, 1991. **5**(6): p. 958-69.

131. Bochman, M.L. and A. Schwacha, *The Mcm complex: unwinding the mechanism of a replicative helicase.* Microbiol Mol Biol Rev, 2009. **73**(4): p. 652-83.

132. Forsburg, S.L., *Eukaryotic MCM proteins: beyond replication initiation.* Microbiol Mol Biol Rev, 2004. **68**(1): p. 109-31.

133. Kearsey, S.E. and K. Labib, *MCM proteins: evolution, properties, and role in DNA replication.* Biochimica et biophysica acta, 1998. **1398**(2): p. 113-36.

134. Kamimura, Y., et al., *Sld3, which interacts with Cdc45 (Sld4), functions for chromosomal DNA replication in Saccharomyces cerevisiae.* The EMBO journal, 2001. **20**(8): p. 2097-107.

135. Tanaka, S., et al., *CDK-dependent phosphorylation of Sld2 and Sld3 initiates DNA replication in budding yeast.* Nature, 2007. **445**(7125): p. 328-32.

136. Ricke, R.M. and A.K. Bielinsky, *Mcm10 regulates the stability and chromatin association of DNA polymerase-alpha.* Molecular cell, 2004. **16**(2): p. 173-85.

137. Aparicio, O.M., D.M. Weinstein, and S.P. Bell, *Components and dynamics of DNA replication complexes in S. cerevisiae: redistribution of MCM proteins and Cdc45p during S phase.* Cell, 1997. **91**(1): p. 59-69.

138. Sheu, Y.J. and B. Stillman, *Cdc7-Dbf4 phosphorylates MCM proteins via a docking site-mediated mechanism to promote S phase progression.* Molecular cell, 2006. **24**(1): p. 101-13.

139. Komamura-Kohno, Y., et al., *Site-specific phosphorylation of MCM4 during the cell cycle in mammalian cells.* The FEBS journal, 2006. **273**(6): p. 1224-39.

140. Ishimi, Y. and Y. Komamura-Kohno, *Phosphorylation of Mcm4 at specific sites by cyclin-dependent kinase leads to loss of Mcm4,6,7 helicase activity.* The Journal of biological chemistry, 2001. **276**(37): p. 34428-33.

141. Hrabe de Angelis, M.H., et al., *Genome-wide, large-scale production of mutant mice by ENU mutagenesis.* Nature Genetics, 2000. **25**(4): p. 444-7.

142. Shima, N., et al., *A viable allele of Mcm4 causes chromosome instability and mammary adenocarcinomas in mice.* Nat Genet, 2007. **39**(1): p. 93-8.

143. Musahl, C., et al., *A human homologue of the yeast replication protein Cdc21. Interactions with other Mcm proteins.* European journal of biochemistry / FEBS, 1995. **230**(3): p. 1096-101.

144. Masai, H., et al., *Phosphorylation of MCM4 by Cdc7 kinase facilitates its interaction with Cdc45 on the chromatin.* J Biol Chem, 2006. **281**(51): p. 39249-61.

145. Fujita, M., et al., *Cell cycle- and chromatin binding state-dependent phosphorylation of human MCM heterohexameric complexes. A role for cdc2 kinase.* The Journal of biological chemistry, 1998. **273**(27): p. 17095-101.

146. Woods, C.G., *DNA repair disorders.* Archives of Disease in Childhood, 1998. **78**(2): p. 178-84.

147. Tischkowitz, M.D. and S.V. Hodgson, *Fanconi anaemia.* Journal of medical genetics, 2003. **40**(1): p. 1-10.

148. Bicknell, L.S., et al., *Mutations in the pre-replication complex cause Meier-Gorlin syndrome.* Nature Genetics, 2011. **43**(4): p. 356-9.

149. Kim, J.S., et al., *Subcapsular cell hyperplasia and mast cell infiltration in the adrenal cortex of mice: comparative study in 7 inbred strains.* Exp Anim, 1997. **46**(4): p. 303-6.

150. Bielinska, M., et al., *Mouse strain susceptibility to gonadectomy-induced adrenocortical tumor formation correlates with the expression of GATA-4 and luteinizing hormone receptor.* Endocrinology, 2003. **144**(9): p. 4123-33.

151. Berthon, A., et al., *Constitutive beta-catenin activation induces adrenal hyperplasia and promotes adrenal cancer development.* Hum Mol Genet, 2010. **19**(8): p. 1561-76.

152. Vlangos, C.N., et al., *Caudal regression in adrenocortical dysplasia (acd) mice is caused by telomere dysfunction with subsequent p53-dependent apoptosis.* Developmental biology, 2009. **334**(2): p. 418-28.

153. Metherell, L.A., et al., *Nonclassic lipoid congenital adrenal hyperplasia masquerading as familial glucocorticoid deficiency.* The Journal of clinical endocrinology and metabolism, 2009. **94**(10): p. 3865-71.

154. Sheu, Y.J. and B. Stillman, *The Dbf4-Cdc7 kinase promotes S phase by alleviating an inhibitory activity in Mcm4.* Nature, 2010. **463**(7277): p. 113-7.

155. Parviainen, H., et al., *GATA transcription factors in adrenal development and tumors.* Mol Cell Endocrinol, 2007. **265-266**: p. 17-22.

156. Wood, M.A. and G.D. Hammer, *Adrenocortical stem and progenitor cells: Unifying model of two proposed origins.* Mol Cell Endocrinol, 2010. **336**(1-2): p. 206-12.

157. Pruitt, S.C., K.J. Bailey, and A. Freeland, *Reduced Mcm2 expression results in severe stem/progenitor cell deficiency and cancer.* Stem Cells, 2007. **25**(12): p. 3121-32.

158. Gineau, L., et al., *Partial MCM4 deficiency in patients with growth retardation, adrenal insufficiency, and natural killer cell deficiency.* The Journal of clinical investigation, 2012. **122**(3): p. 821-32.

159. Tye, B.K., *MCM proteins in DNA replication.* Annu Rev Biochem, 1999. **68**: p. 649-86.

160. Coll, A.P., et al., *The effects of proopiomelanocortin deficiency on murine adrenal development and responsiveness to adrenocorticotropin.* Endocrinology, 2004. **145**(10): p. 4721-7.

161. Dertinger, S.D., et al., *Three-color labeling method for flow cytometric measurement of cytogenetic damage in rodent and human blood.* Environmental and molecular mutagenesis, 2004. **44**(5): p. 427-35.

162. Takahashi, K. and S. Yamanaka, *Induction of pluripotent stem cells from mouse embryonic and adult fibroblast cultures by defined factors.* Cell, 2006. **126**(4): p. 663-76.

163. Suga, H., et al., *Self-formation of functional adenohypophysis in three-dimensional culture.* Nature, 2011. **480**(7375): p. 57-62.

164. Seki, T., et al., *Generation of induced pluripotent stem cells from human-terminally differentiated circulating T cells.* Cell stem cell, 2010. **7**(1): p. 11-4.

165. Staerk, J., et al., *Reprogramming of human peripheral blood cells to induced pluripotent stem cells.* Cell stem cell, 2010. **7**(1): p. 20-4.

166. Loh, Y.H., et al., *Reprogramming of T cells from human peripheral blood.* Cell stem cell, 2010. **7**(1): p. 15-9.

APPENDIX 1

OUR LADY'S HOSPITAL FOR SICK CHILDREN, CRUMLIN, DUBLIN 12.

ETHICS COMMITTEE PROTOCOL FORM

This protocol was developed based on the general principles of medical ethics, the control of clinical trials Acts 1987 and 1990, and European Guidelines of Good Clinical Practice.

Please read the attached introductory notes, then complete the protocol in **typescript.**

All relevant sections must be fully completed. Please place "X" or circle the appropriate response in the boxed areas. NA is the abbreviation for Not Applicable.

1. **Title of research project:**

Investigating the genetics and mechanisms of ACTH resistance in children with Familial Glucocorticoid Deficiency

2. **Name of the Chief Investigator(s)** who should ordinarily be a hospital consultant:

Dr. Colm Costigan

3. **What are the objectives of the research project?**

- Identify further genes responsible for Familial Glucocorticoid Disease in our patients
- Isolate and investigate these genes
- Examine the relationship between the ACTH receptor, new genes identified, and previously identified accessory proteins (MRAP)

4a. **Does the design of the study allow a statistically significant conclusion to be reached?**

YES

4b. **Has statistical advice been sought?** NO

5. **Will the conduct of the project conform to the principles of the Declaration of Helsinki** (Recommendations guiding Medical Doctors in Biomedical Research involving Human subjects)**.**

If not, elucidate: YES

6. **Please itemise here any ethical problems which you perceive to be associated with research project:**

We will need to obtain consent for taking blood samples from patients with Familial Glucocorticoid Deficiency (during routine phlebotomy to monitor clinical progression). We will also need to obtain consent to take blood samples from family members, if they are willing. We will then use these samples for research into the genetics and mechanisms of disease in FGD, in these families.

SECTION A

DETAILS OF PROJECT

7. **Background**

A) **What person or organisation devised this project?**

Dr. Colm Costigan, Dr. Claire Hughes and Dr. Adrian Clarke

B) **Has a detailed research protocol been drawn up?** (If so, such documentation must be submitted to the committee). YES NO

In progress

8.

A) **Has the investigator who will present this project to the Committee studied all the documentation drawn up for the Project, and will the documentation be studied by all the investigators before the project begins?** YES

B) **Briefly describe the scientific rationale for the project:**

FGD is a genetically heterogeneous, autosomal recessive syndrome of ACTH resistance resulting in adrenal failure. The genetic basis of approximately 50% of cases of FGD is known. FGD type 1 (OMIM 202200) results from a mutation in the ACTH Receptor gene, Melanocortin 2 receptor (MC2R). FGD type 2 (OMIM 609196) maps to a mutation in the melanocortin 2 receptor accessory protein (MRAP). This protein may have a role in the trafficking of MC2R from the endoplasmic reticulum to the cell surface. The underlying genetic mutation for the remaining 50% is unknown, but some cases may map to a locus on chromosome 8q.

We have identified 22 patients with FGD, 12 of these patients have been tested for all known mutations and are negative. We intend to use whole genome scanning by single nucleotide polymorphism (SNP) array genotyping and linkage analysis to identify further potential genes that cause ACTH resistance.

7 of our patients have mutations in the MC2R gene, and 3 patients have a mutation in the MRAP gene. We aim to analyse the nature of the interaction between MC2R and MRAP and additional proteins or chaperones discovered. This will lead to a better understanding of MC2R trafficking and signaling and increase the understanding of G protein coupled receptors (GPCRs) and adrenal physiology in general.

By identifying further loci linked to this disease, molecular genetic testing will allow early diagnosis and treatment in high-risk groups and allow carrier testing.

9. **What is the nature and extent of the medical examination that participants and controls are to undergo before participating in this project?**

Dr. Colm Costigan is actively caring for the patients with ACTH resistance, with clinic reviews 3 – 6 monthly. Some patients are already aware of ongoing research through Dr. Sally Ann Lynch, but this new project will be explained to them in detail with further consent obtained for all participating families / patients.

10. **How will the health of the participants and controls be monitored during and after the trial?** (List clinical, laboratory and other examinations):

NA – The family members are not been "treated" so there is no need to monitor health. Regular clinic review is on-going regardless of research.

11. **Will the participants or controls undergo independent medical examinations, before, during or after the trial?** NO

12. **If a placebo group is to be used, will the group receive the best standard therapy?** NA

13. **If the project involves the use of radioactive substances or of laser therapy has the approval of the Head of Radiology been sought?**
(If not, elucidate) NA

SECTION B

INVESTIGATORS AND FACILITIES

14. **Name, qualification and position of each person associated With this project:**

Dr. Colm Costigan, Consultant Paediatric Endocrinologist, OLHSC, MRCPI (Paed)
Dr. Claire Hughes, Specialist Registrar Paediatrics, OLHSC, MRCPI (Paed)
Dr. Adrian Clarke, DSc FRCP, F Med Sci, Professor of Medicine, Bart's and the London School of Medicine and Dentistry

15. **Is each investigator a registered medical practitioner?** YES
If not, elucidate:

16. **Is each investigator a member of a major medical defense body?** YES
If not, elucidate:

17. **What payments, monetary or otherwise, if any, are to be made to any of the investigators** (include payments to any institution or research facility. Please quote account name and number)?

PLEASE NOTE:
Non-disclosure of funds may lead to revoking of the Ethics Approval for this trial.

Dr. Claire Hughes will receive funding as part of a 2 year research fellowship for a salary. The William Harvey institute will receive funding to cover laboratory costs.

18. **What payments, whether monetary or otherwise, if any, are to be made to any person or institution providing facilities to be used for the purpose of the clinical trial?**

The William Harvey Institute will be reimbursed for overheads and consumables from the research funding.

19. **In which hospital or facility will the project take place?**

The project is a joint project between Our Lady's Children's Hospital and the William Harvey Institute, Barts and the Royal London School of Medicine and Dentistry. All laboratory work will be done in William Harvey Institute.

SECTION C

PARTICIPANTS

20. **How many subjects and controls from this centre are expected to participate in this project?** **NUMBER** | 22 |

21. **If this is a multicentre trial please indicate:**

    a) **The expected overall number of subjects:** **NUMBER** | N/A |

    b) **The number and geographical distribution of the centres involved in the study?** **NUMBER** | |

22. **What criteria are to be used for the selection of participants?**

The only criteria includes a diagnosis (clinical and biochemical) of FGD. All patients have already been identified and are aware of their diagnosis. All samples will come from either an affected individual or their family members.

23. **Are women of childbearing potential included?** | NA |

    If so, does the protocol/patient information sheet address the following 8 points:
    (1 - Scientific justification,
    2 - Negative teratogenic studies,
    3 - Warning subject that fetus may be damaged,
    4 - Initial negative pregnancy test,
    5 - Forms of contraception defined,
    6 – Duration of use to exceed drug metabolism,
    7 - Exclude those unlikely to follow contraceptive advice,
    8 - Notify investigator if pregnancy suspected)?

24. **State any other exclusion criteria (age, other illness, other medications etc.):**

    N/A

25. **What are the proposed methods by which participants and controls are to be recruited:**

All affected individuals are receiving ongoing care within the endocrine department. However if a patient is newly diagnosed and wishes to take part we will be happy to include their samples in the analysis upon taking appropriate consent.

26. **Are inducements or rewards, monetary or otherwise, offered to participants and controls:** NO
If yes, elucidate:

27. **What arrangements exist to provide compensation to each participant who may suffer injury or loss as a result of this research project?**

N/A

28. **Have you submitted to the committee, with this form, a patient's information leaflet and consent form prepared by a sponsor or other external group, or a patient information leaflet and consent form based on the committee's guidelines (attached to this form) to be given to each participant and control?** YES
If no, elucidate:

29. **What criteria are to be used to ensure that the identity of each participant and control remains confidential?**

The samples will be kept in a secure DNA bank either in the national centre for medical genetics or in the William Harvey Institute.

30. **Give details of any risks to subjects or to controls from investigative or therapeutic procedures or from withholding of therapy?**
NOTE: *For the protection of both the investigator and the subject this list must be comprehensive and must also appear in full in the patient information leaflet.*

The only procedure will be phlebotomy. The risks would include the risk of bruising and extremely rarely infection following phlebotomy.

31. **Indicate how adverse events are to be notified and evaluated:**

Those of us who will take blood are trained in phlebotomy and have the OLHSC advisory pack on adverse incidents when taking blood. We are also aware of the reporting requirements for adverse incidents

SECTION D

DRUGS AND THE SUBSTANCES

32. **Is the object of this project to assess the effect of a drug or therapeutic substance?** NO

If no, skip to section E:

33. **Name of the substance or preparation which is the subject of the proposed project:**

34. **Name of the company or organisation which produces this substance or preparation:**

34a. **Code number used by the company or organisation for this trial.**

35. **Does the organisation and performance of this trial conform to European Directives on Good Clinical Practice.** YES NO

36. **Give details of the pharmacology, dosage, toxicity and side effects of the substance or preparation:**
NOTE: *For the protection of both the investigator and the subject, the list of side effects must be comprehensive and must also appear in full in the patient information leaflet.*

PRODUCT AUTHORISATION

37. **Is there a Product Authorisation?** YES NO

38. **If there is a Product Authorisation, does the study involve a new use not included in the authorisation, or a dose in excess of the maximum authorised or otherwise exceed authorisation?** YES NO

39. **Irish Medicines Board:**
Application for approval of the study has been made?

NA YES NO PENDING

DATE of application:

Approval has been received.

DATE of approval:

NA YES NO PENDING

40. **Is this preparation or substance given with therapeutic intent?**
(Is the principal purpose of its administration to prevent disease in or to save the life, restore the health, alleviate the condition or relieve the suffering of the patient – in contrast to testing a drug in normal controls or volunteers or giving a drug purely to study pharmocokinetics?)

Note that if the answer is NO patients who are unable to physically sign consent or unable to comprehend the nature, significance, and scope of the consent required, may not participate.

41. **Will the trial begin within 6 days of recruitment?** YES | NO
(In order to allow for mature consideration by the participant, a period of 6 days must elapse from the time a subject is invited to participate in a drug trial (and been given appropriate information) at the beginning of the study. If such a delay is not possible the 6-day rule may be waived by the IMB).

42. **If YES, has a request for a waiver of the 6 day rule been made to the IMB?** YES | NO | NA

43. **Indicate what phase (IMB phase 1 – 4) of drug testing the trial represents.**

Phase 1 – Pharmacokinetics in healthy humans.
Phase 2 – Early studies (kinetics and dose ranging).
Phase 3 – Large safety and efficacy studies in population to be treated.
Phase 4 – Post-marketing/monitoring.

Phase 1 2 3 4

SECTION E

FINANCE

44. **What are the cost/resource implications of this study?**

Please elucidate:

Dr. Claire Hughes is applying for funding from the European Society for Paediatric Endocrinology and from the Barts Research Advisory Board. The funding is to secure a salary to support Dr. Hughes during her research fellowship and to cover laboratory overheads and cost of consumables.

45. **Is the cost of running the trial/research study covered in total by the company/sponsor?** YES | NO | NA

N/A

46. **Please detail all costs under the following headings:**

	Departments	**Head of Department Approval Signature**
Pathology	N/A	_____
Radiology	N/A	_____
Nuclear Medicine	N/A	_____
Pharmacy	N/A	_____
Any other	N/A	_____

Staff

Nursing	N/A	_____
Medical Salaries	N/A	_____
Portering	N/A	_____
Medical Records	N/A	_____
Secretarial	N/A	_____
Any other	Salary for Claire Hughes	_____

The Finance Department will assist with providing costings if required.

47. **Have all <u>tests</u> for this study been discussed with the relevant departments?** YES NO

N/A

48. **Have all <u>costs</u> for this study been discussed with the relevant departments?** YES NO

N/A

49. **Please detail approval.**

Agreed: _____

Head of Department

50. **Have all costs been approved by Accountant/Research Centre Council Department?** YES NO

Agreed: _____ **Date:** _____

Accountant

PLEASE NOTE:

INSURANCE/INDEMNITY ARRANGEMENTS

(a) If the clinical trial is sponsored by a pharmaceutical company please confirm that the sponsor has agreed to accept the Hospital standard Indemnity Form (and append a signed copy). YES NO

N/A

(b) If the standard Indemnity Form has not been signed please explain why.

(c) If there is no sponsor for the clinical trial please specify the insurance arrangement in place and furnish appropriate certification.

(d) If the research is sponsored by a pharmaceutical company, has that company agreed to abide by the current ABPI Clinical Trials Compensation Guidelines? YES NO

SECTION F

I confirm that the information provided in this protocol is correct. I also understand to undertake an annual report on the anniversary of The Ethics Committee approval with details of the number of subjects who have been recruited, the number who have completed the study and details of any adverse events.

Signed: _____
(Project Supervisor)

Date: _____

Ethics Committee Comments:

IMB approval	YES	PENDING	NA
Financial approval	YES	PENDING	NA
Insurance	YES	NO	
Patient Information Sheet approval	YES	NO	
Patient Consent Form approval	YES	NO	

Approved subject to:

Approved:

_____

DIABETES & ENDOCRINOLOGY CENTRE
Telephone: 01-4096399 / Emergency: 01-4096121 / Fax: 01-4560953
Email: diabetes.endocrine@olhsc.ie

Information Leaflet

Project title: Investigating the genetics and mechanisms of ACTH resistance in children with Familial Glucocorticoid Deficiency

I am writing to you to ask if you would like to take part in a research study which aims to find the gene responsible for the genetic condition Familial Glucocorticoid Deficiency, and examine how this gene works. You and your family have previously been seen by the Endocrine Department of Our Lady's' Hospital, Crumlin, because your family has this condition. A sample of blood may have been taken at that time for genetic testing.

We now wish to try and find the cause for the genetic condition in your family. We are asking your consent to take a blood sample, and for this sample and your clinical details to be included in this study.

You are under no obligation to take part in this study, and if you do take part, you may withdraw at any time without having to give an explanation. Your participation in this study will not affect your ongoing medical care.

Your information and sample will be kept confidential at all times. Your blood sample may be sent on for further analysis to another laboratory, and if it is, the sample will be encoded, and your name will not be passed on to the laboratory.

There may not be any direct results for you from the testing carried out. However, we will let you know the outcome of the research project in general and of any specific results that are relevant to you.

If you wish to take part in the study, please sign the attached consent form.

If you have any concerns, or wish for further information, you may contact Dr. Colm Costigan Consultant Paediatrician on 01-4096399, or Dr. Claire Hughes on 01-4096100.

Principal Investigators
Dr. Colm Costigan – Paediatric Endocrinology Consultant
Dr. Claire Hughes – Paediatric Specialist Registrar
Dr. Adrian Clarke – Professor of Medicine, Bart's and the London School of Medicine and Dentistry

DIABETES & ENDOCRINOLOGY CENTRE
Telephone: 01-4096399 / Emergency: 01-4096121 / Fax: 01-4560953
Email: diabetes.endocrine@olhsc.ie

Information Leaflet

Project title: Investigating the genetics and mechanisms of ACTH resistance in children with Familial Glucocorticoid Deficiency

Familial Glucocorticoid Deficiency is a condition that means you have to take steroids every day to keep you well and is why you have to come to see Dr. Costigan and Dr. Cody in the hospital.

We want to study this condition and why some children have it and others don't.

Would you like to take part in this study to help us find the cause of this condition? It would mean taking a blood test and allowing us to look at some of your hospital notes.

You only have to take part in the study if you want to and if you want to stop at any stage (with or without a reason) it's no problem. This study may not help you but it could help others.

Your information and blood sample will be kept secret at all times.

If you would like to take part in the study, please sign the attached form.

If you have any other questions please ask Dr. Colm Costigan or Dr. Claire Hughes on 01-4096100.

Principal Investigators
Dr. Colm Costigan – Paediatric Endocrinology Consultant
Dr. Claire Hughes – Paediatric Specialist Registrar
Dr. Adrian Clarke – Professor of Medicine, Bart's and the London School of Medicine and Dentistry